

CHARACTERIZATION OF THE MOLECULAR DETERMINANTS FOR CLASS A G
PROTEIN-COUPLED RECEPTOR LIGAND BINDING AND FUNCTION: DRUG
DISCOVERY TARGETING THE HISTAMINE H₁RECEPTOR

By

SEAN MICHAEL TRAVERS

A DISSERTATION PRESENTED TO THE GRADUATE SCHOOL
OF THE UNIVERSITY OF FLORIDA IN PARTIAL FULFILLMENT
OF THE REQUIREMENTS FOR THE DEGREE OF
DOCTOR OF PHILOSOPHY

UNIVERSITY OF FLORIDA
2011

© 2011 Sean Michael Travers

ACKNOWLEDGMENTS

To all of my family, friends, colleagues, teachers, professors, my committee members, and my advisor, who have helped me reach this point, I would not be here without each and every one of you. In addition, I would like to acknowledge Dr. Raymond Booth as he has guided me through this process collectively known as graduate school. I would also like to thank Doctors Margaret James, Ken Sloan, and JoannaPeris for their input and expertise while serving on my committee; and Dr. Henry Vischer for his efforts with our BRET studies, as well as all of our post-docs past and present. My thanks also go out to the late Dr. Eugene Gooch of Elon University for his unparalleled teaching ability and for instilling a love of chemistry in me. Last and definitely not least, I would like to thank my parents, Bill and Linda, and my brother Garrett for their unwavering support; and I would be remiss if I did not thank my wonderful girlfriend Laura for putting up with me and supporting me throughout this long, strange trip known as graduate school.

TABLE OF CONTENTS

	<u>page</u>
ACKNOWLEDGMENTS.....	3
LIST OF TABLES.....	6
LIST OF FIGURES.....	7
LIST OF ABBREVIATIONS.....	9
ABSTRACT.....	12
Chapter	
1 G PROTEIN-COUPLED RECEPTORS: ENDOGENOUS AND THERAPEUTIC SIGNIFICANCE OF HISTAMINE RECEPTORS.....	14
Introduction to G-Protein Coupled Receptors (GPCRs).....	14
Ballesteros Numbering System.....	17
Using Ballesteros Numbering to Identify Critical Aminergic Residues	20
Histamine Receptors.....	24
Histamine Biosynthesis and Catabolism	27
Histamine in the Central Nervous System.....	28
Therapeutic Use of Histamine Ligands	36
Previously Established Molecular Determinants for H ₁ Receptors.....	38
H ₁ GPCR Dimerization.....	45
Current GPCR Theory	47
Law of Mass Action and Early GPCR Models	48
Ternary Complex Model	49
Extended Ternary Complex Model.....	49
LITicon.....	50
Goal of This Thesis.....	56
Aim #1: Characterization of the Structure Activity Relationships for PAT Analogue Binding at the Wild Type Human Histamine H ₁ Receptor (HH ₁ R) ..	57
Aim #2: Characterization of the Role of Amino Acid Residue Y5.48 in Dimerization of the HH ₁ R and its Impact on Ligand Binding and Function....	57
Aim #3: Characterization of the Role of HH ₁ R Residue Y7.53A in Ligand Binding and Activation Using Functionally Selective Phenylaminotetralin (PAT) Derivatives	58
2 CHARACTERIZATION OF THE STRUCTURE ACTIVITY RELATIONSHIPS FOR PAT ANALOGUES AT THE WILD TYPE HH ₁ R.....	66
Rationale for Undertaking These Studies	66
Materials and Methods.....	66
Chemicals.....	66

Cell Culture and Transfection	67
HH ₁ R Binding Assays.....	68
Binding Assay Results and Discussion	69
Unsubstituted Parent PAT Compounds.....	70
<i>Ortho</i> -Substituted PATs.....	72
<i>Meta</i> -Substituted PATs.....	73
<i>Para</i> -Substituted PATs	75
N-substituted PAT Derivatives.....	81
Chloro and Hydroxyl Tetrahydronaphthalene Substituted PATs	85
PAT-Like Compounds with Ring Perturbations	86
PAT Binding Summary.....	91
3 INVOLVEMENT OF AMINO ACID RESIDUE Y5.48A IN THE DIMERIZATION/FUNCTIONAL STABILIZATION PROCESSES OF THE HUMAN HISTAMINE H ₁ RECEPTOR	104
Literature Review of Ballesteros Position 5.48.....	104
Materials and Methods.....	106
Experimental Results and Discussion.....	108
Saturation Binding Assay Results	108
Competitive Binding Experiments.....	111
Inositol Phosphate Production Mediated via G _{αQ}	114
Bioluminescence Resonance Energy Transfer (BRET) Studies Comparing dimerization of the WT and Y5.48A H ₁ Receptors	118
Summary	120
4 PROBING THE ROLE OF RESIDUE Y7.53A IN THE LIGAND BINDING AND ACTIVATION OF THE HH ₁ R	126
Rationale for Undertaking These Studies and Literature Review.....	126
Materials and Methods.....	127
Experimental Results and Discussion.....	128
Competitive Binding Studies at Y7.53A	128
Inositol Phosphate Production Mediated via G _{αQ}	129
Adenylyl Cyclase Activity/Cyclic Adenosine Monophosphate Formation Mediated via G _{αS}	132
Summary	132
5 CONCLUDING REMARKS	137
LIST OF REFERENCES	141
BIOGRAPHICAL SKETCH.....	145

LIST OF TABLES

<u>Table</u>	<u>page</u>
1-1	K _i and B _{Max} values for ³ H-mepyramine and (-)-trans-Phenylaminotetralin (PAT) for WT and D3.32A/F6.52A H1 receptors..... 65
2-1	Affinities of the PAT stereoisomers at the WTHH ₁ R 93
2-2	Human Histamine H ₁ Receptor (HH ₁ R) binding affinities of (+)- and (-)-trans-para-substituted PATs 95
2-3	WT HH ₁ R binding affinities of (+)- and (-)-trans-para-substituted PATs 96
2-4	Histamine H ₁ binding affinities of N-alkyl substituted PAT analogues 99
2-5	Affinities of di-OH and Cl-OH PAT analogues at the WT HH ₁ R..... 100
2-6	Affinities of PAT analogues with modified tricyclic ring systems 103
3-1	Compiled K _D and B _{Max} values for 3H-mepyramine and (-)-trans-PAT at the WT and Y5.48A HH ₁ R. 125
3-2	Tabulated K _i values for the HH ₁ R ligands examined in this section at both the WT and Y5.48A point-mutated receptors. 125
3-3	Displays the correlated functional values for the ligands examined in the phospholipase C (PLC) functional assay at the WT and Y5.48A HH ₁ R..... 125
4-1	Compiled affinities of various H ₁ ligands at the WT and Y7.53A receptors 134
4-2	Tabulates the EC/IC ₅₀ and E/I _{max} values of various ligands at the WT and Y7.53A point mutated receptors 136

LIST OF FIGURES

<u>Figure</u>	<u>page</u>
1-1 Generic structure of a G-Protein Coupled Receptor (GPCR).	59
1-2 GPCR activation demonstrating guanine exchange.	59
1-3 Ballesteros numbering proceeds as indicated by the arrow on the generic GPCR structure	60
1-4 Phylogenetic tree for aminergic GPCRs that are closely related to the H ₁ receptor.	60
1-5 Representation of both signaling pathways for the Human Histamine H ₁ Receptor (HH ₁ R).	61
1-6 Histamine catabolism in the central nervous system	62
1-7 The chemical structures of first generation and second-generation (bottom) antihistamines.....	62
1-8 Proposed models of GPCR dimerization	63
1-9 Possible combinations of contact and domain-swapped dimers for D3.32A and F6.52A mutations.	63
1-10 Structures of the β ₂ -adrenergic receptor ligands that were studied using LITicon.....	64
1-11 Illustrates the law of mass action.....	64
1-12 Indicates the changes that were made to the law of mass action in order to incorporate G-proteins.....	64
1-13 Demonstrates the ternary complex model of G-protein activation	64
1-14 Extended ternary complex model	65
2-1 Phenylaminotetralin (PAT) family of stereoisomers demonstrating the stereochemical relationships between each compound.	93
2-2 Representative competitive binding curves for the PAT family of stereoisomers at the human WT H ₁ receptor.....	94
2-3 Enantiomers of (±)-cetirizine that demonstrate high stereoselectivity at the HH ₁ R	94
2-4 Structures of (±)- <i>trans-ortho</i> -Cl-PAT (±)- <i>trans-ortho</i> -CH ₃ -PAT	95

2-5	Structures of (-)-trans- <i>meta</i> -halogenated-PAT derivatives	95
2-6	Structures of the (-)-trans- <i>para</i> -substituted PATs.....	96
2-7	Representative HH ₁ R competitive binding curves for (+)- and (-)-trans- <i>para</i> -substituted PATs.	97
2-8	Structures of N-alkylated-PAT derivatives.	98
2-9	Proposed interaction of aspartic acid D3.32 with (-)and (+)- <i>trans-N,N</i> -diethyl-PAT that may account for higher affinity of the (-)-enantiomer	99
2-10	Structures of racemic di-OH and Cl-OH-PAT ligands	99
2-11	Representative competitive binding curves for di-OH and Cl-OH-PAT at the WT HH ₁ R.....	100
2-12	Proposed H ₁ pharmacophore and the ligands that are derived from it..	101
2-13	Structures for the ring substituted PAT derivatives.....	102
3-1	Saturation binding isotherms for ³ H-mepyramine at the WT and Y5.48A HH ₁ R	121
3-2	Saturation isotherms for of ³ H-(-)- <i>trans</i> -PAT labeled WT and Y5.48A HH ₁ receptors	122
3-3	Structures of ligands examined in this section:.....	123
3-4	Competitive binding curves for (-)- <i>trans</i> -PAT at the WT and Y5.48A HH ₁ R	124
3-5	Ligand mediated Phospholipase C (PLC) functional activity at WT vs. Y5.48A HH ₁ receptors.	124
4-1	GPCR snake diagram for the HH ₁ R illustrating the location of Y7.53 towards the intracellular side of TMD 7.....	134
4-2	Representative competition binding curves for various H ₁ ligandsat the Y7.53A point mutated receptor:.....	135
4-3	Representative PLC functional curves for H ₁ ligands at the Y7.53A HH ₁ R.....	135
4-4	Representative Adenylyl Cyclase functional curves for histamine stimulationat WT and Y7.53A HH ₁ R.	136

LIST OF ABBREVIATIONS

5HT	serotonin, usually accompanied by a receptor subtype as in 5HT _{2A}
AA	arachidonic acid
AC	adenylyl cyclase
AD	Alzheimer's disease
B2-AR	beta-2 adrenergic receptor
BRET ₅₀	concentration of cDNA, at which 50% of the maximum BRET signal is reached
BRET	bioluminescence resonance energy transfer
BRET _{Max}	maximum BRET signal obtained
cAMP	cyclic-3, 5-adenosine-monophosphate
CAT	cyclohexylaminotetralin
CDNA	cloned deoxyribonucleic acid
CNS	central nervous system
COAT	cyclooctylaminotetralin
CSF	cerebrospinal fluid
DAG	diacylglycerols
DOI	2, 5-dimethoxy-4-iodoamphetamine
DNA	deoxyribonucleic acid
EC/IC ₅₀	effective concentration or inhibitory concentration of a ligand that produces 50% of the maximal response
ECL(s)	extracellular loop
E/I _{Max}	maximum stimulation (E) or inhibition (I) over percent basal
G _{αX}	acronym for a particular subunit of a G-protein, where X is Q or S
GC/MS	gas chromatography/mass spectrometry
GABA	γ-amino-butyric acid

GDP	guanine diphosphate
GI	gastrointestinal
GPCR	G-Protein Coupled Receptor
GTP	guanine triphosphate
HDC	histidine decarboxylase
HH ₁ R	Human Histamine H ₁ Receptor, H _x is used to indicate other histamine receptors, as in H ₂ receptor.
HNMT	human N-methyl transferase
HPLC	high performance liquid chromatography
IP or IP ₃	Inositol Phosphates or Inositol Triphosphates
ICL(s)	intracellular loop(s)
IL	ionic lock
K _D	affinity value of a radioligand for its receptor
K _I	affinity value of a ligand, determined by the displacement of a radiolabeled compound from the receptor
MAO-B	mono amine oxidase B
MEM	Eagle's minimum essential medium
PAB	<i>cis</i> -5-phenyl-7-dimethylamino-5,6,7, 8-tetrahydro-9 <i>H</i> -benzocycloheptane
PAT	phenylaminotetralin
PD	Parkinson's disease
PET	positron emission tomography
PL	Phospholipase, usually listed with a subtype as in PLC, equating to phospholipase C
PNS	peripheral nervous system
PTZ	pentylenetetrazol
R-Luc	<i>Renillareniformis</i> luciferase (an enzyme)

RTS	rotamer toggle switch
SAR	structure activity relationships
TH	tyrosine hydroxylase
S.E.M.	standard error of the mean
SPA	scintillation proximity assay
TMD(s)	transmembrane domain(s)
TMN	tuberomammillary nucleus
UV-VIS	ultraviolet visible spectrometry
VLPO	ventrolateralpreoptic area
WT	wild type
YFP	yellow fluorescent protein

Abstract of Dissertation Presented to the Graduate School
of the University of Florida in Partial Fulfillment of the
Requirements for the Degree of Doctor of Philosophy

CHARACTERIZATION OF THE MOLECULAR DETERMINANTS FOR CLASS A G
PROTEIN-COUPLED RECEPTOR LIGAND BINDING AND FUNCTION: DRUG
DISCOVERY TARGETING THE HISTAMINE H₁ RECEPTOR

By

Sean Michael Travers

August 2011

Chair: Raymond Booth

Major: Pharmaceutical Sciences

This PhD thesis research project focuses on drug discovery targeting the human histamine H₁ (HH₁R) G protein-coupled receptor (GPCR). Certain novel phenylaminotetralin (PAT) ligands synthesized in our laboratory interact with mammalian brain H₁ receptors in vivo to modulate catecholamine (dopamine, norepinephrine) neurotransmitter synthesis. Alteration of brain catecholamine neurotransmitter levels is linked to several psychiatric and neurological diseases, including, schizophrenia, depression, insomnia, epilepsy, and Parkinson's disease. Meanwhile, activation of H₁ receptors in the periphery mediates allergic responses. There is evidence that central and peripheral histamine H₁ receptors can signal through different second messenger pathways. The functional selectivity hypothesis suggests that the same ligand may act as an agonist or inverse agonist at the same GPCR, depending on differential G-protein coupling with the receptor. Thus, it is theoretically possible for the same ligand to modulate brain and peripheral H₁ receptor signaling to result in therapeutically useful central H₁ receptor activation without provoking a peripheral H₁-mediated allergic response. A lipophilic, brain-

penetrating ligand, (2*R*,4*S*)-(-)-*trans*-*N,N*-dimethylamino-4-phenyl-1,2,3,4-tetrahydro-2-naphthalenamine (phenylaminotetralin, PAT) possesses the therapeutically useful pharmacological properties of inverse agonism regarding H₁ signaling via the H₁G_{αQ} and phospholipase (PL)-C and inositol phosphate (IP) formation pathway that mediates allergic reaction responses; while acting as an agonist regarding H₁ signaling via the G_{αS} adenylyl cyclase (AC) and cyclic-3,5-adenosine-monophosphate (cAMP) pathway that stimulates brain catecholamine neurotransmitter synthesis. The general goal of this dissertation is to characterize the molecular determinants of PAT-type ligands with the H₁GPCR that govern functionally selective signaling. Results are predicted to characterize H₁ molecular structure, provide structure activity relationships, and functional determinantsto advance H₁ drug design for psychiatric and neurological disorders.

CHAPTER 1
G PROTEIN-COUPLED RECEPTORS: ENDOGENOUS AND THERAPEUTIC
SIGNIFICANCE OF HISTAMINE RECEPTORS

Introduction to G-Protein Coupled Receptors

G protein-coupled receptors (GPCRs) represent the largest family of membrane proteins in the human genome, and comprise approximately 1% of our total genetic code (Johnston & Siderovski, 2007). Knockout models have shown GPCRs that are critical to regulating the signaling processes of the cardiovascular, nervous, endocrine, metabolic, and sensory systems (Kobilka & Rohrer, 1998; Spiegel & Weinstein, 2004). Mutations in the genes encoding for GPCRs have been identified as the root cause of many inherited diseases. For example, a mutation to the gene encoding for G_{α_s} has been linked to bone abnormalities, hormone resistance (pseudohypoparathyroidism) and hormone hypersecretion (McCune-Albright syndrome) (Spiegel & Weinstein, 2004). Due to their ubiquitous distribution throughout the body and their critical role in regulating a vast number of signaling cascades, GPCRs are an obvious therapeutic target, for both peptide and small molecule ligands.

GPCRs share a common structural motif that includes seven transmembrane helices, an extracellular N-terminus, an intracellular C-terminus, and a unique ability to couple to intracellular signaling modifiers called G-proteins, as shown in figure 1-1 (Johnston & Siderovski, 2007). Current estimates state there are approximately 800 GPCR's that are encoded within the human genome. However, the majority of these 800 receptors are characterized as orphans, meaning that their endogenous ligand has yet to be uncovered. By comparing their sequence homologies, GPCRs can be broadly classified into three separate families: the rhodopsin-like family (A), secretin-like (B), glutamate family (C) (Kobilka B. , 2006). It is worth mentioning that GPCR families can

be broken down by the binding location of their endogenous ligand, also called the orthosteric binding site. Class A GPCR's tend to bind their ligands in their transmembrane domains (TMD's). Class B GPCR's tend to bind their endogenous ligand in the extracellular loops, and class C GPCR's bind at their unique N-terminal Venus-Flytrap moiety.

There is currently much debate about the minimal functional unit for class A and B GPCR's. Class C GPCR's (GABA_B), are well documented as dimeric receptors, however this has yet to be demonstrated definitively in the remaining two classes (Pin et al., 2004). A recent paper demonstrated that nucleotide exchange could take place when a monomeric β_2 -Adrenergic Receptor is isolated within a reconstituted high-density lipoprotein (Whorton et al., 2007). Contrary to this, several modeling papers indicate G-proteins have a more energetically favorable interaction with a dimeric subunit (Hamm, 2001; Liang et al., 2003). The present consensus in the literature is that class A and B GPCR's can form dimers and oligomers, but the minimal functional unit has yet to be determined. A more detailed discussion on GPCR dimerization will follow later in this document.

Despite being arranged into several different classes, all GPCR's couple intracellularly to G-proteins. These unique, heterotrimeric proteins allow signals from the extracellular (N-terminal) side of the receptor to exert their influence on the intracellular (C-terminal) side of a cell. G-proteins consist of three distinct subunits, the α , β , and γ . These three subunits are crucial to the function of the entire GPCR unit, as they serve as guanine nucleotide exchange factors. The guanine nucleotide exchange takes

places in the α -subunit and is the catalyst for the intracellular signaling cascade (Johnston & Siderovski, 2007).

It is important to note that many GPCR's have the ability to activate in the absence of an agonist ligand. This phenomenon is caused by the dynamic and flexible nature of GPCR's and is called basal or constitutive activity (Kobilka & Deupi, 2007). Activation of a receptor, with or without an agonist present, causes conformational changes to the receptor that are transmitted to the intracellular loops. These changes result in a conformational change in the G-protein, exchanging a guanine diphosphate (GDP) unit that is bound to the G_α subunit, for a guanine triphosphate (GTP). This nucleotide exchange causes the heterotrimeric G-protein to dissociate into G_α and $G_{\beta\gamma}$, both of which act as intracellular signaling effectors, acting upon ion channels, adenylyl cyclases, phosphodiesterases, kinases, and phospholipases, as shown below in figure 1-2. These are but a few examples from the litany of downstream targets that GPCR's have the ability to modulate (Johnston & Siderovski, 2007).

The downstream target of a particular GPCR is determined by its location in the body and the G-protein to which it is coupled. This is well demonstrated by human Histamine H_1 receptor. In most mammalian tissues the H_1 receptor signals through $G_{\alpha Q}$, which activates PLC, increasing the intracellular concentration of IP and diacylglycerols (DAG). In stark contrast to this, H_1 receptors found in the mammalian brain demonstrate the ability to function through $G_{\alpha s}$, leading to activation of AC and increased intracellular levels of cAMP as well as intracellular Ca^{2+} (Moniri et al, 2004). The ability of a GPCR to couple to several G-proteins is well established and the phenomenon is called functional selectivity (Moniri et al, 2004; Urban et al., 2007). To date twenty different

G_α subunits have been identified in mammalian tissues. These can be further classified into four subfamilies based upon their structure and the functional pathways they modify. These subfamilies are G_{αs}, G_{αQ/11}, G_{αi/o}, and G_{α12/13}. The β and γ subunits exist and function as a single dimeric unit that can be constructed from a pool of five unique β and twelve γ subunits (Offermans, 2003).

The ability of GPCR's to affect such a wide variety of downstream mechanisms, in nearly all regions of the body, has made them very attractive drug targets. A recent study done by Overington et al. in 2006, suggests that rhodopsin-like (Class A) GPCRs account for over twenty-five percent of FDA approved drugs. Class A GPCRs represent only part of the superfamily, so as more information about the other GPCR classes becomes available that number is expected to increase further.

Ballesteros Numbering System

Given the vast array of GPCRs and their structural differences and complexity, it is quite difficult to discuss results across receptors, especially when referring to an amino acid residue as a single number in a chain of 400 plus residues. This issue is compounded by the fact that GPCRs can have differing residue lengths for each of their shared structural features including transmembrane domain, intracellular and extracellular loops, and N and C-termini (Hermans, 2003; Kobilka B. , 2006). For example, amino acid 400 may be located in the intracellular loops for one receptor, yet be in the TMD region for another class A receptor. These numbers provide no indication as to which TMD the residue belongs, which is critical for GPCRs like the H₁ receptor that possess a long third intracellular loop (ICL) of about 200 amino acids. If you used conventional residue numbering, meaning residues from 1-400, the long loop would

cause the residues in TMD 6 and 7 to have much higher numbers than in related receptors where ICL3 is shorter. To help address this issue, a new numbering system specifically for GPCRs was proposed by Ballesteros (Ballesteros et al., 2001). This newer classification proved incredibly useful and caught on quite quickly, so an in-depth discussion is warranted here.

By careful analysis of GPCR sequences, the authors noticed that the origins of both the intracellular and extracellular TMD regions were designated by a positively charged cluster of lysine or arginine residues. These residues associate with the negatively charged phospholipid heads of the cell membrane to create a series of strong ionic bonds that help the receptor associate with the membrane. Arginine and lysine clusters proved to be consistent markers of the beginning and end of the TMD helices across class A GPCRs; however, the residue number was never the same in the overall sequence. The arginine and lysine observation seemed to beg the question; can a specific position within the GPCR architecture be as important as the amino acid number in the sequence? The answer is an emphatic yes. By using the most conserved residue within each TMD helix as a reference point, and selecting the most conserved residues across the entire GPCR superfamily, a numbering system was created (Ballesteros et al., 2001).

The most conserved residue in each TMD was assigned an arbitrary value of X.50, where X indicates the TMD where the residue is located. As an example W6.48, would correspond to a tryptophan residue in TMD 6 that is two residues before the most conserved residue (6.50). In addition, this nomenclature has been extended to point mutations. The principle is the same, each amino acid is given a number relative to the

most conserved residue in that helix; however, the amino acid that the residue is being mutated to is listed in one letter amino acid code immediately following the location.

Taking W6.48 again as an example, an alanine mutant in TMD 6, located two residues before the most conserved residue would correspond to W6.48A. Where W is the native residue, 6 is the TMD, .48 is the position, and A, the one letter code for alanine, is the residue that W is mutated to (Ballesteros et al., 2001).

The last nuance to this numbering system is that the numbers increase or decrease as you move intracellularly, depending upon the TMD you are considering. GPCRs are folded proteins that pass through the membrane seven times. It winds down from the extracellular N-terminus through the cell membrane into TMD 1, across the cytoplasm in ICL 1, up through the membrane for TMD 2, across extracellular loop 1 (ECL1), down through TMD 3, across ICL 2, up through TMD 4, across ECL 2, down through TMD 5, across ICL 3, up through TMD 6, across ECL 3, before winding down through the membrane with TMD 7 and the c-terminus. Residues always count up toward the most conserved residue, but the starting point varies as you follow the peptide chain through the membrane. For TMD 1, 3, 5, and 7 the numbers increase as you move intracellularly because the sequence is heading in that direction as you follow from the N to C terminus. For TMD 2, 4, and 6 the numbers still increase as you move towards X.50, but they now increase as one progresses extracellularly. Again, this is due to the origin of these helices being found at the intracellular loops and proceeding upward towards the extracellular region. An example of this is demonstrated below in figure 1-3, with notations to indicate how the numbering proceeds (Ballesteros et al., 2001).

Using Ballesteros Numbering to Identify Critical Aminergic Residues

The literature is inundated with other examples of a position being important across species subtypes. For example, the DRY (Asp-Arg-Tyr) motif at the intracellular end of TMD 3 has been implicated in the activation of nearly all rhodopsin-like (class A) receptors. Of the three residues Tyr is the least conserved, yet is still found in 67% of class A GPCRs. Arg, which is strongly basic, and Asp/Glu, which are strongly acidic, form an important “ionic lock” interaction that is critical to activation. Not surprisingly, Arg and Asp/Glu are conserved across 87% of class A GPCRs (Mirzadegan et al., 2003). In fact, a GPCR without the DRY motif that was able to function was deemed significant enough to warrant a standalone publication in 2005 (Flanagan, 2005). It is important to note, that even though the residue numbers were changing, all of these GPCRs possess this DRY motif at the same location, the cytoplasmic end of TMD 3. Suggesting that class A GPCRs have conserved structural regions that are critical for receptor function. These regions that are known to be involved in receptor activation are called molecular switches (Kobilka B. , 2006).

A similar trend is found with a cluster of residues in TMD 6 that are collectively called the rotamer toggle switch. These residues C/T/S6.47, W6.48A, and F6.52 form a series of stabilizing interactions that modulate the degree of bending caused by a proline residue in TMD 6. This phenomenon is called the proline kink in TMD 6. Ligands at β_2 -AR and across many other aminergic GPCRs produce strong interactions with these residues, specifically W6.48 and F6.52 that seem to be linked to receptor activation (Shi et al., 2002). In the “off” position, there is a stabilizing interaction between the hydroxyl-containing residue at position 6.47 and W6.48 that reduces the bend caused by P6.50. In the “on” position this stabilizing interaction is lost at the proline kink

becomes much more pronounced leading to a movement in the cytoplasmic end of TMD 6 causing receptor activation (Shi et al., 2002). Here again, it is observed that a particular location within a series of GPCRs is just as critical for activation of the receptor as the amino acids that are located at that position. Therefore when discussing GPCRs and attempting to draw conclusions, it is important to use the Ballesteros numbering system rather than the amino acid number in the sequence. Doing so provides significantly more information about that residue as well as its location within the GPCR architecture, while at the same time allowing comparisons to different receptors.

When the Ballesteros numbering system is employed, and the molecular determinants for several other aminergic receptors are examined, an unusual trend is noticed. Certain residue numbers seem to be important for the binding of endogenous ligands across several aminergic receptors. Residues at positions 5.42 and 5.46 seem to be important for the binding and function of endogenous compounds at the H₁ receptor, the β_2 -adrenergic receptor and at serotonin 2 family (5HT₂) receptors. At the H₁ receptor it has been proposed that an asparagine at position 5.46 (N5.46) forms a critical hydrogen bond with the N _{π} -imidazole nitrogen in histamine. Based upon mutagenesis of this residue it is clear that it has a profound impact upon histamine binding and function. Specifically the affinity (K_i) for histamine is reduced by approximately 40 fold, with PLC activation being similarly impacted; demonstrating a dramatic EC₅₀ reduction of about 300 fold (Smit et al., 1999; Fang, Travers, and Booth.,2009 pre-publication). Interestingly, the maximum signal (E_{Max}) for PLC activity was not reduced and the potency and efficacy of cAMP accumulation was not impacted.

Position 5.42 is a threonine in the H_1 R and displays a significant reduction in affinity and efficacy when compared to the WT receptor. A 10-fold reduction in binding affinity and a significant drop in efficacy (EC_{50} values) were observed for this point mutant. Preliminary molecular modeling, with homology to bovine rhodopsin, indicated that this residue has an important stabilizing interaction with N5.46, and holds this residue in an ideal location to bind to the imidazole ring of histamine (Fang, Travers, and Booth., 2009 pre-publication).

When the β_2 -AR is considered, its endogenous agonist epinephrine forms extremely strong hydrogen bonding contacts in this exact same region. At this receptor, 5.42 and 5.46 are both occupied by serine residues. Upon mutation to non-functional alanine residues, affinity for epinephrine was found to decrease markedly. At S5.42A, the affinity dropped 25-fold and at 5.46A, the affinity was reduced 39-fold. This sharp drop in affinity is attributed to hydrogen bonding between the two serine residues and the hydroxyl groups on the catechol ring (Carmine et al., 2004; Bhattacharya et al., 2008). It is interesting to note that the drop in ligand affinity for S5.46 in β_2 -ARs (39-fold), is nearly identical to the reduction in affinity for histamine at H_1 N5.46A receptors (40-fold).

When the more closely related 5HT₂ receptor family is considered, things become slightly more complex as there are three subtypes A, B, and C of this receptor. In the interest of keeping this brief, the focus will be on human 5HT_{2A} receptors. In human 5HT_{2A} receptors position 5.46 is a serine, and has been strongly implicated in ligand binding differences that have been observed between human and rat_{2A} receptors (Miller et al., 2009). In rats, this residue is an alanine, and mutagenesis studies have shown

that by mutating the rat receptor from an alanine to a serine “rescues” the binding profile observed in the human receptor. This effect was originally observed in 1992 by Kao et al, with the well-known radioligands ketanserin and mesulergine. Briefly, mesulergine displayed a low affinity for human 5HT receptors and a high affinity at rat 5HT receptors. By creating a S5.46A mutation to the human receptor, and mimicking the rat sequence, the affinity of ³H-mesulergine was dramatically increased and resembled the affinity for rat receptors. The researchers concluded that position 5.46 was critical for ligand binding at 5HT receptors (Kao et al., 1992; Johnson et al., 1993). Interestingly, residue 5.46 has also been proposed to interact with the indole nitrogen of serotonin, which is quite similar to the imidazole interaction seen at this position with histamine (Braden and Nichols, 2007).

The same paper concludes that the serine residues at positions 5.43, and possibly 5.42, have hydrogen bond interaction with the hydroxyl moiety of serotonin and other tryptamines. These results fit with the interactions of epinephrine and residues S5.42 and S5.43 at the β_2 -AR. Upon examining the whole picture, it seems that positions 5.42/5.43 are polar residues at these aminergic receptors and produce stabilizing interactions, either directly with a hydrogen bonding moiety on the ligand, or by stabilizing a nearby residue that is critical for ligand binding. The 5.46 position seems to have strong, direct interactions with the endogenous ligands of these aminergic receptors. In 5HT_{2A} and H₁ receptors, 5.46 forms a strong hydrogen bonding interaction with the nitrogen atoms in the heteroaromatic rings in both serotonin and histamine. When the β_2 -AR is considered, the interaction with the nitrogen is lost, but a hydrogen bond is formed with the second hydroxyl on the catechol ring of epinephrine. These

results, when taken together, suggest that there may be an overall similarity in the way these aminergic GPCRs are binding their endogenous ligands. The fact that these receptors are all derived from a common ancestor fits with this observation and could suggest that each receptor evolved residues at key positions in order to bind its endogenous ligand specifically. The conservation of these positions across receptor families also suggests that these positions are critical for causing the conformational changes that are responsible for receptor activation, and could suggest that there is a common mechanism of activation among these aminergic GPCR's. This adds significance to probing the molecular determinants of the H₁receptor, as the results can be extrapolated across aminergic receptors.

Histamine Receptors

There are four subtypes of histamine receptors, H₁, H₂, H₃, and H₄, each of which is a GPCR. H₄ is the most recently discovered and it can be found in bone marrow, leukocytes, and mast cells. The H₄ subtype shares approximately 40% of its sequence with H₃ and about 18% with H₁ and H₂. H₄ receptors couple to G_{αi/o} and inhibit cAMP formation and can also activate PLC/IP signaling (Nakamura et al., 2000). The remaining histamine subtypes (H₁-H₃) are expressed in mammalian brain tissue, and are known to play roles in regulating metabolic states, sleep-wake cycles, and behavior patterns (Haas and Panula, 2003).

The H₃ receptor share approximately 20% of their sequencing with H₁ and H₂ subtypes, and couple to G_{αi/o}/AC/cAMP signaling, inhibitingcAMP release, and are found in central nervous system (CNS) and peripheral nervous system(PNS) cells. It can act as either an autoreceptor to inhibit further release of histamine or as a

heteroreceptor, which regulates the release of other neurotransmitters like serotonin, norepinephrine, acetylcholine, dopamine and γ -amino butyric acid (GABA) (Lovenberg et al., 1999; Esbenshade, 2003; Yanai & Toshiro, 2007; Haas et al., 2008). Because of their ability to control the release of a variety of biogenic amines H_3 receptors have been proposed as a novel antipsychotic targets (Ito, 2009).

The H_2 receptor shares 21% of its overall homology with H_1 and couples mainly to G_{α_s} /AC/cAMP signaling. It is found in gastric parietal cells, vascular smooth muscle, heart muscle, and in the brain (Hill et al, 1997; Smit et al., 1999). Antagonists for the H_2 receptor are used clinically in the treatment of gastrointestinal (GI) ulcers, acid reflux disease, and Zollinger-Ellison syndrome. Each disorder is characterized by an overproduction of gastric acid, administering a selective H_2 antagonist will decrease acid secretion from gastric parietal cells and result in an amelioration of the symptoms (Leurs et al, 1995; Smit et al., 1999). This approach has lost favor in recent years, as proton-pump inhibitors have shown to be more efficacious (Haas et al., 2008; Malfertheiner et al, 2009)

Interestingly, the H_1 receptor has its highest transmembrane homology (44%) with the muscarinic M_1 receptor and is more closely related to the muscarinic M_1 - M_5 and the serotonergic $5HT_2$ family than to the H_2 receptor (Leurs et al., 1995; Smit et al., 1999). The phylogenetic tree for the receptors that are related to H_1 can be found in figure 1-4 below.

The traditional therapeutic role for H_1 R is already well defined. As early as 1910, Dale and Laidlaw observed that injection of histamine into the body produced symptoms that were identical to an allergic response (Brunton, Lazo, & Parker, 2006). In the years

since this initial discovery, the H₁ receptor has been largely associated with this allergic response. The histamine H₁ receptor, however, is a G-protein coupled receptor, and as such, it has the ability to couple to several different G-proteins. This phenomenon is called functional selectivity. (Hermans, 2003; Urban et al., 2007)

The G-proteins linked to the human H₁receptor include the G_{αQ}/PLC second messenger pathway that is associated with allergic responses in the peripheral nervous system. In addition to this pathway, it has been well established that the receptor can stimulate the adenylyl cyclase pathway in mammalian brain tissues (Moniri et al, 2004). It is believed to be mediated through G_{αS}, but this has yet to be conclusively demonstrated and there is at least some debate in the current literature about G_{αS} involvement (Maruko et al., 2005). A third signaling pathway is mediated by phospholipase A2 (PLA₂), which cleaves the fatty acid from the second carbon of glycerol, resulting in the Ca²⁺ dependent release of arachidonic acid (AA) from the cell membrane(Leurs et al, 1995). It has been shown that PLC and DAG's stimulate the release of AA. Due to activation by the second messengers, Ca²⁺ and DAG's, there is significant cross-talk between signaling pathways and AA release has yet to be tied to a specific G_α subunit. Studies have implicated a direct G-protein interaction with PLA₂, but this phenomenon has only been conclusively demonstrated in *Sporothrixschenkii*, a pathogenic fungus (Berrios et al., 2009). The pathways for G_{αS} and G_{αQ}signaling can be found in figure 1-5 below.

H₁ receptors have been characterized using the radioligand, ³H-mepyramine, in a wide variety of mammalian cells. In 1986, Donaldson et al. demonstrated that H₁ receptor activation led to smooth muscle contraction via the G_{αQ}/PLC/IP signaling

pathway. This response can present itself as respiratory distress (bronchial constriction), diarrhea (GI contraction), or edema and hypertension (cardiovascular contraction). However, in the adrenal gland and in mammalian brain tissue, occupation of H₁ by a suitable agonist produces cAMP, TH stimulation, catecholamine synthesis, and the release of epinephrine/norepinephrine (Marley and Robotis 1998; Booth & Moniri, 2006).

Histamine Biosynthesis and Catabolism

Histaminergic neurons possess the ability to synthesize the neurotransmitter histamine. Biosynthesis of histamine is quite efficient, even by the standards of the human body. Histamine's precursor, L-histidine, is taken up by the cerebrospinal fluid (CSF) and by the L-amino acid transporters found directly on histaminergic neurons (Haas et al., 2008; Stahl, 2008). Once taken up, histamine is acted upon by the enzyme histidine decarboxylase (HDC) to synthesize histamine. Contrary to other neurotransmitters, the rate limiting step in histamine synthesis is the bioavailability of the precursor (Haas et al., 2008). This is unusual among the biogenic amines and can be explained by the relatively simple biosynthetic pathway for histamine.

Histamine is stored in cell somata and is packaged into vesicles by vesicular monoamine transporter 2 by exchanging two protons. Histamine is released when an action potential arrives, and is regulated by the histamine H₃receptor (an autoreceptor) through feedback inhibition. Histamine is predominantly inactivated in the extracellular space of the CNS by two enzymes, histamine N-methyltransferase and monoamine oxidase B (HNMT and MAO-B, respectively) (Haas et al., 2008; Stahl, 2008). Initial inactivation occurs by HNMT, using S-adenosyl-methionine (SAM) as a methyl donating substrate, to yield tele-methylhistamine. When in the brain, this metabolite is acted upon

by MAO-B to produce the inactive metabolite t-methyl-imidazolacetic acid, as depicted in figure 1-6 below. In the periphery, histamine is metabolized directly to imidazolacetic acid by the enzyme diamine oxidase.(Haas et al., 2008)

Histamine in the CNS

Histaminergic neurons express the enzyme L-histidine decarboxylase, which confers the ability to synthesize histamine, and are located exclusively in the tuberomammillary nucleus (TMN) in the posterior hypothalamus. Despite their limited location, histamine neurons project broadly throughout the entire brain and are found in the cerebral cortex, thalamus, basal ganglia, and amygdala(Haas et al., 2008; Stahl, 2008). Ascending pathways innervate the cortex and thalamus and play important physiological roles in arousal and learning. Histamine projections also innervate cholinergic neurons in the basal forebrain, which are postulated to play roles in learning and arousal. Projections extend into the hippocampus, nucleus accumbens, and amygdala to modulate additional behaviors. Descending pathways innervate brainstem functions and regulate further neurotransmitter pathways capable of modifying neuronal activity and release(Stahl, 2008). Because of their extensive projections from the TMN histaminergic neurons are postulated to play significant roles in a number of neurological pathologies including, but not limited to insomnia, allergic responses, Alzheimer's disease, Parkinson's disease, depression, and schizophrenia.

Histamine receptors have been associated with sedation since the first antihistamines were produced. In fact, the second generation of antihistamines was created to help alleviate prolonged sedation associated with many of the original antihistamines such as diphenhydramine (Benadryl), azatadine, hydroxyzine, triprolidine, and chlorpheniramine(Leurs et al, 1995). The structures for each of these compounds

can be found in figure 1-7 below, along with their second-generation (non-sedating) counterparts. Many early antipsychotic drugs, such as doxepin and amitriptyline, were originally classified as anti-histamines. Both compounds have strong activity as H₁ inverse agonists, but exert their antipsychotic activity by blocking serotonin and norepinephrine transporters. Regardless, these compounds also display the strong sedative properties associated with H₁ inverse agonism(Stahl, 2008).

These observations and many years of research have tightly interwoven histamine H₁ inverse agonism and prolonged sedation. However, recent results have caused this link to come under scrutiny. A study by Stahl in 2008 revealed that many H₁ ligands that demonstrate prolonged sedative actions are given in amounts that significantly exceed the necessary concentrations to effectively target H₁ receptors. Amitriptyline and doxepin both have H₁ inverse agonism as their most potent property, yet amitriptyline is dosed at 400x its H₁K_D(Stahl, 2008). At their pharmacological dose, amitriptyline and doxepin should be considered dirty drugs, as they can target serotonin and norepinephrine transporters, muscarinic M₁, Alpha₁, and serotonin 2_A receptors. Of these antihistamines with a mixed pharmacology, doxepin is considered to be the most selective, demonstrating H₁ selectivity of greater than two orders of magnitude(Stahl, 2008). By giving doxepin in a low dose of 1-6 mgs, the long-term sedation associated with antihistamines has been eliminated, while the soporific qualities associated with H₁ inverse agonism remain. This result has been confirmed in two separate clinical trials, which will be discussed later, and seems to suggest that selective H₁ inverse agonists do not exhibit the prolonged sedation traditionally associated with antihistamines(Roth et al., 2007; Scharf et al., 2008).

The body's ability to sleep is controlled by a variety of wake and sleep promoting neurotransmitters and hormones that are released in a tightly regulated manner to match circadian rhythms(Stahl, 2008). This balance between wake and sleep promoting compounds can easily be perturbed, leading to excesses in wake-promoting neurotransmitters and causing insomnia. Wake-promoting neurotransmitters include histamine, acetylcholine, norepinephrine, serotonin, and the peptide orexin. Interestingly, the tuberomammillary nucleus is the location where histaminergic neurons arise and a location where these additional pathways converge. Because of this, the TMN is considered to be one of the most critical brain regions for arousal(Stahl, 2008). The litany of wake-promoting compounds, is balanced primarily by the sleep promoter GABA. A second thalamic region called the ventrolateralpreoptic area (VLPO) has projections into the wake-promoting brain centers, allowingGABA to exert its effects on each wake-promoting neurotransmitter system. Effects on histaminergicneurons include 3 types of interaction with varying GABA sensitivities that have been identified s (Haas et al., 2008; Stahl, 2008). Histamine neurotransmission displays an obvious link to circadian rhythm, as concentrations wax during high activity levels and wane during sleep periods. This has been observed in fish, monkeys, rodents, and humans, suggesting that histamine levels are critical to governing the sleep-wake cycles across species (Haas et al., 2008).

Insomnia is characterized by a state of hyperarousal, and in the case of chronic insomnia is hypothesized to occur during the day and night. Perturbations of this nature can be extremely disruptive to a patient as they cannot sleep at night and are unable to make up for lost sleep during the day(Stahl, 2008). Treatments for insomnia must either

inhibit wake-promoting neurotransmitters, especially histamine, but also including epinephrine, norepinephrine, acetylcholine, and serotonin, or act by enhancing the inhibitory effects of GABA.

Traditional therapeutics for insomnia focuses on the GABA pathways to suppress all wake-promoting regions of the brain. These approaches not only produce excessive sedation, but also can be dangerous when used incorrectly; as is the case with barbiturates. Positive allosteric modulators of GABA, which bind and potentiate the effects of GABA, such as benzodiazepines and zolpidem (Ambien) are the most commonly prescribed current treatments(Stahl, 2008). However, these newer ligands are not perfect. The half-life of the compound should not extend past the duration of sleep. If it does, the compound can accumulate in the body and cause severe sedation or present with a “hangover” effect where sedation is carried into the next day. Neither of these are desired pharmacological properties and some severe cases of side effects have been reported for zolpidem. Side effects range from sleep eating, talking, walking, and even driving have been reported. More severe side effects such as temporary amnesia, ataxia, hallucinations, reduced inhibition, and increased sexual libido have also been observed. Prolonged use of Ambien has shown addictive properties and has significant abuse potential(Hoque& Chesson, 2008)

By taking the alternate route and suppressing wake-promoting neurotransmitters, it is possible to target one wake-promoting brain region at a time. The selective H₁ inverse agonist doxepin is able to fill this niche. As mentioned previously, low-dose doxepin has been show to be extremely effective in the treatment of insomnia and does not possess the dramatic side effect profile of Ambien. In fact, double-blind studies

showed that doxepin had a side effect profile less than placebo and produced no next day sedation(Roth et al., 2007; Scharf et al., 2008).These results strongly suggest that selective H₁ inverse agonists are efficacious in the treatment of insomnia and seem to eliminate or at least dramatically lessen the side effect profile of other sleep aids.

Recent advances in imaging techniques, particularly positron emission tomography (PET) studies have allowed for real-time monitoring of neurotransmission within the human brain. The development of a¹¹C-doxepin allowed this technique to be applied to the histaminergic system and comparisons to be drawn between patients with varying behavioral and pathological disorders. A review of these studies was undertaken, comparing histaminergic neurotransmission in control patient groups against those that were aging, presenting with various stages of Alzheimer's disease, depression, schizophrenia, and epilepsy (Yanai & Toshiro, 2007). Each patient group will be addressed briefly here.

In the aging brain, it has been well documented that attention, learning, and memory decline in humans and animals. Senescence-accelerated mice, used as a model for the aging brain, demonstrate significant age-related deficits in passive avoidance tests. Interestingly, the administration of an H₃ antagonist thioperamide markedly improved the results for the same mice in avoiding the constant current and voltage shocks in the passive avoidance tests (Meguro et al., 1995). H₃receptors are autoreceptors that provide feedback inhibition to prevent excessive histamine release, blocking these receptors will drastically increase histamine neurotransmission. Thus, increases in histaminergic neurotransmission appear to improve memory and cognition significantly in non-human subjects(Meguro et al., 1995; Haas et al., 2008). It has been

established that the concentration of histamine metabolites in CSF and histamine levels in the human brain increase with age, suggesting a possible disconnect between histamine release and neurotransmission. In keeping with this, PET studies reveal a pronounced reduction in H₁R binding sites in elderly patients (Yanai et al., 1992; Yanai & Toshiro, 2007). It is hypothesized that the excessive release of histamine is able to downregulate the available H₁R population, resulting in a decrease in overall histaminergic neurotransmission and explaining the detrimental effects on memory and cognition observed in murine studies (Haas et al., 2008). The downregulation of H₁R's by histamine is also firmly established, being demonstrated in guinea pigs by Quach et al. in 1991.

Alzheimer's disease (AD) is traditionally characterized by deficiencies in neurotransmission of the cholinergic neurons of the brain. However, deficiencies in neurotransmission have also been observed in cholinergic receptors, both muscarinic and nicotinic subtypes, and also in acetylcholinesterase levels. Autopsied human brains have also been examined to help unravel the etiology of AD, they have revealed the characteristic neurofibrillary tangles in hypothalamus and reported a loss of large histaminergic neurons in the TMN (Nakamura et al., 1993). Thorough analysis by Schneider et al. in 1997 reported that the levels of HDC and choline acetyltransferase, the enzymes responsible for the synthesis of histamine and acetylcholine respectively, were drastically reduced in AD patients. Additional reports suggest that histamine levels in the brain are reduced in patients with AD (Panula et al., 1998).

The use of PET imaging in conjunction with ¹¹C-doxepin examined the levels of H₁R expressed in the brains of mild to severe AD patients and compared them with

age-matched control groups. A decrease in H₁R brain density was observed that was proportional to the severity of AD. Despite its limited scope, this study was the first to establish deficits in histamine neurotransmission in the brains of living AD patients. The study concludes that disruption of histamine neurotransmission and the death of histaminergic neurons could play a significant role in the etiology of AD (Higuchi et al., 2000; Haas et al., 2008; Yanai & Toshiro, 2007)

Depression is a psychiatric disorder characterized by alterations in the patients' normal behavior patterns. This can manifest as disturbances in sleep, appetite, and/or physical potential. Symptoms include prolonged feelings of helplessness, unnecessary guilt, extreme fatigue, insomnia or excessive sleep, and difficulty concentrating. Given the vast array of symptoms, some of which are contradictory (sleep/wake cycles), it is perhaps unsurprising that an exact mechanism for the etiology of depression has yet to be produced (Yanai & Toshiro, 2007). Regardless, it has long been established that many antipsychotic drugs possess strong H₁ receptor affinity. In fact, chlorpromazine and amitriptyline, used clinically as first generation treatments for schizophrenia and depression respectively, were originally labeled as "antihistamines". Advances in molecular biology, such as receptor cloning and expression, later showed chlorpromazine acted by blocking dopamine D₂ receptors and that amitriptyline treated depression by blocking serotonin and norepinephrine transporters (Stahl, 2008). Nevertheless, strong evidence remains for a role of H₁ receptors in the etiology of depression.

It is interesting to note that many of the symptoms associated with depression, such as disturbances in sleep, appetite, and physical potential can be linked to the

functions of the histaminergic neuronal system. Loss of histamine or histamine receptors has also been established as an animal model for human depression (Haas et al., 2008). Despite this knowledge, there is currently little investigation into the possible role of histamine receptors in depression. As of 2007, only one human PET study examining ^{11}C -doxepin binding in the brain of depressed patients has been performed (Yanai & Toshiro, 2007; Haas et al., 2008). Results were compared between patients, who had completed a self-rating depression scale to assess the severity of their depression, and healthy, age-matched patients. Data examined from 10 depressed patients showed a strong correlation between the severity of the depression and a reduction in H_1 binding sites found in the frontal, temporal, occipital cortex, and the cingulate gyrus. (Yanai & Toshiro, 2007) Although preliminary, these results seem to suggest a possible role for histamine and histamine receptors in the etiology of depression. Further studies, with anti-depressant naïve patients, must be undertaken to validate this hypothesis.

Histaminergic neurons have also been implicated in schizophrenia. In murine methamphetamine induced schizophrenia models, blockade of H_1 receptor neurotransmission has been shown to attenuate changes in animal behavior (Yanai & Toshiro, 2007). Schizophrenic patients demonstrate a pronounced increase in the levels of N-tele-methyl-histamine, a histamine metabolite, in their CSF. Upon imaging the schizophrenic human brain with PET, Iwabuchi et al. demonstrated a significant decrease in H_1 receptor density in the frontal, temporal, occipital, and cingulate cortices, as well as in the striatum and thalamus (Haas et al., 2008; Yanai & Toshiro, 2007).

Therapeutic Use of Histamine Ligands

Histamine H₁ receptors have been linked with the weight gain associated with atypical antipsychotics, specifically olanzapine and clozapine, in a number of publications (Kirk et al., 2009; Deng et al., 2009; Reynolds and Kirk, 2010).

Unfortunately, this literature is inundated with indirect observations based largely upon the affinity of atypical antipsychotics for serotonergic, muscarinic, dopaminergic, and histaminergic receptors. These papers report that H₁ antagonism alone is unlikely to explain the weight gain observed with these drugs. As stated in Reynolds and Kirk (2010),

“These studies (demonstrating circumstantial H₁ receptor involvement) do not, however, exclude effects on histamine systems being secondary to, or in addition to, 5-HT_{2c} receptor antagonism.”

This quote demonstrates the consensus in the literature, that H₁ receptors may play a role in atypical antipsychotic associated weight gain, but there is scant evidence that H₁ receptors are solely responsible for this effect.

A thorough study performed by Stephen Stahl (Stahl, 2008), demonstrated that one of the original tricyclic antidepressants, doxepin, possesses a significant H₁ receptor selectivity (greater than two orders of magnitude) when compared to serotonin and norepinephrine transporters, muscarinic M₁, alpha₁, and 5HT_{2A} receptors. However, the dose required to treat depression is large enough to impart a “dirty pharmacology”; meaning doxepin is able to target serotonin and norepinephrine transporters in addition to H₁ receptors. In the same paper, Stahl demonstrates that lower doses (1-6 mg vs. 150-300 mg for antidepressant treatment) of doxepin, which specifically target H₁ receptors at the aforementioned lower dose, acts as a novel hypnotic that is extremely effective in the treatment of insomnia (Stahl, 2008). Stahl eloquently demonstrates that

many first generation “antihistamines” that display long-term sedation, including diphenhydramine (Benadryl) and doxylamine (the sedating ingredient in Nyquil), are dosed far beyond the amount that would selectively target H₁receptors. At the administered doses, both compounds have significant anti-muscarinic effects that could easily account for the excessive next day sedation observed with these compounds. It is significant to note that next day sedation was not observed during the clinical trials performed with low-dose doxepin (Roth et al., 2007; Stahl, 2008).

Clinical trials have been undertaken with low-dose Doxepin for the treatment of insomnia and the results have been quite positive. In a trial of elderly insomniac patients using 1-6mg of doxepin, all patients showed significant ($p < 0.001$) improvement in wake time after sleep onset, total sleep time, and overall sleep efficiency (Scharf et al., 2008). A second study examining the effects of similar doses in adults (ages 18-64) with primary insomnia demonstrated similar results. 1, 3, and 6 mg doses of doxepin produced improvements in objective and subjective sleep maintenance and duration up until the final hour of the night (Roth et al., 2007). Both studies reported side effects that were comparable or less than the placebo and there were no reported anticholinergic effects, memory impairment, or next day hangover(Roth et al., 2007; Scharf et al., 2008).This is an intriguing result, suggesting selective histamine H₁antagonism is a novel therapeutic route for the treatment of insomnia, which appears to overcome the limitations of many sleep aids currently on the market.

Current research suggests that histamine plays a critical role in the CNS by acting as an all-natural anti-convulsive agent (Haas et al., 2008; Yanai & Toshiro, 2007; Chen et al., 2003). Alpha-fluoromethylhistidine, an inhibitor of histidine decarboxylase, has

been shown to enhance the severity of clonic convulsions, and accelerate seizure development in mice where pentylentetrazol (PTZ) was used to induce a seizure model. This PTZ-induced murine seizure model has been recognized as an effective model for human absence epilepsy, as well as myoclonic or generalized tonic-clonic seizures (Chen et al., 2003). Interestingly, histamine and selective H₁ agonists act as neuroprotective agents, while mepyramine and ketotifen, which are H₁ inverse agonists, have been shown to increase focal and general epileptic fits in patients (Yanai & Toshiro, 2007). Diphenhydramine, a similar brain-penetrating H₁ antagonist/inverse agonist, has a similar effect when given via an intraperitoneal injection; it exacerbates epileptic fits (Haas et al., 2008). Local histamine concentrations have been shown to increase around the foci of complex partial seizures in order to prevent their spread (Chen et al., 2003).

These studies strongly emphasize the role of brain histamine as a protective factor against the formation, spread, intensity, and duration of seizure activity. It is interesting that our lead compound (-)-*trans*-PAT is also a selective, brain penetrating, H₁ agonist. The literature failed to mention what “selective” means from a GPCR standpoint. However, based upon the literature shown above, PLC/IP inverse agonists diphenhydramine, mepyramine, and ketotifen aggravate seizure development, it is reasonable to infer that the selective pathway they are referring to is the adenylyl cyclase/ cAMP pathway. This is the same pathway where our lead compound is an agonist and could represent an additional therapeutic role for (-)-*trans*-PAT.

Previously Established Molecular Determinants for H₁ Receptors

When the biogenic amine systems were originally characterized by *o*-phthalaldehyde fluorescence chemistry in the 1960's, the brain localization of serotonin

and catecholamine systems became the focus of neuroscientists everywhere (Haas et al., 2008; Haas and Panula, 2003). The litany of neuropsychiatric disease states that are characterized by these receptor systems is extensive and intensive research was undertaken on these neurotransmitter systems. However, histamine was not identified as a neurotransmitter at this time, as the widespread amino acid spermidine cross reacted with pthalaldehyde, obscuring the location of histaminergic neurons. Eventually, histamine received its due and was identified as a neurotransmitter, this was verified individually by Panula's group in Washington and Wada's in Osaka in 1984 (Panula et al., 1984; Wada et al., 1984). The belated recognition of histamine as a neurotransmitter, allowed approximately twenty extra years of research to be performed on the catecholnergic and serotonergic systems before work was even begun on histamine. Since then, large strides have been made in characterizing the four subtypes of H₁ receptors and the g-proteins with which they are associated. Much work has been placed into identifying the amino acid residues that are critical to the binding and function of histamine ligands. These critical amino acid residues are called molecular determinants and the established literature for the more well known H₁ compounds will be discussed here.

It is important to discuss the previously established loci that have been identified as important for H₁ ligand binding in the literature before delving into novel data. As previously mentioned, the radioligand ³H-mepyramine has long been used to characterize histamine H₁ receptors. Keeping with this, there is a litany of data in the literature about the molecular determinants involved in the binding of mepyramine and the endogenous agonist histamine. Comparing the molecular determinants involved in

the binding of mepyramine, an inverse agonist, and histamine, a full agonist, will provide a solid framework and a point for comparison in the investigation into the binding of PAT scaffold in TMD 5,6, and 7.

It is pertinent to begin the discussion of H₁ receptor binding by discussing the endogenous agonist, histamine. Histamine, whose chemical name is imidazoylethylamine, creates strong contacts with polar amino acid residues in TMD 5, as mentioned briefly above. However, there is a stronger interaction that is conserved across aminergic receptors and is critical to ligand binding, D3.32; this aspartic acid residue forms an ionic bond with the protonated amine moiety of aminergic ligands (Smit et al., 1999). D3.32 appears to be the most critical residue involved in ligand binding to the H₁ receptor, as both antagonists and agonists require this ionic interaction for proper binding (Smit et al., 1999; Gillard et al., 2002; Jongejan & Leurs, 2005). Radioligand studies using ³H-mepyramine and ³H(-)-*trans*-PAT in our own lab indeed confirm this result (Fang, Travers, and Booth., 2009 pre-publication). The residues T5.42 and N5.46 play a role in binding histamine to TMD 5, as mentioned briefly earlier, these contacts are important as TMD 5 connects to the ICL₃, which is responsible for G-protein coupling and subsequent signal transduction. Out of the TMD 5 residues, N5.46 possesses the strongest interaction with histamine and demonstrates a 40-fold reduction in affinity when an alanine is inserted in its place (Jongejan & Leurs, 2005; Booth et al., 2008; Fang, Travers, and Booth., 2009 pre-publication).

Two additional residues in TMD 5, K5.39 and T5.42, are well established as molecular determinants for the binding of histamine. T5.42A is postulated to have a stabilizing hydrogen bond with N5.46A that keeps the receptor in the proper

conformation to bind histamine. Several H₁ receptor models have demonstrated this hydrogen bond, however a direct interaction with the imidazole ring of histamine has not been ruled out. The affinity for histamine is reduced at T5.42A by approximately ten-fold (Jongejan & Leurs, 2005; Fang, Travers, and Booth., 2009 pre-publication). K5.39A interacts directly with histamine at the N_π of the imidazole ring (Jongejan & Leurs, 2005; Booth et al., 2008). Mutating this residue to a non-functional alanine residue resulted in an 8-fold reduction in histamine affinity, illustrating that K5.39 is important for maintaining proper histamine binding, but the interaction is not quite as strong as N5.46 or D3.32 (Fang, Travers, and Booth., 2009 pre-publication). There is evidence for an aromatic π-π stacking interaction of the imidazole ring with F6.55, which causes about a 1000-fold reduction of histamine affinity (Wieland et al. , 1999; Jongejan & Leurs, 2005). Histamine makes its strongest HH₁R interactions with polar residues TMD's 3 and 5 and appears to have a strong aromatic interaction in TMD 6. Interestingly, F6.55A produces a large effect on histamine's potency, while nearby aromatic residues associated with the rotamer toggle switch and antagonist binding (F6.52) have little effect on histamine's ability to activate the receptor (Wieland et al. , 1999; Bruyesters et al., 2004; Jongejan & Leurs, 2005).

Mepyramine, also known as pyrilamine, is the traditional radiolabel that has been used to identify H₁ receptors. It is an inverse agonist at H₁ receptors, with a high affinity and a strong inverse agonist response. Due to its availability as a radioligand ³H-mepyramine has been studied at a wide array of point mutations and a great deal is known about its binding. D3.32, the highly conserved aspartic acid residue in TMD 3, is again critical for ligand binding. Mutation to an alanine results in the complete

abolishment of receptor binding, demonstrating once again that the ionic interaction with the protonated amine is necessary for any ligand, agonist or antagonist, to bind to this aminergicreceptor(Wieland et al. , 1999; Bruysters et al., 2004; Jongejan & Leurs, 2005; Fang, Travers, and Booth., 2009 pre-publication). By comparing the structure and function of histamine and mepyramine, one can and should conclude that the similarities in binding end there. Histamine is a small, polar, heteroaromatic compound with few degrees of rotational freedom. Mepyramine, while possessing the critical protonated amine pharmacophore, is a much larger, bicyclic compound, with many rotatable bonds that provide the ligand with significant flexibility.

An early H₁ model, with homology to bacterial rhodopsin, predicted that mepyramine would interact with aromatic residues in TMD 4 and 6(Wieland et al. , 1999). In contrast to this, histamine is known to form its strongest contacts (D3.32 aside) with a series of polar residues in TMD 5. The residues originally predicted to be significant in the binding of mepyramine were designated Trp¹⁶⁷ (W4.56), Phe⁴³³ (F6.52), and Phe⁴³⁶ (F6.55). These three predicted interactions turned out to be conserved residues across all known H₁ receptor sequences, suggesting they play some integral role in H₁receptor binding and/or activation(Wieland et al. , 1999). While the Ballesteros numbers assigned here correspond to the same amino acid in the human receptor, the original model was based upon the guinea pig H₁sequence so the sequence numbering does not exactly match the human sequence. In the human receptor, these three residues correspond to Trp¹⁵⁸, Phe⁴³², and Phe⁴³⁵, respectively. By referring to these positions by the Ballesteros number, rather than their sequence

number, it is possible to avoid the confusion that occurs when cross-referencing results across differing species.

Invoking saturation binding assays with the alanine mutants of these identified residues allowed Wieland et al. to confirm their hypotheses through experimental results. When W4.56 was mutated to an alanine, a complete loss of binding was observed for ^3H -mepyramine. This strongly suggests that this position and residue are critical to the binding of this H_1 inverse agonist and has been confirmed by mutagenesis studies at the HH_1R as well (Fang, Travers, and Booth., 2009 pre-publication)(Jongejan & Leurs, 2005). It is interesting to note there have been no residues identified in TMD 4 that have been directly linked to histamine binding, suggesting there are different binding modes for H_1 agonists and inverse agonists.

The F6.52 and F6.55 residues also were predicted to interact strongly with H_1 inverse agonists and the ^3H -mepyramine saturation studies revealed similar results. The F6.52 position is located at the rotamer toggle switch in TMD 6, given its role in receptor activation, it is logical to conclude F6.52 would have strong interactions with H_1 ligands. F6.52A saturation isotherms revealed that ^3H -mepyramine was unable to bind appreciably (no difference when compared to mock transfections) to the F6.52A mutated H_1 receptor. This result has been confirmed at the HH_1R by our lab and several others, indicating F6.52 is critical for the binding of antagonists to the human H_1 receptor (Bruysters et al., 2004; Bakker et al., 2004; Fang, Travers, and Booth., 2009 pre-publication). An intriguing result came from Wieland's same paper, when F6.52A was examined in the inositol phosphate functional assay. Despite an inability to bind ^3H -mepyramine, F6.52A produced a functional response that was identical to the WT

receptor when histamine was administered as the agonist(Wieland et al. , 1999); lending further credence to the hypothesis of at least two unique binding pockets, one for agonists and one for inverse agonists, at the H₁ receptor.

The F6.55 residue did not produce as dramatic a decrease in binding as the previous two mutations, however in the case of the guinea pig H₁ receptor the affinity (K_D) was still reduced from approximately 1nM at the WT to > 15 nM at F6.52A (Wieland et al. , 1999). When the HH₁R is examined, the reduction is slightly lessened, yielding an affinity of 4.76 ± 0.8 nM and a P-value of 0.011(Booth Lab unpublished data). F6.55 does seem to have relatively strong interactions with mepyramine, as indicated by the statistically significant p-value, however these aromatic interactions are weaker than W4.56 and F6.52.

Having mentioned “second generation” histamine antagonists briefly, a discussion of their unique binding profile is warranted here. In general, second generation antihistamines are more selective for the H₁ receptor and lessen the severity of the sedation commonly associated with first generation drugs (Wieland et al. , 1999). The decrease in side effects was due to more selective H₁ targeting, and a simple structural change that alleviated much of the sedative action possessed by these ligands. The introduction of a polar carboxylic acid moiety into the ring structures of triprolidine and hydroxyzine, resulted in the development of acrivastine and cetirizine, respectively. These ligands were able to decrease the amount of drug that crossed the highly lipophilic blood-brain barrier, preventing sedation from occurring.

The introduction of the carboxylic acid moiety had a second impact on the overall profile of these new ligands, it created a second strong contact point for anchoring the

ligand to the H₁ receptor. As predicted by the modeling studies performed by Wieland et al., the carboxylic acid of cetirizine and acrivastine has an ionic interaction with the basic side chain of K5.39. A litany of studies confirmed this result, with mutagenesis data indicating that the affinity of triprolidine (parent compound) is not affected by K5.39A, while the affinity of acrivastine was reduced fifty fold (Wieland et al. , 1999; Jongejan & Leurs, 2005).

H₁ GPCR Dimerization

Based upon the current evidence available, it is now relatively well accepted that GPCR's have the ability to exist as monomers, dimers, and even higher order oligomers (Gurevich and Gurevich, 2007). The diverse library of ligands produced by our chemistry lab has provided unique stereochemical probes to carry out a wide array experiments to help characterize the structure and function of the human histamine H₁ receptor. The ligand called (-)-*trans*-PAT has been shown to activate the AC/cAMP pathway through G_{αS}, as well as being an inverse agonist at G_{αQ}. (-)-*cis*-PAB has been shown to activate G_{αQ} and the PLC second messenger pathway (Fang, Travers, and Booth., 2009 pre-publication). These two ligands alone provide very interesting tools for probing the molecular determinants involved in activation and signaling of the HH₁R. However, previous work from our lab and its collaborators has determined that (-)-*trans*-PAT binds to a specific subpopulation of H₁ receptors. Upon further investigation, it was proposed that (-)-*trans*-PAT preferentially labeled dimers while the traditional radioligand ³H-mepyramine was able to label both monomers and dimers (Booth et al., 2001,2004).

Currently, there are two dominant hypotheses about how GPCR dimers and oligomers are formed. These are contact dimers (B) and domain-swapped dimers (C)

as illustrated in figure 1-8(adapted from Booth et al., 2004). It is proposed that in contact dimers certain transmembrane domains interact, through mainly hydrophobic residues, to form the necessary stabilizing interactions while maintaining their individual binding pockets. In domain-swapped dimers, two full transmembranes of each receptor are exchanged forming two complete chimeric receptors, each of which maintains a binding pocket for the ligand.

Based upon a clever series of mutagenesis experiments it was determined that the ligand (-)-*trans*-PAT prefers to bind to domain swapped H₁ receptors (Booth et al., 2004). Coexpression of two mutations, D3.32A and F6.52A, both of which individually result in a complete loss of radioligand binding, were able to regenerate a binding site for both ³H-(-)-*trans*-PAT and ³H-mepyramine. This regenerated site possessed an identical K_D for the two radioligands at the WT HH₁R, however it possessed a significantly lowered B_{MAX}. At the WT receptor, mepyramine possessed a B_{MAX} that was 7x larger than (-)-*trans*-PAT. The differences in B_{MAX} between the two ligands are not a cause for concern and have been previously reported, along with the fact (-)-*trans*-PAT is known to bind to a subset of H₁ receptors, while mepyramine is able to label all H₁ receptors (Booth et al, 2001).

Coexpression of D3.32A and F6.52A significantly lowered both B_{Max} values to 0.33 pMol/mg protein, a 10-fold reduction for PAT and nearly 100-fold reduction for mepyramine. Actual B_{MAX} and K_i values are listed below in table1-1 (Booth et al, 2004). When the coexpressed mutant is considered, it stands out that the B_{max} values are identical. This suggests that the two ligands that normally occupy different cross sections of the H₁ receptor population, are now sharing the same unique binding site.

Regeneration of binding with two non-functional mutations is quite significant, because it can only take place through dimerization, and more specifically domain-swapped dimerization.

Domain-swapped dimers are similar to chimeric receptors in that an individual receptor subunit is composed of helices from two separate receptors. Because of this unique interaction, it is possible to quarantine the non-functional point mutations into a single subunit, leaving the other half of the dimer unperturbed. To demonstrate this point, a schematic from this paper is illustrated below in Figure 1-9 (Bakker et al., 2004). Possible receptor combinations of contact and domain swapped dimers are displayed, with the TMD's containing the mutation highlighted in gray and non-binding receptors marked with an X. Receptors that bind ligand are marked with an L through their center. Contact dimers have no chance of forming a functional receptor, as one of the mutations is always present on each side of the dimer. Because of their unique structure, domain swapped dimers are able to place both mutations in one half of the dimer, allowing the other half to bind radioligand normally. This argument is strengthened by the fact that the B_{Max} values of the co-mutation are greatly reduced, from wild type (WT), suggesting that extenuating circumstances are necessary to recreate a binding site. In this case, the receptor must assemble as a domain-swapped dimer with the caveat that TMD's 3 and 6 must be from different receptors and be trafficked to the membrane surface.

Current GPCR Theory

Our understanding of GPCRs has come a long way since the lock and key, bimodal switch, and law of mass action models for GPCR activation were first proposed. Significant discoveries such as constitutive activity, inverse agonism, and

allosterism have quickly forced GPCR models to become increasingly complex. Culminating in the extended ternary complex model and the cubic ternary complex model, proposed by Samama et al in 1993, and Weiss et al in 1996, respectively (Christopolous & Kenakin, 2002). The extended ternary complex model was significant because it addressed the possibility of allosterism and accounted for constitutive activity. The cubic ternary complex model is more sophisticated from a thermodynamics standpoint, however its bulky nature significantly hinders its laboratory applications. Recent evidence suggests that the GPCR model may need to be adapted yet again. Modeling results and recent data suggest that there is not one agonist, basal, or inverse agonist conformation of the receptor, instead there are thousands. It seems that every ligand induces a unique receptor conformation, with unique functional properties (Kobilka & Deupi, 2007; Bhattacharya et al., 2008). Each of these models will be discussed in detail in the coming sections.

Law of Mass Action and Early GPCR Models

The simplest GPCR models followed enzyme kinetics and ion channels, suggesting that an agonist bound to a receptor, causing a physiological response in the process. This concept is called the law of mass action and was defined by the formula listed below. This equation was governed by the equilibrium association constant K_a , which governs the association and dissociation of the ligand from the receptor. A represented the agonist molecule, R the receptor, and AR the ligand-receptor complex as demonstrated below in figure 1-11.

The discovery of intracellular G-proteins forced this model, which was originally designed for ion channels, to adapt. At this time it was believed that the agonist bound

to the receptor, which could isomerize into an active form, which was able to function or couple to a G-protein. This adaptation is illustrated below in figure 1-12.

Ternary Complex Model

Further understanding of GPCRs demonstrated that an agonist could bind to a receptor, yet produce no functional effect if it was not attached G-protein. This observation led to the original ternary complex model, proposed by DeLean et al in 1980. It is significant to note that the only active species in this model is the ARG complex, indicating that the receptor must be complexed with a ligand and the G-protein in order to exert its function (Christopolous & Kenakin, 2002). The ternary complex model is illustrated in figure 1-13.

Extended Ternary Complex Model

When constitutive activity was first demonstrated conclusively by Costa and Hertz in 1989, it was clear that the previous theories would not be able to describe the complex GPCR activation process accurately. Around the same time, it was shown that the binding of GTP to the G-protein (the critical activating step) resulted in a conformational change reducing the affinity of the receptor. Thus, receptors demonstrate differing affinities for both ligand and G-protein, depending upon which bound to the receptor first. This resulted in the emergence of cooperativity factors (α , β , and γ), which are constants that affect the equilibrium involved in agonist-receptor and receptor-G-protein interactions. The use of cooperativity factors allowed the equilibrium constants to take into account what species was able to bind to the receptor first. By incorporating the law of mass action and the ternary complex theory into one formula, and allowing for constitutive activation, Samama et al. were able to create the extended ternary complex model in 1993. This model expanded on the ternary complex model

with the addition of cooperativity factors and allowed the receptor to adopt an active conformation in a spontaneous, or agonist mediated manner before coupling to the G-protein.

This expanded model still uses the equilibrium constants K_A and K_G for the binding of the agonist A and G-protein G, to the receptor. It adds the equilibrium constant L for the isomerization of the receptor from the inactive R conformation, to the active R^* conformation. The cooperativity factors α , β , and γ have also been added as constants that modify these equilibrium constants. As mentioned above, the observation that agonist or G-protein pre-coupling was able to alter the binding affinity of the latter, necessitated that there be unique equilibrium constants for each transition in the model. For example, the equilibrium between the inactive R conformation and the R^* representing basal activity, would not be governed by an identical equilibrium as the AR to AR^* transition. The equilibria may be similar, but the binding of an agonist will alter the equilibrium constant L by some factor. This factor represented by α was termed a cooperativity factor. The incorporation of these cooperativity factors made the extended ternary complex model incredibly versatile and represented a significant leap forward in GPCR theory. There are additional complex models like the cubic ternary complex model and the quaternary complex model, which are more thermodynamically correct, yet both models are incredibly complex and become unwieldy in a laboratory setting (Christopolous & Kenakin, 2002). For these reasons, it has been the extended ternary complex model that has been used as the template for GPCR studies.

LITicon

The extended ternary complex model significantly advanced our understanding of the complex processes that govern GPCR binding and function. However, as

technology has continued to progress there have been findings that call into question even the basic tenants of the ternary complex model. The extended ternary complex assumes there are only several conformations that a receptor must choose. Making this assumption allowed researchers to create a model that described their experimental results and helped elucidate the major steps in G-protein activation. Yet, the variety of functional states available to GPCR's including full, partial, neutral, and inverse agonism, as well as allosteric agonists, positive and negative allosteric modulators, and ago-allosteric modulators seems to suggest a litany of unique conformations exist. Describing all of these functional properties in the context of the ternary complex model yields the quaternary complex model that was alluded to earlier (Christopolous & Kenakin, 2002). This model becomes unwieldy rather quickly, with equilibrium constants that can have up to seven unique cooperativity factors. It should be mentioned that despite its unwieldiness, the quaternary ternary complex model is able to describe allosteric receptor interactions accurately, with unique equilibrium constants for each conformation.

Despite this incredible accomplishment, a question that needs to be addressed is whether or not agonists all induce an identical receptor conformation. A 2007 paper made use of a novel molecular modeling technique called LITicon, to address this question. LITicon is an acronym for Ligand Induced Transmembrane Rotational Conformational Changes. Traditional molecular modeling freezes the backbone of the transmembrane domains and allows free movement to the amino acid side chains to interact with the ligand. This artifact creates a litany of problems for extrapolating modeling to experimental results. First, the binding of a ligand becomes highly

dependent upon the crystal structure template that was selected. As defined by the extended ternary complex model, a ligand possesses different affinities for the active and inactive state of the receptor. It follows that the way the ligand binds, especially with frozen TMD backbones that restrict movement, will differ between the active and inactive crystal structures. This presents the researcher with an unavoidable choice that will bias their results.

Freezing the backbones of the helices would significantly hinder the movement of a receptor that is renowned for its dynamic nature and flexibility. If the backbones of the TMDs were frozen in GPCRs, there would likely be no observed constitutive activity, and one of the defining features of GPCRs would not exist; thus freezing the TMD backbones results in an unnatural environment for ligand binding. In addition, freezing the backbones prevents molecular modelers from observing ligand specific effects on molecular switches (Bhattacharya et al., 2008). Both the ionic lock and rotamer toggle switch require significant movement from TMDs that is difficult to replicate with a rigid helical backbone. The ionic lock between TMDs 3 and 6 is lost during the activation process as the helices pull away from each other (Prioleau et al., 2002; Shi et al., 2002; Kobilka & Deupi, 2007). The rotamer toggle switch is a more subtle movement that is governed by the proline residue 6.50. Upon activation, a series of stabilizing interactions is lost and the proline kink becomes the dominant factor in the TMD structure, causing a pronounced bending of the cytoplasmic end of helix 6 (Prioleau et al., 2002).

LITicon addresses these pitfalls associated with traditional molecular modeling and allows a ligand to determine the lowest energy receptor conformation. The process is begun by identifying the helices, or TMDs, that are perturbed during the docking

process. Once this process is completed and the ligand is located within the orthosteric binding pocket, each helix is rotated 180° in each direction. The energy of each rotational combination was then compared to the energy of the ligand-free receptor. The resulting differences in energy were tabulated for each conformation, and the lowest energy receptor-ligand complex was assumed to be the proper ligand binding conformation (Bhattacharya et al., 2008).

This technique produced several advantages over traditional molecular modeling, the most critical of which is a flexible backbone for each helix. Reducing the constraints on each backbone allows the formation and breaking of new hydrogen bonds, as the ligand and receptor move towards equilibrium. This results in more accurate modeling predictions and molecular determinants. It also allows the ligand-receptor complex to trigger molecular switches, potentially allowing this model to attain the golden fleece for molecular modeling, reliably predicting the functionality of ligands. An important caveat to this statement is that this model does not take into account G-protein coupling and therefore cannot predict functional selectivity. However, when the norepinephrine bound LITicon receptor conformation was used to select a series of 60 β_2 -AR agonists from a pool of 10,060 compounds, a 38% increase in success rate was observed when compared to a ligand naïve receptor (Bhattacharya et al., 2008).

The increased hit-rate for LITicon was not the only significant finding in this paper. When a diverse series of β_2 -AR ligands were examined using LITicon, an extremely interesting series of results was noticed. The ligands screened included the full endogenous agonist norepinephrine, the partial agonists dopamine, salbutamol, and catechol, and the inverse agonist ICI118551. Each ligand that was studied using

LITicon produced a unique receptor conformation, and induced changes in the receptor that fit its functional profile. Structures for these ligands can be found in figure 1-10.

These conformations will be briefly discussed here, and will exclude the redundant D3.32-amine interaction and instead focus on the remaining molecular determinants and the ionic lock and rotamer toggle switch. The full endogenous agonist norepinephrine showed strong hydrogen bonding interactions with a series of serine residues in TMD 5. These residues were S203, S204, and S207. When converted into Ballesteros numbers they correspond to 5.42, 5.43, and 5.46, all of which were implicated in the binding of norepinephrine through mutagenesis studies (Carmine et al., 2004; Bhattacharya et al., 2008). Interestingly, S204 and 207 were not initially located within the binding pocket of the receptor, but after rotating the helices in LITicon these strong hydrogen-bonding interactions were observed. There is an additional strong hydrogen bond that is observed with N293 (N6.55). To corroborate these findings both the rotamer toggle switch (RTS) and the ionic lock(IL) are perturbed by norepinephrine binding, suggesting correctly that this ligand should be a full agonist.

Dopamine, a partial agonist at β_2 -AR, was the next ligand examined. S5.43 and 5.46 again interacted with the *p*-OH group on the catechol ring. Yet, there was no longer an interaction between S5.42 and the *m*-OH on the catechol ring and no hydrogen bond with N6.55. Dopamine was able to disrupt the ionic lock, but only partially disrupted the RTS. The partial activation of the rotamer toggle switch was determined by an intact hydrogen bond between N7.45 and C6.47, and a lack of a hydrogen bond between W6.48 and M5.54 (Bhattacharya et al., 2008). Both of these interactions were observed with the norepinephrine bound receptor and further confirm that dopamine

and norepinephrine induce different conformations of the β_2 -AR. With only weak perturbations to the RTS, LITicon predicted dopamine to be a partial agonist at the β_2 -AR, confirming experimental results.

Salbutamol was docked using the LITicon method and was shown to disrupt the ionic lock, but not the RTS. This finding already hinted at a different receptor conformation, but a detailed assessment of the molecular determinants was necessary. Salbutamol made strong contacts with the three serines in TMD 5, but was unable to interact with N6.55, the residue closest to the RTS. The loss of this interaction prevented the hydrogen bonding pattern mentioned above that is indicative of RTS activation (Bhattacharya et al., 2008). With only the ionic lock disrupted, one would predict salbutamol to be a partial β_2 -AR agonist, just as is observed in vitro.

The weak partial agonist catechol, which is simply 1,2-di-hydroxy-benzene, was next to be examined. Since it was lacking the protonated amine moiety, there would be no ionic interaction to hold the ligand in the binding pocket. Instead, catechol interacts with S5.46 and N6.55 by hydrogen bonding to these residues. There was no observed disruption of the IL, and only a weak interaction at the rotamer toggle switch that is unable to replicate the hydrogen bonding patterns caused by norepinephrine (Bhattacharya et al., 2008). With the ionic lock unperturbed and only a weak interaction with N6.55, affecting the RTS it would be predicted that catechol would be a weak partial agonist at the β_2 -AR. This prediction mirrors catechol's function and demonstrates another unique receptor conformation.

The last ligand to be studied was the inverse agonist ICI115881. This compound made no contacts with TMD 5, and caused it to rotate in the opposite direction as the

full and partial agonists. It did form a hydrogen bond with N6.55, but it also hydrogen bonded to H6.58, a residue located only one helical turn below that residue. This two-pronged hydrogen bond was only observed with this inverse agonist and prevented the rotation of TMD 6 (Bhattacharya et al., 2008). With the ionic lock left intact and the RTS switch stabilized by the forked hydrogen bonds in TMD 6, the LITicon conformation predicted a less active receptor conformation for the salbutamol docked receptor. As an inverse agonist, this is exactly the effect salbutamol exerts on the β_2 -AR, it reduces the constitutive activity of the receptor.

As this paper demonstrates, it seems that each ligand creates a unique drug-receptor complex that is defined by the position and types of functional moieties on the ligand itself. This is in stark contrast to the ternary complex models, which propose a single receptor conformation for the inactive, active, and constitutively active states. It is more likely that GPCRs have a limitless number either of conformations that they can adopt at random or in the presence of a ligand. Ligands serve to stabilize specific conformations from this subset that are able to produce an observable and reproducible physiological effect. These comments are not meant to trivialize the extended ternary complex by any means, as it has been and remains critical to understanding the minutiae of GPCR ligand binding assays. To the contrary, this theory seeks to build on the concepts put forth in ternary models, while painting the most accurate picture of GPCR activation.

Goal of This Thesis

It is hypothesized that through a detailed characterization of the molecular determinants involved in ligand binding and function that a better understanding of the molecular events involved in H_1 GPCR functional selectivity can be obtained and

exploited for drug design purposes. The goal of these thesis studies is to determine which H₁ receptor amino acid residues are critical for PAT analog H₁ ligand binding, as well as selectively activating the AC/camp vs. PLC/IP signaling pathways. Investigating the mechanism of binding and activation for HH₁R's will provide valuable insight into future drug design for the treatment of psychiatric and neurological disorders. Insight into how ligands influence H₁ receptor activation of G-proteins is expected to aid design of efficacious drugs with predictable and fewer adverse side effects. Information learned about drug discovery targeting the H₁ GPCR can be applied to other related aminergic GPCRs (e.g., receptors for the neurotransmitters acetylcholine, dopamine, norepinephrine, and serotonin) with implications for both GPCR structure and function and drug discovery.

Aim #1: Characterization of the Structure Activity Relationships for PAT Analogue Binding at the Wild Type HH₁R

Characterizing the structure activity relationships of PAT analogues synthesized in our lab is crucial to guiding future syntheses and as a tool to guide our molecular modeling program. This aim means to determine the affinity of a variety of PAT derivatives at the WT HH₁R receptor, with a particular emphasis on stereochemistry. Examining the binding modes of these varying ligands will provide crucial structural information about the binding pocket of the HH₁R that will serve as a guide for future synthesis and molecular modeling experiments.

Aim #2: Characterization of the Role of Amino Acid Residue Y5.48 in Dimerization of the HH₁R and its Impact on Ligand Binding and Function.

This aim tests the hypothesis that the HH₁GPCR transmembrane domain (TMD) 5 amino acid residue Y5.48 is involved in receptor dimerization that affects ligand binding and/or activation of the receptor. The (-)-*trans*-(2S,4R)-PAT compound is known to bind

to domain-swapped dimers, and this aim addresses the possibility that Y5.48 is involved in the domain-swapped dimerization.

Aim #3: Characterization of the Role of HH₁ Residue Y7.53A in Ligand Binding and Activation Using Functionally Selective PAT Derivatives

Studies indicate that TMD 7 amino acid 7.53 plays a critical role in the signaling of the closely related 5HT_{2C} receptor. This aim focuses on elucidating whether or not this effect is specific to 5HT_{2C} receptors, or can be found in the HH₁R as well. This aim will determine whether or not a particular signaling pathway and/or a particular ligand are affected by this point mutation. A novel addition to this HH₁R investigation, is the concept of functional selectivity. In particular, the focus will be on the efficacy of histamine at Y7.53A, and the effects this mutation has on the ability of the HH₁R to couple to G_{αS} and G_{αQ}.

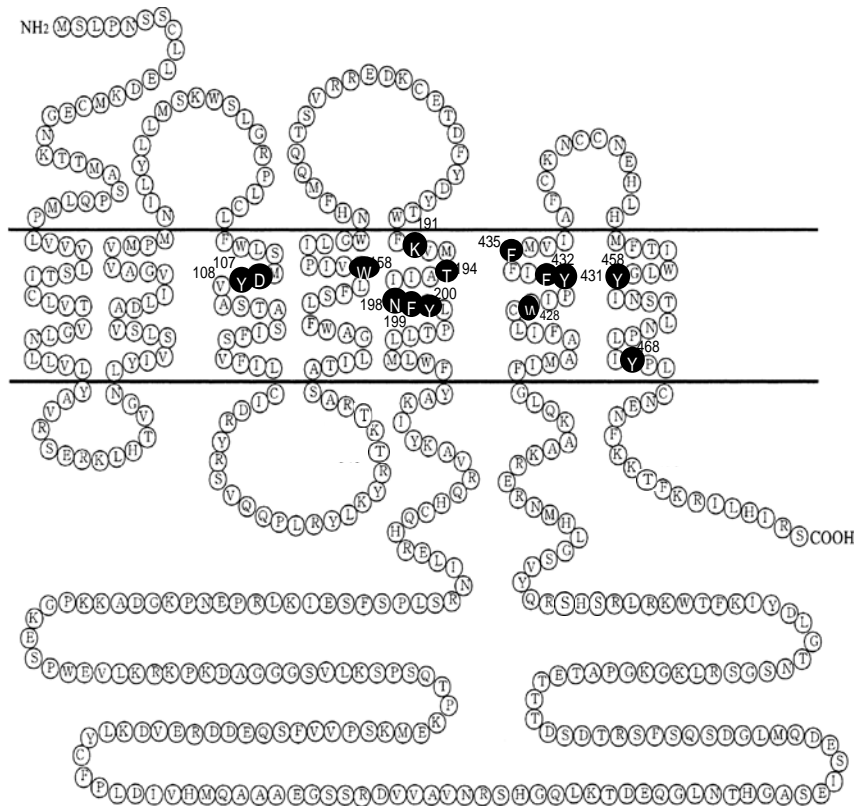


Figure 1-1. Generic structure of a GPCR.

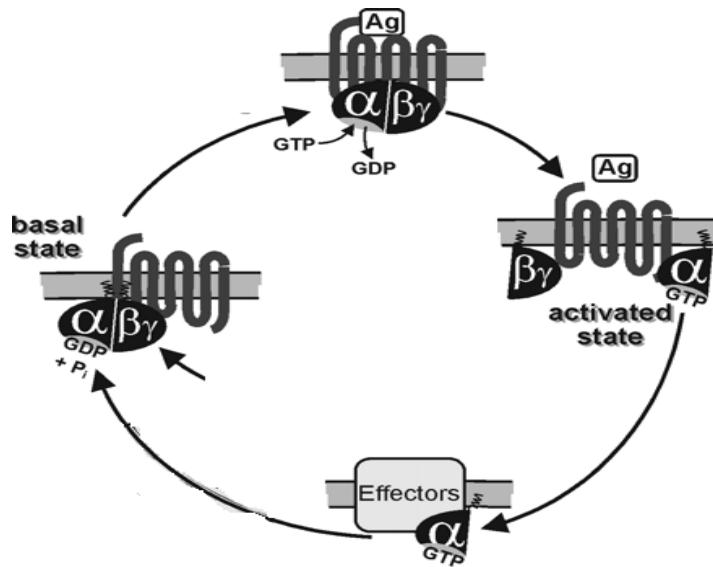


Figure 1-2. GPCR activation demonstrating guanine exchange.

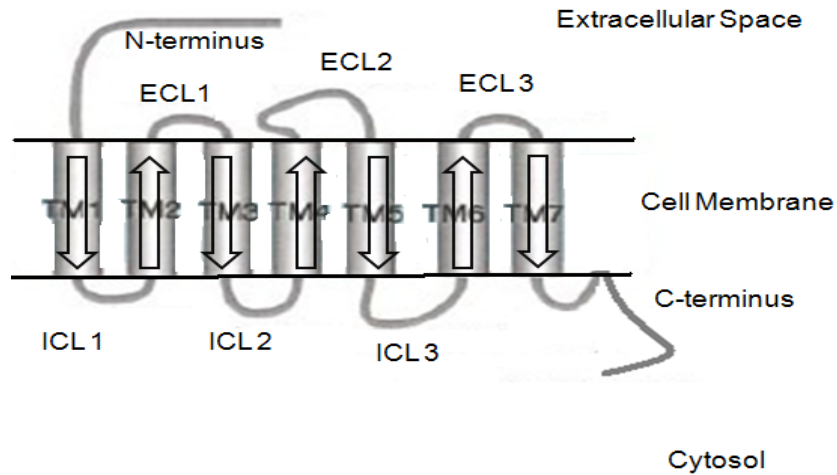


Figure 1-3. Ballesteros numbering proceeds as indicated by the arrows on the generic GPCR structure

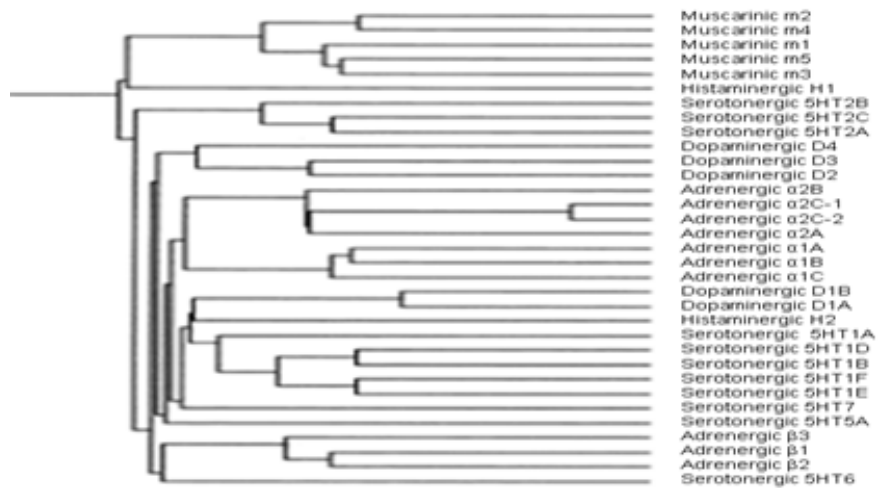


Figure 1-4. Phylogenetic tree for aminergic GPCRs that are closely related to the H₁ receptor.

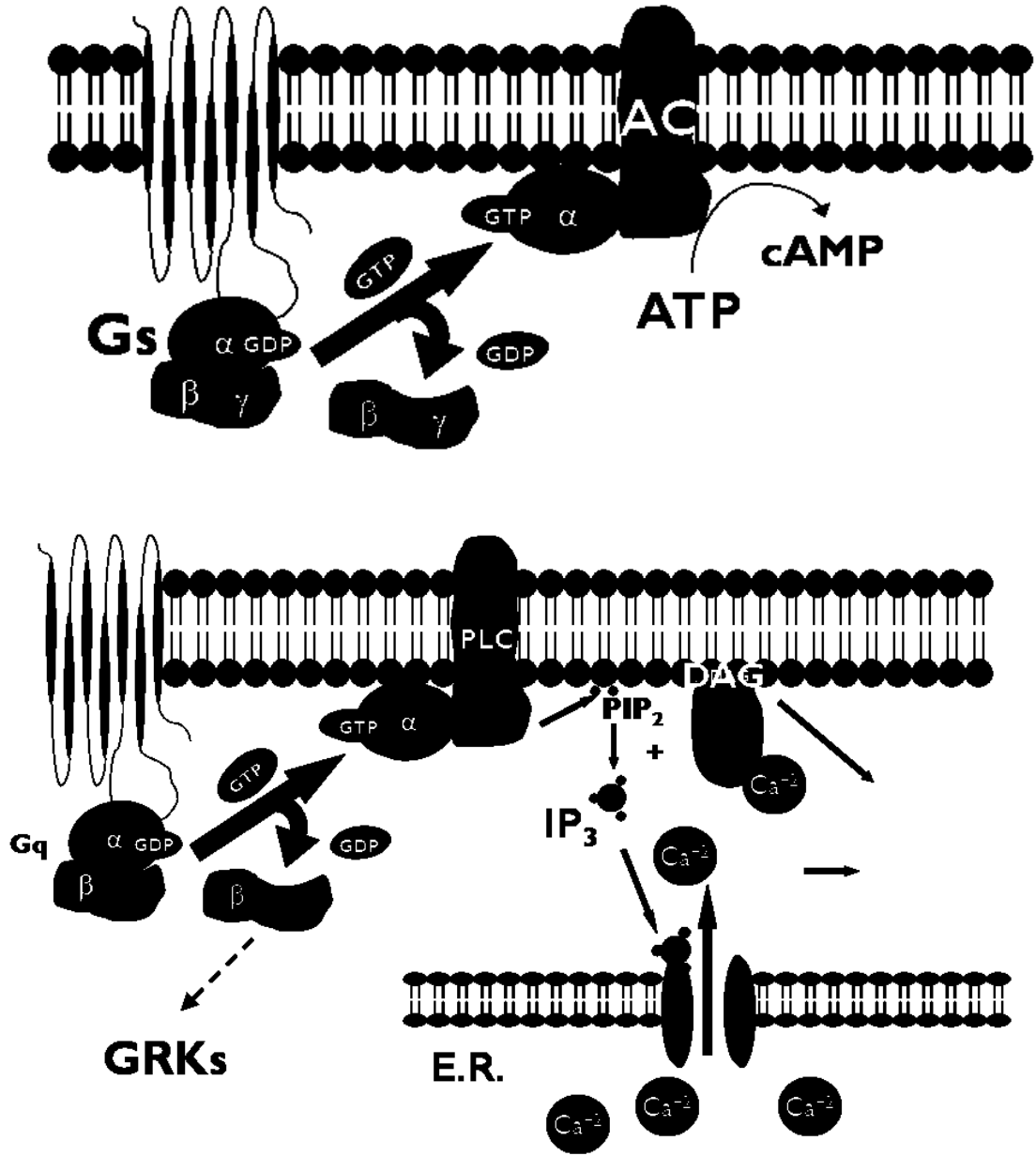


Figure 1-5. Representation of both signaling pathways for the production of A) cAMP mediated via G_{α_s} . B) Inositol triphosphate production mediated via G_{α_q} .

Figure1-6. Histamine catabolism in the central nervous system .

Figure 1-7. The chemical structures of first generation (top row) and second-generation (bottom row) antihistamines.

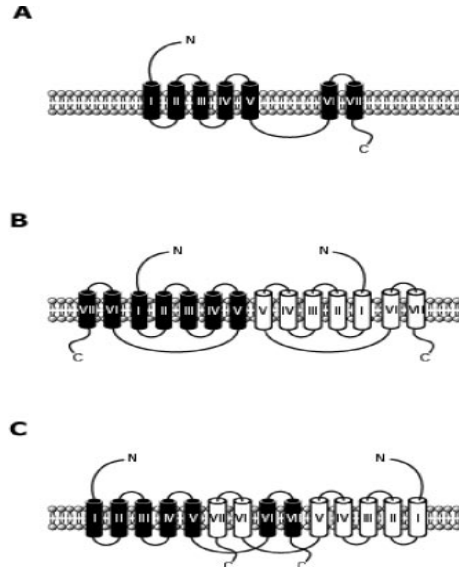


Figure 1-8. Proposed models of GPCR dimerization. This diagram illustrates GPCR monomers (A), contact dimers (B), and domain-swapped dimers (C).



Figure 1-9. Possible combinations of contact (middle) and domain-swapped dimers (bottom) for D3.32A and F6.52A mutations.



Figure 1-10. Structures of the β_2 -adrenergic receptor ligands that were studied using LITicon. Compounds illustrated are: salbutamol (top left), dopamine (top right), catechol (left center), ICI-118551 (right center), and norepinephrine (bottom)

Law of mass action: $A + R \leftrightarrow AR \rightarrow \text{Response}$

Figure 1-11. Illustrates the law of mass action



Figure 1-12. Indicates the changes that were made to the law of mass action in order to incorporate G-proteins.

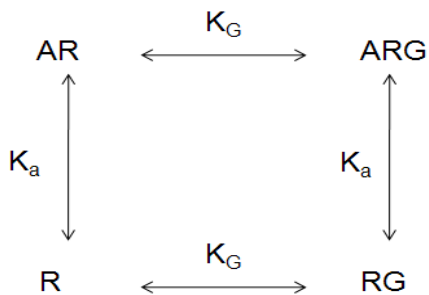


Figure 1-13. Demonstrates the ternary complex model of G-protein activation

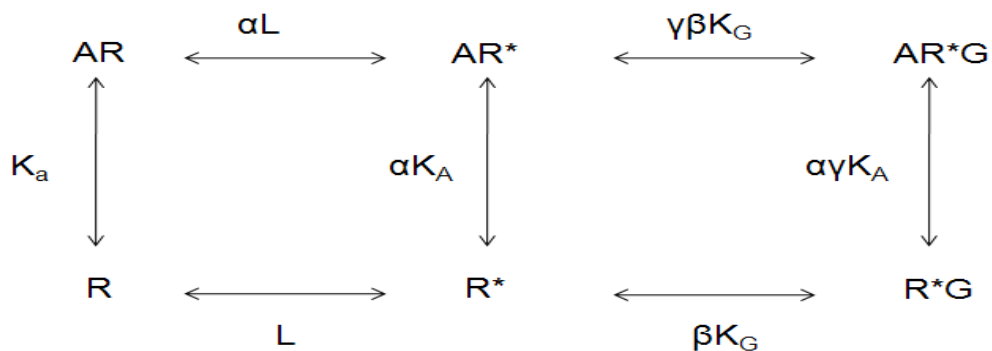


Figure 1-14. When constitutive activity was discovered, the ternary complex model was modified to incorporate this new concept. The resultant extended ternary complex model that is illustrated here.

Table 1-1. K_i and B_{Max} values for 3H -mepyramine and (-)-trans-PAT for WT and D3.32A/F6.52A H1 receptors (Bakker et al., 2004).

Receptor	3H -mepyramine K_D (nM)	3H -mepyramine B_{max} (pMol/mgprotein)	3H -(-)-trans- PAT K_D (nM)	3H -(-)-trans-PAT B_{max} (pMol/mgprotein)
H ₁ RWT	1.2 ± 0.1	21 ± 4	1.2 ± 0.4	3.4 ± 1.0
H ₁ R D3.32A + F6.52A	1.8 ± 0.1	0.34 ± 0.1	3.0 ± 0.6	0.32 ± 0.1

CHAPTER 2 CHARACTERIZATION OF THE STRUCTURE ACTIVITY RELATIONSHIPS FOR PAT ANALOGUES AT THE WILD TYPE HH₁R

Rationale for Undertaking These Studies

Our lead compound, (-)-*trans*-PAT possesses therapeutic potential for the treatment of Parkinson's Disease, via activation of the HH₁R receptor which leads to increased tyrosine hydroxylase activity and dopamine synthesis in the brain (Moniri and Booth, 2006). HH₁Rs also have been implicated in the etiology of insomnia, depression, Alzheimer's disease, schizophrenia, and epilepsy (Yanai & Toshiro, 2007; Haas et al., 2008). In addition, (-)-*trans*-PAT has potential as a therapeutic agent for the treatment of psychosis, obesity, and drug addiction via interactions at the 5-HT₂GPCR family (Booth et al., 2009). By conducting a thorough survey of the PAT ligands that have been synthesized in our laboratories, it is hypothesized that functional moieties can be identified that confer selective binding to the H₁ receptor. Previous PAT studies examining structure activity relationships (SAR) used racemic compounds (Bucholtz et al., 1999). Advances in asymmetric synthesis and HPLC have allowed resolution of PAT enantiomers and an updated SAR, including a litany of new PAT derivatives, is warranted.

Materials and Methods

Chemicals

Synthesis of (+) and (-)-*trans*-PAT, (+)- and (-)-*cis*-PAT, (+)- and (-)-*trans*-PAB, and (+)- and (-)-*cis*-PAB are previously reported (Wyrick et al., 1993; 1995). Histamine, as the dihydrochloride salt, was purchased from Sigma-Aldrich (St. Louis, MO).

The H₁ radioligand [pyridinyl-5-³H]-pyrilamine (mepyramine; specific activity 30.0 Ci/mMol) was purchased from Amersham Biosciences (GE healthcare, Piscataway, NJ)

and myo-[2-³H-(N)]-inositol (specific activity 18.5 Ci/mMol) was purchased from Perkin Elmer (Waltham, MA). Unless otherwise noted, all other compounds were obtained in highest purity from Sigma-Aldrich.

Cell Culture and Transfection

The cDNA encoding the WT human histamine H₁ receptor was purchased from UMR (Rolla, MO). The H₁ K5.39A, T5.42A, N5.46A, Y5.48A, Y7.53A point mutations were prepared using the WT cloned deoxyribonucleic acid (cDNA) subcloned in the pAlter plasmid (Promega), according to the manufacturer's protocol (Altered Sites II, Promega). Mutations in the cDNA were verified by deoxyribonucleic acid (DNA) sequencing using the dideoxy chain termination method. WT and point-mutated cDNA's were subcloned into the expression plasmid pcDEF3 (Goldman et al., 1996).

Human embryonic kidney 293 cells (HEK-293; from ATCC, number CRL-1573) were maintained in Eagle minimum essential medium (MEM) with 10% fetal bovine serum and 2 mM L-glutamine, 0.1 mM non-essential amino acids, 1.5 g/L sodium bicarbonate, 1.0 mM sodium pyruvate.

The cDNA of wild type and mutants of human histamine H₁ receptors in pcDEF3 expression vectors was prepared with Promega Wizard Plus Midipreps DNA Purification System (Promega A7640). Transfection was carried out with Lipofectamine 2000 (Invitrogen, CA) by following manufacture's procedures. Briefly, approximate 1-3 x 10⁶ cells were seeded onto a 100mm tissue culture dish and allowed to grow to 85-95% confluence, then transfected by 12 µg of plasmid DNA mixing with 50 µl of Lipofectamine 2000 for 24 hours. Expression was allowed for another 24 hours in growth medium without antibiotics. Membranes were harvested in ice-cold 50 mM Na₂/K

phosphate ($\text{Na}_2\text{HPO}_4/\text{KH}_2\text{PO}_4$) buffer, pH7.4 (assay buffer) after total 48 hours transfection and expression.

HH₁R Binding Assays

HH₁R saturation and competition binding assays were performed using membrane homogenates prepared from the transfected HEK cells. [³H]-mepyramine was used to label the H₁ receptors (Booth et al., 2002; Moniri et al., 2004). Briefly, 48-hrs following transfection, cells were harvested and homogenized in 50 mM Na²⁺/K phosphate buffer, pH7.4. The homogenate was centrifuged at 35,000g for 10 min and the resulting membrane pellet was re-suspended in assay buffer. Protein concentration was determined by BioRad protein assays. For saturation binding assays, membrane suspension containing 5 µg total protein was incubated with 0.625 to 10.0 nM [³H]-mepyramine in a total assay buffer volume of 250 µl. Non-specific binding was determined in the presence of 1 µM triprolidine. Competition binding assays were conducted under the same conditions using 1.0 nM [³H]-mepyramine (~K_D concentration). Radioreceptor binding assay mixtures were incubated for 30 minutes at room temperature, with termination by rapid filtration through Whatman GF/B filters using a 96-well cell harvester (Tomtec, Hamden, CT). The membrane-bound mepyramine retained on the filter discs was quantified by liquid scintillation spectrometry. Data were analyzed by nonlinear regression using the sigmoidal curve-fitting algorithms in Prism 5.02 (GraphPad Software Inc., San Diego, CA). Ligand affinity is expressed as an approximation of K_i values by conversion of the IC₅₀ data to K_i values using the equation $K_i = \text{IC}_{50} / (1 + L/K_D)$ where L is the concentration of radioligand having affinity K_D (Cheng, 1973). Each experimental condition was performed in triplicate and

each experiment was performed a minimum of three times to determine S.E.M. Statistic analysis was carried out with Prism 5.02 using t tests (and nonparametric tests), unpaired t test, and ANOVA. P value > 0.05 is considered as 'not significant', 0.01<P<0.05 as 'significant *', 0.001<P<0.01 as 'very significant **', and P<0.001 as 'extremely significant ***'

Binding Assay Results and Discussion

A series of novel N,N-dimethylamino-4-phenyl-1,2,3,4- tetrahydro-2-naphthalenamines (PATs) were found to have high affinity and functional activity at histamine H₁ receptors of both humans and other species (Booth et al., 2002). It was discovered that (2S,4R)-(-)-*trans*-PAT (structure in figure 2-1) activates H₁ receptors in mammalian forebrain to stimulate TH and dopamine neurotransmitter biosynthesis in vivo (Choski et al., 2000). Another PAT derivative, (±)-*cis*-5-phenyl-7-(dimethylamino)-5,6,7,8-tetrahydro-9H-benzocycloheptane (PAB, more potent (-)-*cis*-PAB shown in figure 2-13) also stimulates dopamine synthesis via TH stimulation (Moniri and Booth, 2002, 2003). A series of experiments indicated that (-)-*trans*-PAT and (±)-*cis*-PAB activate different signaling pathways to stimulate brain TH and dopamine synthesis. (-)-*trans*-PAT activates the H₁-linked AC/cAMP pathway consistent with activation of G_{αs}, while (±)-*cis*-PAB activates H₁-linked PLC/IP signaling, consistent with activation of G_{αQ}. (Moniri et al., 2004, Moniri and Booth 2006)

Stimulation of TH, the rate-limiting step in dopamine synthesis, holds vast therapeutic potential in treating neurodegenerative and psychiatric disorders, in addition to cardiovascular diseases that involve catecholamine neurotransmission (Booth & Moniri, 2006). Perhaps the most obvious therapeutic use for stimulation of TH would be

in Parkinson's disease (PD). In this disorder, there is a pronounced dying off of the dopaminergic neurons within the substantia nigra. The loss of these neurons, and the dopamine they produce, leads to a disconnect between the brain and the muscles causing resting tremors, bradykinesia, a pronounced stooping posture, loss of balance, akinesia, and depression (Zhou et al 2008). Since neuronal death permanently prevents further synthesis of dopamine, PD is classified as a neurodegenerative disorder. By stimulating TH with small molecules, like PAT and PAB, it is believed the dopamine output from the remaining neurons can be increased, resulting in a potential amelioration of the symptomology of PD.

In order to assess the ability of each compound to affect H₁ receptor signaling, one must first determine how well the compounds of interest are binding to their target. This is accomplished through competitive binding assays, where the ligand in question displaces ³H-mepyramine from a cloned HH₁R transiently expressed in a cell line. The cell lines used in these experiments were either CHOK₁ (CHO, ATCC CCL-61) or HEK-293 (HEK, ATCC CRI-1573) cell lines.

Unsubstituted Parent PAT Compounds

Significant effort has been placed upon the synthesis and isolation of the enantiomers of cis and trans-(±)-PAT. Enantiomeric separation was originally performed by recrystallization with camphor sulfuric acid, as described in our previous papers (Booth et al., 2002; Moniri et al, 2004). As more compound was needed for binding assays, functional, and animal studies it quickly became clear that a more efficient and higher throughput method of enantiomeric purification was necessary. This was made clearly evident by the fact that the resolution of the more potent (±)-*trans* compound produced a yield of less than 10% under recrystallization conditions. By employing a

chiral polysaccharide column (Kromasil, AkzoNobel, Brewster, NY), it was possible to increase yields for the more potent trans diastereomers, while reducing the need for labor-intensive recrystallizations (Booth et al., 2009).

It is important to note that some of the data presented under this specific aim consists of racemic compounds. These compounds either had binding data previously reported, were difficult to separate by any means (Cl-OH and di-OH PATs), or had affinities that were too low to warrant further investigation (NH₂-PATs). It is important to keep in mind that these compounds are 50% mixtures of two different enantiomers, making any comparison beyond simple structure activity relationships rather difficult. However, some of the data provided by these racemic mixtures has been instrumental in streamlining the design of future PAT ligands and will be discussed in the following pages.

The general trend in HH₁ affinities for PAT stereoisomers is that the (-)-enantiomer is more potent than (+), and the *trans* configuration is more potent than the *cis*-configuration. The affinities for the four PAT stereoisomers are 2S, 4R(-)-*trans* > 2S, 4S(-)-*cis* > 2S, 4S(+)-*trans* > 2R, 4R(+)-*cis*. The structures for these compounds are in figure 2-1. The K_i values for each of these compounds and their p-values in reference to the lead compound (-) *trans*-PAT are in table 2-1, and representative binding curves are in figure 2-2. The results suggest that stereochemistry is a crucial factor in PAT binding to the HH₁ receptor and confirm that the (S) stereochemistry at the amine as the most important structural feature for determining H₁ receptor affinity (Bucholtz et al., 1998).

The affinity of these two pairs of enantiomers varies from 1 nM to 100 nM. The results indicate that the ligand binding pocket for PAT's at the HH₁ receptor is quite

selective and can easily differentiate between two enantiomers of the same compound. This effect previously was observed for enantiomers of cetirizine, (R)-levocetirizine and (S)-cetirizine at the HH₁R (structures in figure 2-3). The K_i values for levocetirizine and its enantiomer at the HH₁R, ranged from 3.16 nM for (R)-levocetirizine, to 79.4 nM for (S)-cetirizine (Gillard et al., 2002). These results set a precedent that the binding pocket of the HH₁ receptor is highly stereoselective and lend credence to this PAT binding data. These results fit closely with previously determined K_i values in our lab and with previously published data using both guinea pig and human H₁ receptors (Bucholtz et al., 1998; Booth et al., 2002).

***Ortho*-Substituted PATs**

A series of *o*-substituted PATs were synthesized to probe the structure activity relationships of the pendant phenyl ring. These compounds were (±)-*trans*-*o*-Cl and *o*-CH₃-PAT, whose structures can be found in figure 2-4. As these were older ligands, the binding data consists of the racemic mixture of the (-) and (+)-*trans* enantiomers. Both compounds exhibit a pronounced reduction in affinity when compared with (-)-*trans*-PAT. Previous modeling studies in our lab reveal that the pendant phenyl moiety of (-)-*trans*-2S,4R-PAT possesses aromatic contacts with W6.48, Y6.51, and Y7.43. The (±)-*trans*-*o*-Cl-PAT compound had a K_i value of 24.82 ± 2.7 nM, a ten-fold reduction in affinity compared to its unsubstituted parent compound. The (±)-*trans*-*o*-CH₃-PAT compound has an affinity of 12.7 ± 0.6 nM. Insertion of the methyl group or a chlorine at the *ortho* position seems to produce a negative steric effect with these residues; resulting in the observed drop in affinity compared to the parent ligand. It can be concluded that the effect is steric, as the opposing electronegativities of the chlorine

atom and the methyl group, would have opposing effects on any nearby polar residue. Since both substituents did the same thing, it follows that the effect is likely steric.

Meta-Substituted PATs

Following up on possible pendant phenyl derivatives, our chemists synthesized a series of *meta*-substituted PAT compounds, *trans*-*m*-F, *m*-Cl, and *m*-Br-(structures of each are found in figure 2-5). The affinity of the *m*-F enantiomers will be discussed first. The (-)-*trans*-*m*-F-PAT compound was shown to have a potency similar to that of our lead compound. The K_i value obtained (-)-*trans*-*m*-F-PAT for was 3.03 ± 0.26 nM. For (+)-*trans*-*m*-F-PAT, the K_i value was increased approximately thirty fold (compared to the [-]-enantiomer to 93.56 ± 15.2 nM. The compiled K_i values for binding affinities of the *meta*-halogenated compounds are found in table 2-2.

This series of compounds demonstrates a decrease in stereoselectivity when compared to (-) and (+)-*trans*-PAT, which demonstrate a well-documented 10-fold difference in enantiomers. The pronounced reduction in affinity for the (+)-enantiomer of the *meta*-halogenated series was an unexpected result, s. The p-value for the comparison of (-) and (+)-*trans*-*m*-F-PAT is $P = 0.0147$, indicating a significant difference in the binding of the two enantiomers. In keeping with the compact size of the fluorine atom, the *m*-F substituent has little effect on the affinity of the (-)-isomer, reducing the affinity from 1.95 nM to 3 nM ($P = 0.2926$). The (+)-*trans*-PAT compound has an affinity of 30 nM, that is reduced to nearly 100 nM with the introduction of the *meta*-fluorosubstituent found in (+)-*m*-F-PAT ($P = 0.0262$). Given that the affinity of (-)-*trans*-*m*-F-PAT was unaffected, the result for the (+)-*m*-F-PAT enantiomer is rather surprising. The significant reduction in affinity for the (+)-enantiomer, coupled with an unperturbed affinity for the (-) isomer is suggestive of unique amino acid interactions for

the two stereoisomers. Knowing that the pendant moiety of the (-)-*trans*-PAT scaffold interacts with W6.48, Y6.51, and Y7.43, it seems that accommodating the small fluorine atom is not a problem for this aromatic cluster. In the case of the (+)-*trans-p*-F enantiomer, the drastic reduction in affinity is suggestive of a strongly negative interaction with a completely different set of residues. These opposing effects on affinity for the enantiomeric pair strongly suggest that the pendant phenyl moiety of each stereoisomer is seeing a distinct region of the HH₁R.

In order to glean further information about the HH₁ binding pocket, (+) and (-)-*trans-m*-Cl-PAT were examined in a series of binding assays. The resulting K_i values were 10.19 ± 2.4 nM for the (-)-isomer and 79.48 ± 23 for the (+)-enantiomer. Even though chlorine atoms are larger than fluorine, the affinity of (+)-*trans-m*-F-PAT and (+)-*trans-m*-Cl-PAT are similar. Comparing the (+)-*m*-Cl isomer to its parent enantiomer demonstrates a significant reduction in affinity with a p-value of 0.0262. The (-)-*trans*-PAT and (-)-*trans-m*-Cl-PAT compounds also show a significant reduction in affinity (P = 0.0057). This trend illustrates that insertion of a *meta*-chloro substituent into either the (-) or (+)-*trans*-PAT scaffold results in a reduction in affinity when compared to the parent ligand.

In order to confirm these trends, the affinity of a third *meta*-halogen compound was required. The (+) and (-)-*trans-m*-Br-PAT were synthesized. Bromine is the next largest halogen atom after chlorine and fluorine, and possesses a reduced electronegativity when compared to fluorine and chlorine. The K_i values for the (+) and (-)-isomers of *trans-m*-Br-PAT were determined to be 62.52 ± 10.1 and 27.94 ± 1.5 nM, respectively. The K_i values for the (+)-*para*-halogenated PATs range from 94 nM for *m*-F, to 62 nM for

m-Br and show no significant differences when compared to each other with ANOVA ($P > 0.05$). When placed in their rank order from high to low affinity, the results are (+)-*trans-m*-Br-PAT > (+)-*trans-m*-Cl-PAT > (+)-*trans-m*-F-PAT. It is important to recall that the K_i value for (+)-*trans*-PAT is 30 nM, thus, substituting a halogen atom in the meta-position does not provide HH1 ligands with enhanced affinity.

In contrast to the (+)-*trans-meta*-halogens, the (-)-*trans-meta*-halogens illustrate a clear trend. The rank order of affinity of the (-)-*trans* compounds is (-)-*trans-m*-F-PAT > (-)-*trans-m*-Cl-PAT > (-)-*trans-m*-Br-PAT. As the halogen substituents on the pendant phenyl ring increase in size, the HH1 affinity of the (-)-*trans-meta*-halogenated-PATs decreases. Contrasting the effects of *meta* halogen substitution on the (-) and (+) enantiomers of PAT, reveals two unique pictures. The (+) enantiomers seem to be unaffected by the size of the halogen substituent ($P > 0.05$ between compounds), while the (-)-isomers show a significant reduction in affinity as the halogen size increases ($P_{F-Cl} = 0.0103$ and $P_{Cl-Br} = 0.0321$). These findings suggest that the (-) and (+) enantiomers of PATs are binding differently to the H_1 receptor and that the pendant phenyl moiety is an important determinant of the binding mode. Despite the intriguing lack of affinity differences with the (+)-*trans-m*-substituted-PATs, it is important to keep a sense of scope, as none of the compounds examined improved the affinity of (-)-*trans*-PAT; and therefore would not make suitable H_1 ligands.

Para-Substituted PATs

To further our understanding of the molecular determinants of PAT at the HH_1R it was necessary to look at additional derivatives. In a search for more potent analogues, a series of compounds were synthesized with an array of substituents at the *para* position of the pendant phenyl ring. Included among them were a series of halogen-

substituted compounds, *p*-F, *p*-Cl, *p*-Br-PAT, and a methyl substituent, *p*-CH₃-PAT. The structures of these compounds are found in figure 2-6. The compiled competitive binding data for all of the *para*-substituted compounds is located in table 2-3. Intriguingly, each of these *para* substituted compounds showed a reduced stereoselectivity between enantiomers. For quite some time, PAT enantiomers have illustrated approximately a ten-fold difference in H₁ receptor affinity with the (-) being the more potent of the stereoisomers (Bucholtz et al., 1999; Booth et al., 2002)

The *p*-methyl-PAT was the first *para* derivative that was resolved into its respective (+) and (-) enantiomers and was the first compound investigated. Intriguingly, there is no difference in affinity regarding stereoselectivity for the (+)-*trans* vs. (-)-*trans* enantiomers ($P = 0.19$). Binding curves for the *p*-substituted PATs are located in figure 2-7. This result was unique among the previous trends that were established for PATs and was quite unexpected. Based upon the differing affinities for (+) and (-)-*trans*-PAT at the H₁ receptor ($P = 0.015$), and the lack of stereoselectivity between the *p*-CH₃-PATs ($P = 0.19$), it is clear that the interactions formed by the pendant phenyl ring with the receptor are being perturbed. This is supported by the fact that the introduction of a small, lipophilic methyl group on the *para* position of this ring had opposing effects on the binding affinity of the (-) and (+) isomers. The (-)-*trans*-*p*-CH₃ isomer demonstrated a ten-fold reduction in affinity, when compared to its parent compound ($P = 0.023$). In contrast, (+)-*trans*-*p*-CH₃-PAT exhibited a three-fold increase in affinity from (+)-*trans*-PAT ($P = 0.037$). The dichotomy between the effects of (-) and (+)-*p*-CH₃-PAT when compared to their parent compounds suggests that the binding pocket of the (+) isomer has more space around the *para*-position of the pendant phenyl ring, with which to

accommodate the extra methyl group. Contrary to this, the area surrounding the pendant phenyl of the (-) isomer seems to be unable to accommodate the same moiety. Whether this negative interaction is caused by perturbations in the π - π stacking interactions with W6.48, Y6.51, and Y7.43 or by simple steric bulk is difficult to say without modeling results. Regardless, it is clear that the introduction of a *p*-methyl group onto the pendant phenyl ring of the PAT scaffold causes significant changes in H₁ receptor binding.

The *para*-F compound was the next ligands to be resolved into its enantiomers. (-) and (+)-*trans-p*-F-PAT represent excellent ligands to further probe the binding pocket of the H₁ receptor. Methyl and fluorine have approximately the same mass, but quite different steric and electronic properties. Fluorine is sterically smaller than its methyl counterpart is, but is much more electronegative and creates a polar C-F bond. Methyl has little effect on stereoelectronics when compared to a highly electronegative fluorine atom that is capable of forming hydrogen bonds (Torrice et al., 2009). It was originally anticipated that the F-substituent would create additional hydrogen bonds with the receptor to increase its H₁ receptor affinity.

When the binding of the *p*-F-PAT enantiomers was examined, the results proved similar to the *p*-methyl derivatives. Again the first observation was the reduction of stereoselectivity between the (+) and (-) isomers. Rather than the ten-fold selectivity between the (-) and (+) enantiomers, only a two-fold selectivity was observed for the H₁ receptor ($P=0.0098$). In this case, the (-) was still the more potent of the two isomers having an affinity of $4.065 \pm 0.5\text{nM}$, similar to (-)-*trans-m*-F-PAT's 3 nM affinity and not statistically different from (-)-2*S*,4*R*-*trans*-PAT's 2 nM affinity ($P=0.0542$) . Keeping with

the trend established by (+)-*trans-p*-CH₃-PAT, (+)-*trans-p*-F-PAT was significantly more potent than its parent compound by three-fold, having an affinity of $8.268 \pm 0.6\text{nM}$ at the WT receptor ($P=0.026$). The insertion of a fluorine at the *para* position of the pendant phenyl ring produced nearly identical results to the methyl substituent in the same position. This result was rather surprising, as some electronic effects were anticipated from the highly electronegative fluorine atom. As the affinity for the (-)-*p*-F isomer is nearly as potent as the parent compound (-)-*trans*-PAT, it could be gleaned that there was no additional hydrogen bonding taking place. It is intriguing that both (+)-*p*-CH₃ and F-PAT demonstrate a three-fold increase in affinity from their parent compound, suggesting that their increase in affinity is not due to hydrogen bonding interactions. Perturbations involving the nearby aromatic residues in TMD 6 can likely be ruled out, due to the fact that methyl and fluorine substituents have opposing effects on electronic density in an aromatic ring. The methyl group would donate additional electron density, while the fluorine would pull electron density from the aromatic system, weakening the aromatic interactions. With these effects ruled out, it is likely that the increase in affinity for the (+)-isomer is caused by favorable steric interactions or additional Van der Waals interactions, which are only possible if the (+) isomer is seeing a different microdomain of the orthosteric binding pocket than its (-)-enantiomer.

Chlorine was the next substituent on the *para*-PAT derivatives produced by our chemistry lab. Upon investigating their binding to the H₁ receptor, it quickly became clear that the similar trend of reduced stereoselectivity would continue. The (+) and (-)-*p*-Cl enantiomers showed no stereoselectivity, with K_i values of 6.08 ± 0.75 and $8.38 \pm 1.1\text{nM}$, respectively ($P= 0.24$). When the *p*-Cl-PATs are compared to their parent

enantiomers, a familiar trend emerges. The affinity (-)-*trans*-*p*-Cl-PAT is reduced by about four-fold from the parent ($P=0.036$), and the (+)-*trans*-*p*-Cl isomer is five times more potent than its parent ($P=0.022$). These results suggest that the (+) isomer is able to better accommodate a variety of structural changes at the *para* position than its (-) enantiomer. Again suggesting that the (-) and (+) PATs, and more specifically their pendant phenyl moieties, are seeing different regions of the H₁ binding pocket.

(+ and -)-*trans*-*p*-Br-PAT were synthesized to investigate the steric and electronic effects of *para* substitutions on the pendant phenyl ring. Br is the largest of the halogen moieties that has been inserted at the *para* position so far, and should allow information to be gleaned about the amount of space surrounding the *para* position. The electronic effects should be similar to the chloro-substituted isomers as there is some bond-polarity, but a lack of strong hydrogen bonding. The (+) and (-) isomers yielded K_i values of 531.8 ± 62.1 and 1058.2 ± 53.0 nM, respectively and when compared yield a p-value of 0.023. The affinities for both compounds are reduced by approximately 100-fold when compared to the other *p*-halogenated PAT molecules.

Such a drastic reduction in affinity for both stereoisomers, is best explained by steric hindrance. The progression from *p*-F to *p*-Cl yielded only slight differences in affinity between the compounds and slight deviation from the 1 nM K_i of our lead compound (-)-*trans*-PAT. The lack of affinity differences between the *p*-F/Cl and CH₃substituted enantiomers strongly suggests that hydrogen bonding is not involved in the way these ligands bind to the receptor. If hydrogen bonding were involved, one would expect the F-PATs to possess a higher affinity, while the Cl-PATs would show a slightly reduced affinity, as they possess a reduced ability to hydrogen bond. This is

clearly not the case, as the F and Cl-PATs are nearly indistinguishable in binding assays, meaning steric hindrance offers a better explanation of the data. As the halogens increase in size, a schism appears between the affinities of *p*-Cl and *p*-Br-PAT. The atomic radii for halogens increase as one progresses down group VII in the periodic table. Fluorine the smallest halogen has an atomic radius of 0.0709 nM, chlorine's is 0.0994 nM, and bromine is the largest with 0.1145 nM (Visual Elements Group 17: The Halogens, Royal Society of Chemistry). It seems that the binding pocket of the H₁ receptor is tolerant of the size increases at the *para* position until bromine. Once this point is reached, neither the (+) nor (-)-isomers can accommodate the large bromine atom within their binding pockets, resulting in the observed reduction in affinity. It does seem that (+)-*p*-Br isomer has slightly more room in its binding pocket to accommodate the bulky bromine moiety, as evidenced by its higher affinity. However, the reduction in K_i is significant enough to rule out *p*-Br as an effective derivative of the PAT scaffold.

The stereoelectronics of the PAT derivatives examined, varied from strongly electron withdrawing (F and Cl), to electron donating (CH₃) and still produced increases in affinity for the (+) stereoisomer; suggesting that there are no strong electronic interactions formed by these compounds. If a polar amino acid were interacting with the (+)-isomer there would have been a weaker or no gain in affinity for (+)-*p*-methyl-PAT. The same logic can be used to rule out additional aromatic interactions. If an aromatic amino acid was interacting with the pendant phenyl of the (+)-isomer, diverging effects on affinity would have been observed for (+)-*trans-p*-Cl/F-PAT and *p*-CH₃-PAT, as their substituents have opposing effects on aromatic electron density. Cl and F would have

pulled electron density away from the ring, while the CH₃ would have donated electrons to the aromatic system. With these two interactions ruled out, it seems likely that the differences in binding are occurring due to steric and/or Van der Waals effects. Perhaps the simplest explanation is that there is more room to accommodate a *para*-substituted functional moiety at the region of the receptor where the pendant phenyl ring of the (+)-*trans*-isomers is binding. However, it is important to note that this binding pocket for the (+)-*trans* isomers does have steric limitations, as evidenced by the dramatic reduction in affinity observed for (+)-*p*-Br-PAT

This is in contrast to the (-)-*para* substituted isomers, which all demonstrate a reduction in affinity when compared to our lead compound (-)-*trans*-PAT. The (-)-*trans*-*p*-F and Cl isomers retain an affinity that is within 4-fold of the parent compound. However at the present time, it seems that none of the (-)-*trans*-*p*-substituted-PATs was able to improve on the affinity of the parent compound.

In summary, it seems that moieties added to the *para* position of the pendant phenyl ring increase the affinity for the (+) isomer, while reducing the affinity for the (-). The result is that stereoselectivity between the (-) and (+) isomers that has been so well documented, is no longer observed with these *para* substituted derivatives. The diverging effects on affinity observed for the (-) and (+) stereoisomers suggests the enantiomers have unique environments within the orthosteric binding site for the H₁ receptor. The *p*-Br-PATs follow this trend, however their larger bromine atom prevents either enantiomer from effectively binding to the H₁ receptor

N-substituted PAT Derivatives

To probe the area surrounding D3.32, the residue providing the critical ionic interaction for binding to all aminergic receptors, (+) and (-)-*trans*-N,N-diethyl-PAT were

synthesized. These ligands provide important information about the region surrounding residue D.3.32, the most important residue of the H₁ receptor binding pocket. The addition of lengthening aliphatic chains around the lone nitrogen of PAT was predicted to have little effect on the strength of the ionic interaction with D3.32A. However, the larger side chains may provide significant steric hindrance and prevent the protonated amine from coming into contact with the desired aspartic acid residue.

In the case of (-)-*trans*-N,N-diethyl-PAT this proved not to be the case. It was determined that this compound bound quite similarly to (-)-*trans*-PAT, showing only a 4-fold reduction in affinity with a K_i of 8.59 ± 0.53 nM. Contrary to this, (+)-*trans*-N,N-diethyl-PAT showed a pronounced reduction in affinity with a K_i of 193.76 ± 3.3 nM. Tabulated affinity values for all N-alkyl PAT derivatives are located in table 2-4. The structures for the compounds discussed in this section are found in figure 2-8. These results reiterate how crucial stereochemistry is when binding to the H₁ receptor. In order to produce such a drastic decrease in affinity, there must be a significant difference in the binding mode of (+)-2S,4R and (-)-2S,4R-diethylPATs.

Since all aminergic ligands interact with D3.32, this amino acid can be thought of as an anchor point for ligand binding. Once this interaction has formed, the ligand can form the other Van der Waals, hydrogen bonding, and/or aromatic interactions that allow it bind to the receptor. Although D3.32 can be considered an anchor point, it by no means restricts the regions of the receptor with which a ligand interacts. This point was eloquently demonstrated in the β₂-AR using a modeling technique called LITICON, as is discussed in detail in chapter 2. Briefly, it was shown that partial, inverse, and full agonists at the β₂-AR all stabilized unique receptor conformations with unique residue

contacts, despite maintaining the same anchor point at D3.32 (Bhattacharya et al., 2008). It was proposed that after the initial ionic bond is formed, the ligand and receptor adopt the most energetically favorable conformation, leading to unique conformations for each ligand-receptor complex. Unique molecular determinants and by extension receptor conformations, were shown for the partial agonists dopamine, salbutamol, and catechol, the inverse agonist ICI-118551, and the full endogenous agonist norepinephrine (Bhattacharya et al., 2008). By applying a similar logic to the histamine H₁ receptor it is possible to explain the binding differences between (+) and (-)-N,N-*trans*-diethyl-PAT.

The most crucial factor in the loss of affinity for the (+) isomer is certainly steric hindrance, as the only difference between the enantiomers is stereochemistry. It is possible that the two different binding modes of (+) and (-)-PAT force the protonated amine group into diverging conformations. For example, the aromatic interactions that aid in the binding of the (-)-*trans*-N,N-diethyl-PAT enantiomer may allow this compound to interact with D3.32 in a favorable “forked” interaction demonstrated in figure 2-9. This conformation would allow the protonated amine to interact strongly with D3.32, while minimizing the negative steric effects of the longer diethyl side chains. The inversion of the stereocenters in the (+)-isomer causes a change in the aromatic amino acids that are required for binding. This change would alter the most stable conformation of the receptor and the angle with which the amine moiety approaches the crucial D3.32 residue. Even a slight steric clash that weakened the ionic interaction would result in a significant drop in affinity, as the ionic interaction is the strongest factor in determining the affinity of any aminergic ligand.

This point is clearly illustrated by examining the affinity of older PAT analogs. Our lab has previously synthesized PATs with a litany of N-substituted alkyl derivatives ranging from methyl to allyl. The racemic mixtures of *cis* and *trans*-trimethyl-PAT demonstrate that increasing the number of N-alkyl substituents does not increase H₁ receptor affinity. The K_i values for these compounds are 107 ± 4.1 and 120 ± 15 nM, respectively; whereas the affinity for (±)-*cis*-PAT is 13.6 nM and (±)-*trans*-PAT is 4.26 nM at the HH₁R (Bucholtz et al., 1999). The only structural difference between these ligands and the current generation is the addition of a third methyl group, yet the high affinity and *cis/trans* stereoselectivity that is so evident with the dimethyl-PATs is lost. This result has been previously explained by the loss of a proton at the amine, creating a permanent positive charge and preventing proper hydrogen bonding with D3.32. It seems that a permanent positive charge on the amine is not conducive to binding to the H₁ receptor with high affinity (Bucholtz et al., 1999).

Removing alkyl groups from the amine moiety also causes pronounced drops in H₁ affinity. (±)-*trans*-NH₂-PAT, a synthetic intermediate in the production of (+) and (-)-*trans*-PAT lacking two N-methyl groups, has little affinity for the H₁ receptor with a K_i = 1270 nM. A slight structural analog, (±)-*trans*-NH(CH₃)-PAT increased H₁ receptor affinity approximately twenty-fold to 64 nM. The addition of a N-allyl group to the free amine created (±)-*trans*-NH(C₃H₅)-PAT and again yielded a significant increase in receptor affinity from the free amine (K_i = 45 nM). The addition of a methyl group to this compound created (±)-*trans*-N-CH₃(C₃H₅)-PAT and further increased the affinity of the ligand to a K_i of 3.4 nM. Substituting a second allyl group for the N-methyl yielded (±)-*trans*-N(C₃H₅)₂-PAT. This compound was not as potent as its predecessor was (K_i =

10.2 nM) and suggested that there were steric limitations for alkyl substitutions on the amine (Bucholtz et al., 1999). As these results clearly indicate, the most potent PAT analogs all contain a N,N-dialkyl substitutions. The rank order of H₁ affinities for N,N-dialkylated-PATs from high to low affinity is dimethyl > diethyl > diallyl. It is clear from this trend and the affinity values shown above that the dialkyl substituents have a profound effect on H₁ affinity and that the shorter the alkyl side chain the greater the H₁ receptor affinity. The addition or subtraction of any alkyl moiety from the N,N-dialkylated scaffold negatively affects the ability of the protonated amine moiety to form its ionic bond with D3.32, and consequently the affinity of the ligand in question for the H₁ receptor. Based upon this data, it was concluded that N,N-dialkyl-PAT's have the strongest interactions with the receptor and that N,N-dimethyl was the most effective alkyl substituent.

Chloro and Hydroxyl TetrahydronaphthaleneSubstituted PATs

The synthesis of *trans* and *cis*- (±)-6-hydroxy-7-chloro-PAT and *trans* and *cis*- (±)-6,7- di-hydroxy-PAT was first reported in 1993, before the H₁ receptor was even recognized as their most potent target(Booth et al., 1993). The structures of these compounds are found in figure 2-10, with representative curves in figure 2-11. Interestingly, the chloro/hydroxyl substituted PATs retained high affinity and the ability to stimulate TH in rodent forebrain, while the di-hydroxy compounds did not (Bucholtz et al., 1999). It was originally hypothesized that the di-hydroxy substituents would mimic the catechol ring observed in β-2 agonists to produce a more efficacious ligand. In hindsight and with the knowledge that differing GPCR's evolved to discriminate between neurotransmitters, this result makes sense. A receptor that had evolved to bind histamine specifically would have scant affinity for a catechol ring that is possessed by

many catecholamine neurotransmitters. If it did the “histamine-specific” receptor would likely have high affinity for epinephrine, norepinephrine, and dopamine as these structures contain protonated amines with a catechol ring.

As briefly mentioned earlier, the chloro-hydroxy derivatives proved to be more potent than the di-OH PATs with a rank order of (\pm)-*trans*-6-Cl-7-OH > (\pm)-*cis*-6-Cl-7-OH > (\pm)-*cis*-di-OH > (\pm)-*trans*-di-OH-PAT. The affinities listed in table 2-5 were performed using the cloned HH₁R and vary slightly from the original publications that used guinea pig brain homogenates (Booth et al., 1993; Bucholtz et al., 1999). The rank order for the ligands remained the same, with the slight exception that (\pm)-*cis* and (\pm)-*trans*-6-Cl-7-OH-PAT had very similar affinities in guinea pig brain tissue. Despite their high affinities, the Cl-OH-PATs have proved difficult to separate into their respective enantiomers. The Cl and OH substituents interact very strongly with the polar polysaccharide column used in chiral separation and cannot be resolved in this manner.

PAT-Like Compounds with Ring Perturbations

A large portion of clinically relevant histamine antagonists, such as triprolidine, hydroxyzine and acrivastine, possess a 1,1-diaryl-3-aminopropyl moiety, found in figure 2-12 (Bucholtz et al., 1999). PAT's structure closely resembles this established pharmacophore for the H₁ receptor as demonstrated by the overlay in the same figure. Two additional successful compounds, chlorphenamine and mepyramine, that make use of this pharmacophore are also depicted. Having already explored the majority of this pharmacophore's chemical space, it is necessary to discuss permutations to its tricyclic ring structure in order to complete a thorough SAR analysis. To date several ligands that are PAT-like, but possess modifications to their tricyclic ring systems have been synthesized. These ligands are *cis* and *trans* (+ and -)-PAB, (+ and -)-*trans*-N,N-

dimethylamino-4-cyclohexyl-1,2,3,4- tetrahydro-2-naphthalenamine, or CyclohexylAminoTetralin(CAT), (+ and -)-*trans*-*N,N*-dimethylamino-4-cyclooctyl-1,2,3,4-tetrahydro-2-naphthalenamine or CycloOctylAminoTetralin (COAT), and (+ and -)-*trans*-*m*-phenyl-PAT. Of these compounds, only the PABs have been previously reported, making the majority of these results novel and providing new SAR's to examine (Bucholtz et al., 1999; Moniri et al, 2004). The structures of these compounds can be found in figure 2-13, with their K_i values tabulated in table 2-6.

As they have been previously reported, the PAB family provides an ideal starting point for the discussion of the tricyclic structure activity relationships. PAB is slightly different from our lead compound (-)-*trans*-PAT, the only difference being an extra methylene group in the fused ring system. This trivial modification, which creates a fused cycloheptyl ring as opposed to a fused cyclohexyl, causes profound changes in the ability of these ligands to bind to, and activate the H_1 receptor. The binding order of the PAT's, (-)-*trans* > (-)-*cis* > (+)-*trans* > (+)-*cis*, is now completely inaccurate. In fact, the affinity of (\pm)-*trans*-PAB was so low (> 10 μ M) that it was never resolved into its enantiomers. (\pm)-*cis*-PAB did show some promise and its enantiomeric pair was resolved. (-)-*cis*-PAB proved to be the more active stereoisomer with a respectable K_i of 57.5 ± 9.25 nM. (+)-*cis*-PAB demonstrated a K_i of 300 ± 40 nM. Despite its modest affinity, (-)-*cis*-PAB proved to be an interesting compound, as it was the first $G_{\alpha Q}$ partial agonist within the PAT family. This result is quite remarkable, as it demonstrates just how fickle GPCRs can be when selecting an agonist. The four PAT stereoisomers, which differ only in stereochemistry and lack the additional methylene moiety, show no activation of $G_{\alpha Q}$. In fact, (-)-*trans*-PAT is an inverse agonist at this same pathway. By

introducing a cycloheptyl ring, the conformation of the H₁ receptor stabilized by (-)-*cis*-PAB is now unique enough to cause G_{αQ} to activate instead of dissociate as it would with the inverse agonist (-)-*trans*-PAT. This example illustrates how critical it is to examine each stereoisomer individually when investigating GPCRs and lends credence to this SAR analysis.

The pendant phenyl is the next area of the PAT scaffold to consider. A variety of ligands were synthesized to probe the region of the receptor surrounding the pendant phenyl ring. These ligands include *m*-phenyl-PAT, CAT, and COAT. The *m*-phenyl-PATs investigate the possibility of further aromatic interactions in the region surrounding the pendant phenyl ring. COAT and CAT examine how critical the aromatic portion of PAT is for effective H₁ binding.

The *trans-m*-phenyl-PATs have been synthesized, resolved, and investigated at the WT H₁ receptor. A solid K_i was obtained only for (-)-*trans-m*-phenyl-PAT, which displaced ³H-mepyramine with a value of 213.0 ± 20.4 nM. (+)-*trans-m*-phenyl-PAT was unable to displace mepyramine effectively even at concentrations > 10 μM. Both compounds are significantly less potent than their parent PATs, but the drastic difference between (+) and (-)-*m*-phenyl-PAT does provide a few clues about the environment surrounding the pendant phenyl region. Despite its lowered affinity, the (-) isomer is able to tolerate the additional phenyl group, confirming that the (-)-pendant phenyl region binds within or close to a cluster of aromatic residues.

Based upon previous saturation binding studies it seems that the aromatic residues in TMD 6 are the most likely interaction site. It has been previously reported that the F6.52A mutation abolishes the binding of (-)-*trans*-PAT (Bakker et al., 2004).

Similar unpublished saturation experiments revealed the surrounding aromatic residues W6.48, Y6.51, and F6.55 are involved in the binding of ^3H -*trans*-PAT. These residues could stabilize the *m*-phenyl-group sufficiently to allow binding of the (-) isomer to take place. The (+) isomer clearly lacks either the steric space in the region around the pendant phenyl ring or the proper amino acid residues to create a strong enough interaction with the ligand. Either way, these results clearly suggest a differing chemical environment in the regions surrounding the (+) and (-) enantiomers. It is interesting to note that the *p*-Br compound showed an opposite trend, where the (+) isomer could better tolerate the bulky bromine atom. This can be explained by differing amino acid sequences surrounding the pendant phenyl groups of the (+) and (-) isomers. The (+) isomers demonstrate an increase in affinity for *para*-pendant phenyl substituents like F and Cl, suggesting the presence of polar residues in that region. Aromatic substituents are better tolerated by the (-) enantiomers that are postulated to interact with the aforementioned aromatic residues in TMD 6. The same (-) enantiomers show either no change in affinity or a decrease in affinity with non-aromatic pendant phenyl substituents, suggesting a lack of suitable polar amino acids in the region surrounding the pendant phenyl moiety of (-)-*trans*-PAT. Regardless of the substituent that is present, it seems that the bulkier the group that stems from the pendant phenyl ring the lower the H_1 affinity becomes. Future H_1 ligand design should focus on pendant phenyl substituents that are no larger than a chlorine atom, as both the *p*-Br and *m*-phenyl substituents drastically reduce binding affinity regardless of stereochemistry.

The next two ligands CAT and COAT are radically different from their parent ligands. The parent compound (-)-*trans*-PAT has a pendant phenyl ring at the 4-

position of its tetrahydronaphthyl ring. This phenyl has been previously established as a critical region of the PAT scaffold, as its removal decreased the affinity of (-)-*trans*-PAT by 100-fold (Bucholtz et al., 1999). These studies confirmed the importance of the aromatic ring, but due to a lack of suitable compounds, no further SAR results were obtained. CAT and COAT replace the pendant phenyl ring with non-aromatic cycloalkyl rings of six and eight carbons respectively, and are perfectly suited to fill this empty niche in the SAR of the PAT family.

Both the (-) and the (+)-*trans* isomers of CAT and COAT have been synthesized, and their binding results are discussed here. The introduction of the more flexible cycloalkyl substituents in place of the pendant phenyl ring explores new regions of the chemical space surrounding the binding pocket for the (+) and (-) Pats' Both the (-) and (+)-CAT isomers demonstrated high binding affinity at the H₁ receptor. (-)-*trans*-CAT has an affinity of 1.58 ± 0.5 nM, which is strikingly similar to (-)-*trans*-PAT. (+)-CAT demonstrated a nearly identical affinity for the H₁ receptor of 1.7 ± 0.2 nM. These results suggest that the cyclohexyl ring is as effective as the phenyl in producing a high affinity H₁ ligand. This result was extremely surprising given the established interactions that (-)-*trans*-PAT has with the aromatic residues in TMD 6. Based on the high affinity, it seems that the additional flexibility of the cyclohexyl ring and the sum of the cyclohexyl Van der Waals forces is able to create an interaction with the receptor that is as strong as the aromatic π - π stacking interactions with the parent scaffold. The potent binding of the (+)-isomer is not quite as surprising, given that the binding pocket around the pendant phenyl ring was able to tolerate larger halogen substitutions more effectively

than the (-)-isomer. This tolerance suggested a larger and more flexible binding pocket for the pendant phenyl position of the (+)-isomer.

As observed with the *p*-Br compounds, even the most accommodating binding pocket does have its limits. The COAT isomers appear to push these limits too far, given that both isomers demonstrate a pronounced reduction in affinity when compared to either the PATs or CATs. (-)-*trans*-COAT, which was the only isomer that produced a valid K_i , still possessed a meek affinity of 432 ± 60.1 nM. The enantiomer (+)-*trans*-COAT was unable to displace ^3H -mepyramine from the receptor even at a $10\mu\text{M}$ concentration. As the affinity of both (+ and -)-COAT was reduced by at least 100-fold from PAT and CAT, this particular analog was not potent enough for further derivatization.

PAT Binding Summary

Recent advances in GPCR theory have demonstrated that each ligand stabilizes a unique receptor conformation. This result validates and helps explain previous observations of stereoselective binding to the H_1 receptor (Bucholtz et al., 1999; Gillard et al., 2002; Booth et al., 2002). Enantiomers are defined as two identical compounds, meaning their physical properties and structures are the same, but they are non-superimposable mirror images of each other. Yet somehow, these receptors are able to discriminate between enantiomers when very sensitive chemical techniques such as Infrared spectrometry (IR), Ultraviolet-Visible spectrometry (UV-VIS), Gas chromatography coupled with mass spectrometry (GC/MS), and most high performance liquid chromatography (HPLC) are unable to do. Traditional GPCR theory involved active, inactive, and constitutively active states that interacted with a ligand and a G-protein to form the ternary complex model. Unfortunately, these models assumed there

would be only one active or inactive conformation of a receptor and had difficulty explaining concepts like allosterism and partial agonism. Current GPCR theory assumes that every ligand will produce a different conformation of the receptor and is flexible enough to accommodate these observations.

The series of ligands produced by our labs provides an excellent example of modern GPCR theory at work. This chapter details a series of stereospecific ligands that demonstrate functional selectivity and can even exert opposing effects on a signaling pathway with the addition of a simple methylene group. Invoking Accam's razor, the simplest explanation for these diverse observations is if each ligand is indeed creating a unique GPCR conformation. This explanation is supported by the stereospecific binding demonstrated by the PAT analogues in the preceding chapter.

Figure 2-1. PAT family of stereoisomers demonstrating the stereochemical relationships between each compound.

Table 2-1. Affinities of the PAT stereoisomers at the WTHH₁R

Compound Name	Histamine H ₁ Affinity in nM (K _i ± S.E.M.)	P-value compared to (-)- <i>trans</i> -PAT
(-)- <i>trans</i> -PAT	1.95 ± 0.51	N/A
(-)- <i>cis</i> -PAT	13.7 ± 2.0	0.0307*
(+)- <i>trans</i> -PAT	29.79 ± 3.5	0.0157*
(+)- <i>cis</i> -PAT	177.166 ± 9.4	0.0083**

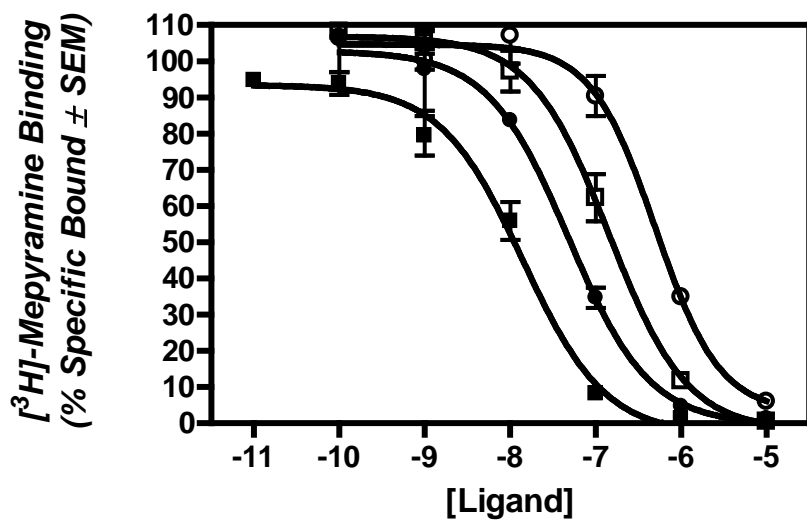


Figure 2-2. Representative competitive binding curves for the PAT family of stereoisomers at the human WT H₁ receptor. The ligands represented are as follows: (-)-*trans*-PAT (■), (-)-*cis*-PAT (●), (+)-*trans*-PAT (□), and (+)-*cis*-PAT (○).

Figure 2-3. Enantiomers of (±)-cetirizine that demonstrate high stereoselectivity at the H₁R

Figure 2-4. Structures of (\pm)-*trans-ortho*-Cl-PAT (left) and (\pm)-*trans-ortho*-CH₃-PAT (right)

Figure 2-5. Structures of (-)-*trans-meta*-halogenated-PAT derivatives, where X is F, Cl, or Br

Table 2-2. HH₁Rbinding affinities of (+)- and (-)-*trans-para*-substituted PATs

Compound Name	HH ₁ Affinity in nM (K _i \pm S.E.M.) and P-values for enantiomeric comparison	P-value compared to parent enantiomer (e.g. (-)- or (+)- <i>trans</i> -PAT)
(-)- <i>trans-m</i> -F-PAT	3.03 \pm 0.26	0.29
(+)- <i>trans-m</i> -F-PAT	93.56 \pm 15.2 (P = 0.014)	0.026*
(-)- <i>trans-m</i> -Cl-PAT	10.19 \pm 2.4	0.0060**
(+)- <i>trans-m</i> -Cl-PAT	79.48 \pm 23 (P = 0.021)	0.039*
(-)- <i>trans-m</i> -Br-PAT	27.94 \pm 1.5	0.0167*
(+)- <i>trans-m</i> -Br-PAT	62.52 \pm 10.1 (P = 0.020)	0.0022**

Figure 2-6. Structures of the (-)-*trans-para*-substituted PATs , where X = F,Cl,CH₃, or Br

Table2-3. WT HH₁R binding affinities of (+)- and (-)-*trans-para*-substituted PATs

Compound Name	Histamine H ₁ Affinity in nM (K _i ± S.E.M.) and P-values for enantiomeric comparison	P-value compared to parent enantiomer (e.g.(-)- or (+)- <i>trans</i> -PAT)
(-)- <i>trans-p</i> -CH ₃ -PAT	17.33 ± 2.7	0.0008**
(+)- <i>trans-p</i> -CH ₃ -PAT	11.30 ± 1.03 (P = 0.0018)	0.0068**
(-)- <i>trans-p</i> -F-PAT	4.07 ± 0.5	0.054
(+)- <i>trans-p</i> -F-PAT	8.268 ± 0.6 (P = 0.0098)	0.026*
(-)- <i>trans-p</i> -Cl-PAT	8.38 ± 1.10	0.036*
(+)- <i>trans-p</i> -Cl-PAT	6.08 ± 0.75 (P =0.2378)	0.022*
(-)- <i>trans-p</i> -Br-PAT	1058.2 ± 53.0	0.0025**
(+)- <i>trans-p</i> -Br-PAT	531.8 ± 62.1 (P = 0.0232)	0.015*

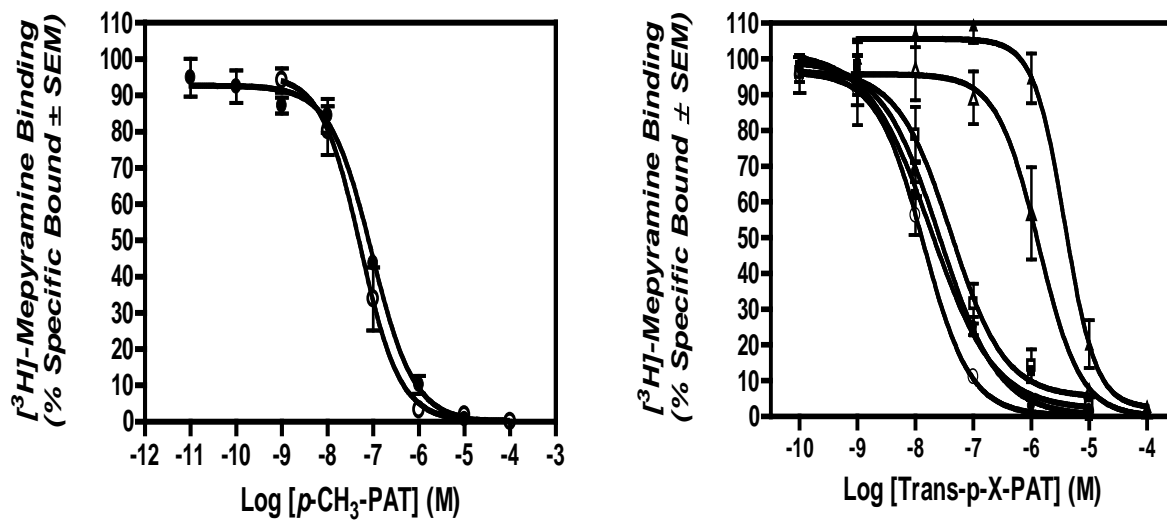


Figure 2-7. Representative HH₁R competitive binding curves for (+)- and (-)-trans-*para*-substituted PATs. A) (●) represents (-)-*trans*-*p*-CH₃; (○) represents (+)-*trans*-*p*-CH₃. B) (-)-*trans* (●) & (+)-*para*-F-PAT (○), (-)-*trans* (■) & (+)-*trans*-*para*-Cl-PAT (□), and (-)-*trans* (▲) & (+)-*trans*-*para*-Br-PAT (△)

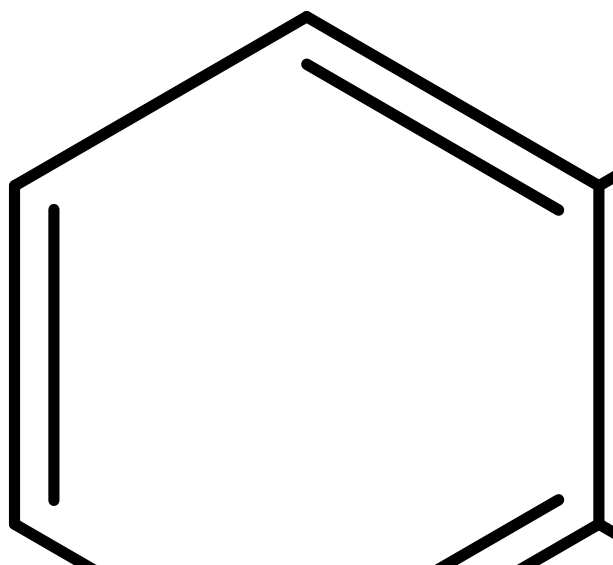


Figure 2-8. Structures of N-alkylated-PAT derivatives. The names of the compounds are as follows; top row: *trans*-N,N-diethyl-PAT (left), *trans*-trimethyl-PAT (center), *cis*-trimethyl-PAT (right), center row: *trans*-N-methyl-N-allyl-PAT (left), *trans*-N,N-diallyl-PAT (center), *trans*-N-allyl-PAT (right), bottom row: NH₂-PAT (left), and N-methyl-PAT (right).

Table 2-4. Histamine H₁ binding affinities of N-alkyl substituted PAT analogues

Compound Name	Histamine H ₁ Affinity in nM (K _i ± S.E.M.)
(-)- <i>trans</i> -N,N-diethyl-PAT	8.589 ± 0.53
(+)- <i>trans</i> - N,N-diethyl-PAT	193.761 ± 3.3
(±)- <i>trans</i> -N ⁺ (CH ₃) ₃ -PAT	120 ± 15
(±)- <i>cis</i> - N ⁺ (CH ₃) ₃ -PAT	107 ± 4.1
(±)- <i>trans</i> -NCH ₃ (C ₃ H ₅)	3.4 ± 0.3
(±)- <i>trans</i> -N(C ₃ H ₅) ₂	10.2 ± 1.7
(±)- <i>trans</i> -NH(C ₃ H ₅)	45 ± 11
(±)- <i>trans</i> -NH ₂ -PAT	1270 ± 92
(±)- <i>trans</i> -NH(CH ₃)-PAT	112 ± 31

Figure 2-9. Proposed interaction of aspartic acid D3.32 with (-)-(left) and (+)- (right) *trans*-N,N-diethyl-PAT that may account for higher affinity of the (-)-enantiomer between the binding of (+) and (-)-*trans*-N,N-diethyl-PAT.

Figure 2-10. Structures of racemic di-OH and Cl-OH-PAT ligands

Table 2-5. Affinities of di-OH and Cl-OH PAT analogues at the WT HH₁R.

Compound Name	Histamine H ₁ Affinity in nM (K _i ± S.E.M.)
(±)- <i>trans</i> -di-OH-PAT	~ 20
(±)- <i>cis</i> -di-OH-PAT	24.5 ± 1.04
(±)- <i>trans</i> -7-OH-8-Cl-PAT	2.424 ± 0.44
(±)- <i>cis</i> -7-OH-8-Cl PAT	~ 150

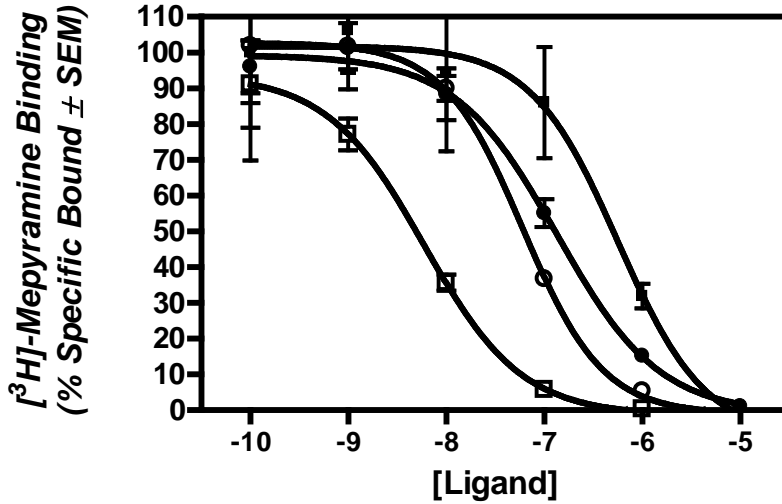


Figure 2-11. Representative competitive binding curves for di-OH and Cl-OH-PAT at the WT HH₁R. The ligands represented here are: *cis*-(±)-Cl-OH-PAT (○), and *trans*-(±)-Cl-OH (□), *cis*-(±)-di-OH-PAT (●), and *trans*-(±)-di-OH-PAT (■)

Figure 2-12. Proposed H₁pharmacophore and the ligands that are derived from it. Left to right (top row): the 1,1-diaryl-3-aminopropane moiety, (-)-trans-PAT structure superimposed on the 1,1-diaryl-3-aminopropane moiety, and acrivastine. Left to right (bottom row): hydroxyzine, triprolidine, and chlorphenamine.

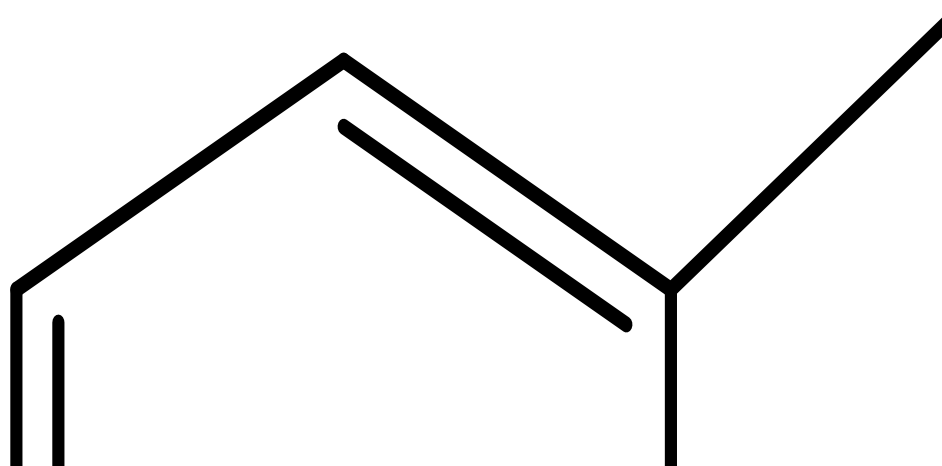


Figure 2-13. Structures for the ring substituted PAT derivatives: (-)-*cis*-PAB (top left), (-)-*trans*-PAB (top center), (-)-*trans*-COAT (right), (-)-*trans*-*m*-phenyl-PAT (bottom left), and (-)-*trans*-CAT (bottom right)

Table 2-6. Affinities of PAT analogues with modified tricyclic ring systems

Compound Name	Histamine H ₁ Affinity in nM (K _i ± S.E.M.)
(±)- <i>trans</i> -PAB	> 10,000
(-)- <i>cis</i> -PAB	57.5 ± 9.3
(+)- <i>cis</i> -PAB	300 ± 40
(-)- <i>trans</i> -CAT	1.58 ± 0.5
(+)- <i>trans</i> -CAT	1.7 ± 0.2
(-)- <i>trans</i> -COAT	432 ± 60
(+)- <i>trans</i> -COAT	> 10,000
(-)- <i>trans</i> - <i>m</i> -phenyl-PAT	213.0 ± 20.4
(+)- <i>trans</i> - <i>m</i> -phenyl-PAT	> 10,000

CHAPTER 3
INVOLVEMENT OF AMINO ACID RESIDUE Y5.48A IN THE
DIMERIZATION/FUNCTIONAL STABILIZATION PROCESSES OF THE HUMAN
HISTAMINE H₁RECEPTOR

Literature Review of Ballesteros Position 5.48

Interestingly, there has been little speculation in the literature about the amino acid residues in Ballesteros position 5.48, when compared to its neighboring positions like 5.42, 5.43, 5.46, and 5.47. In 5HT_{2A} receptors, which have about 70% TMD sequence structural homology to HH₁R's, this position (F5.48) is implicated in ligand binding. A mutation to a non-functional alanine residue resulted in a decrease in binding affinity, efficacy, and potency of 5-HT. F5.48A also reduced the binding affinity of α -methyl-5-HT, N- ω -5-HT and DOI (Shapiro et al. 2000, Roth et al. 2002). Shapiro's paper predicted that F5.48 played a role in stabilizing the aromatic residues around the binding pocket indirectly, by allowing neighboring amino acids to achieve their correct orientation for ligand binding. From the same paper, it is said that in a normal α -helical structure (4 amino acids per helix turn) it is not possible to have residues 5.46 and 5.48 both pointing into the binding pocket(Shapiro et al, 2000).

Residue 5.46 is known to be a key position when differentiating the pharmacology of the rat from the human 5HT_{2A} receptor, as well as in the binding of endogenous ligands at the H₁ and β ₂-AR (Smit et al., 1999; Carmine et al., 2004; Bhattacharya et al., 2008; Fang, Travers, and Booth., 2009 pre-publication). Polar residues inserted into this position in the rat 5HT_{2A}receptor, (S (human endogenous residue), T, and N) shift the pharmacological profile towards the human receptor (Kao et al. 1992, Johnson et al. 1994). Since ligand binding and the pharmacological profile are altered by mutations to this position, it follows that this particular residue is expected to face into the binding

pocket of the receptor. And by extension from the Shapiro 2000 paper, that position 5.48 does not. A second possibility is that position 5.48 is not directly involved in ligand binding, but is critical in stabilizing the GPCR in the proper conformation to bind its endogenous ligand. This result would manifest itself as a reduction in ligand affinity that could easily be misinterpreted as a direct interaction with the ligand in question.

In the β_2 -adrenergic receptor, position 5.48 is again occupied by a phenylalanine. In this case, the residue is not predicted to be within the binding pocket of the receptor. Even with the novel modeling technique LITiCON that allows rotation of the TMD helices based upon the most favorable interaction with the ligand, this position remains exterior to the binding pocket (Bhattacharya et al., 2008). These results mesh closely with the HH₁R, constructed through Rho homology modeling in our lab, and a second model with the homology to the newly solved β_2 -AR crystal structure. Both models demonstrate position 5.48 as an interface between the critical TMDs 5 and 6, and away from the binding pocket and.

To lend further credence to this hypothesis a series of proteomics studies were compiled from GPCR sequences by Weinstein's group out of Cornell. They used several different bioinformatics methods to compile the most likely interfaces for the formation of dimers and/or oligomers (Filizola and Weinstein, 2005). By studying the evolutionary relationship between the sequence of different GPCR's and eliminating the conserved residues known to be directly involved in ligand binding, the group was able to focus their search to residues that have the potential to be involved in dimer formation. Their predictions pointed to residues located in transmembranes 4-6. Specifically for aminergic receptors, which include the HH₁R, the most likely

dimerization residues as predicted by lipid exposure, fall within transmembrane 5-6 (Filizola and Weinstein, 2005). When all of the data from these studies was compiled, a histogram of the most frequently selected residues was assembled. The most frequently selected position turned out to be 5.48. At the time of the publication, there was no known data about the involvement of this particular residue in the dimerization/oligomerization of rhodopsin like GPCR's (Filizola and Weinstein, 2005). In fact, there is very little mutagenesis data that implicates specific amino acids in the dimerization/oligomerization process of class A GPCRs. The reported residues as of 2005 are I1.54 and V4.47 in chemokine receptors, C4.58 in the Dopamine 2 (D2) receptor, and G6.42 in the β 2-adrenergic receptor (Filizola and Weinstein, 2005). The predictions made in this paper lend further credence to our investigation of the Y5.48A mutation to the HH₁R, and help confirm this as a novel discovery.

Materials and Methods

The techniques and chemicals described in chapter two were used in this chapter as well. Any additional techniques that were employed are described below.

Measurement of PLC activity/[³H]-inositol phosphate formation

The methods for measurement of [³H]-IP was as described previously (Booth et al., 2002). HEK293 cells were transiently transfected with wild type or mutant receptors in 100-mm plates by following manufacturer's instructions with 12 μ g of plasmid DNA and 50 μ l of Lipofectamine 2000 (Invitrogen). Cells were aliquoted into wells of 12 or 24-well plates and labeled with 1 μ Ci/ml myo-[2-³H(N)]-Inositol in inositol-free DMEM medium (Chemicon D-101) with supplements of 5% dialyzed fetal bovine serum (Invitrogen Gibco 26400) and 1% nonessential amino acids overnight (approximately 12-24 hrs). Then cells were treated with drugs for 1 hrs with supplement of 35

mMLiCl and 10 μ M of pargyline. Accumulated inositol phosphates were released from cells by 50 mM formic acid incubated for 1 hr at room temperature. [3 H]-Inositol phosphates were separated by AG1-X8 columns (formate form) and eluted by 0.8 M ammonium formate into scintillation vials for counting. Data was analyzed using the nonlinear regression algorithm in Prism 5.02 (GraphPad Software Inc., San Diego, CA) and expressed as mean percentage of basal.

Due to variations in constitutive activity of the mutants, calculations were based on corresponding mutant basal receptor activity and presented as percentage of basal (%basal), not wild type basal receptor activity. Thus allowing comparisons to be made between the point mutations and the WT receptor.

Accumulation of [3 H]-Inositol phosphates by phosphoinositide hydrolysis were also measured by scintillation proximity assay (SPA) (Brandish et al., 2003; Bourdon et al., 2006). Transfected cells were labeled with 10 μ Ci/ml of myo-[2- 3 H(N)]-Inositol in inositol-free DMEM medium (Chemicon D-101) with supplements of 5% dialyzed fetal bovine serum (Invitrogen Gibco 26400-036), 2 mM glutamine and nonessential amino acids overnight. Then [3 H]-Inositol phosphates were detected 0.2mg/well of yttrium silicate RNA binding resin (Amersham Biosciences RPNQ0013, Piscataway, NJ). Radioactivity was quantified with reading at MicroBetaTriLux. Data was analyzed using the nonlinear regression algorithm in Prism 5.02 (GraphPad Software Inc., San Diego, CA) and expressed as mean percentage of basal, EC_{50} and E_{MAX} .

BRET Analysis

BRET constructs were made by subcloning Y5.48A (obtained from Booth) into H₁-eYFP/pcDEF3 and H₁Rluc/pcDEF3 (van Rijn et al., 2006). Sequence of all constructs was verified.

HEK-293 cells were transiently transfected in white 96-well plates with 50 ng GPCR-Rluc and 0-1000 ng GPCR-eYFP DNA/10⁶ cells using PEI (1:3). Total DNA was kept constant at 2050 ng/10⁶ cells by supplementing with empty plasmid. Two days after transfection, the culture medium was replaced with 50 μ L PBS and eYFP fluorescence was measured in a Victor 3 plate reader (ex @ 485 nm; em @ 535 nm). Next, 50 μ L PBS supplemented with 10 μ M coelenterazine H was added, and bioluminescence (em @ 460 nm) and a BRET signal (em @ 535 nm) was recorded after 5 minute incubation. Corrected BRET ratio is $(BRET/Rluc)_x - (BRET/Rluc)_0$. Where "x" was cotransfection of Rluc and eYFP, and "0" transfection of only Rluc. YFP/Rluc corrected is the YFP/Rluc ratio minus the lowest YFP/Rluc (left-shifted curve). BRET_{Max} and BRET₅₀ values are fitted by one-site binding (hyperbola) using GraphPad Prism 4. This technique and its data analysis were performed by Dr. Henry Vischer, a collaborator of ours from Vrije university in Amsterdam.

Experimental Results and Discussion

Saturation Binding Assay Results

The following results are discussed based on the finding that that ³H- (-)-trans-PAT binds preferentially to H₁ dimers, while the radioligand ³H-mepyramine binds to H₁ monomers and dimers (Booth et al., 2004). Investigation into the Y5.48A point

mutations was begun by quantifying the transiently transfected receptor level with the standard H₁ radioligand ³H-mepyramine. All data is reported as the mean ± the standard error of the mean (S.E.M), unless otherwise noted. Results produced a B_{MAX} of 3.085 ± 0.65 pMol/mg protein and a K_D value of 1.790 ± 0.18 nM for the Y5.48A receptor. When contrasted with the H₁ wild type (WT) receptor using a t-test, which has a B_{MAX} of 2.981 ± 0.5 nM and a K_D of 1.024 ± 0.22 nM, the resulting p-values were P = 0.89 and P = 0.40, respectively. Neither the difference in B_{MAX} values, nor the K_D values of ³H-mepyramine at the WT and Y5.48A point mutated receptor breaks the bottom significance level of P < 0.05. Taken together, these results indicate that there is no difference in the receptors ability to bind mepyramine effectively, or in its ability to express at the cell surface. Actual saturation binding curves are shown below in figure 3-1 and B_{max} and K_D values for WT and Y5.48A are tabulated in table 3-1.

These results were not in themselves surprising, given that this particular point mutation is oriented away from the ligand binding pocket. However, when our radioligand ³H-(-)-*trans*-PAT was tested with identical membrane preparations, in the same exact plate as the successful ³H-mepyramine saturation assay, a complete loss of ligand binding was observed. This was initially explained away as a failed experiment, or a batch of protein that had denatured. After several repetitions, with protein concentrations ranging from 0.01-0.1 mg/mL of transiently transfected protein, the result was confirmed ³H-(-)-*trans*-PAT was unable to bind to the Y5.48A point mutated HH₁R at concentrations up to 10nM. Representative saturation isotherms for (-)-*trans*-PAT at various protein concentrations are also located in figure 3-2. For a point of comparison, ³H-(-)-*trans*-PAT is able to bind to the WT H₁ receptor with high affinity. It

possesses a B_{MAX} of 0.345 ± 0.06 pMol/mg protein and a K_D value of 1.34 ± 0.34 nM in transiently transfected HEK-293 cells. Data is displayed below in figure 3-2.

The WT B_{MAX} values differ slightly from those published in Baaker et al. 2004, and from Booth et al. 2001. Although, it should be noted that the HH_1R was expressed in a different cell line in each of those papers. They expressed the HH_1R in COS-7, an African green monkey kidney cell, and in Chinese Hamster Ovary (CHO) cells respectively. In these experiments, the HH_1R is expressed in Human Embryonic Kidney cells (HEK-293).

The use of various cell lines over the course of our investigation has told us that receptor expression levels can vary significantly between cell lines. K_D values remain constant despite the receptor level, as they are dependent upon the sequence of the receptor, which does not vary with the cell line. This makes B_{MAX} comparisons rather difficult, especially with transient transfections, where expression levels can vary based upon: the health of the cell, the passage number, how effectively the cDNA is taken up, and the amount of cDNA that is used for the expression (Dimond, 2007). Fortunately, it has been observed that 3H -(-)-*trans*-PAT consistently labels one-seventh of the entire HH_1R population that is identified by 3H -mepyramine. This has remained true across CHO and COS-7 cells and has served as an internal control to confirm proper 3H -(-)-*trans*-PAT binding (Booth et al., 2001.;Baaker et al., 2004). Based upon the above results, this ratio is confirmed in HEK-293 cells, and lends credence to the WT binding results for both 3H -Mepyramine and (-)-*trans*-PAT.

The Y5.48A saturation results are more difficult to interpret. The previous molecular determinants obtained through mutagenesis studies indicate very similar

binding pockets for (-)-*trans*-PAT and mepyramine. In fact, Y5.48A is the first mutation examined by our lab to produce differing effects for the two ligands. Every other mutation examined produced either no effect on ligand binding, or caused the loss of both (-)-*trans*-PAT and mepyramine binding. The positions that resulted in a complete loss of radioligand binding were D3.32A, Y3.33A, W4.56A, F5.47A, W6.48A, and F6.52A. These interactions have been previously confirmed for ³H-mepyramine by Wieland et al. in 1999. Based upon these mutagenesis results, it was inferred that (-)-*trans*-PAT and mepyramine are interacting with a similar set of residues. They engage the critical D3.32A residue in TMD 3, possess an interaction with W4.56A, and engage the cluster of aromatic amino acids in TMDs 5 and 6. The loss of (-)-*trans*-PAT binding at Y5.48A, caused us to re-evaluate that position. As detailed earlier, it was previously established that (-)-*trans*-PAT is a domain-swapped dimer preferring ligand that binds a subset of the overall H₁ receptor population. Therefore, it was postulated that Y5.48A somehow disrupts the formation of these dimers, causing the observed loss of ³H-(-)-*trans*-PAT binding.

Competitive Binding Experiments

In order to follow up on these binding results properly, it was necessary to further probe the binding of a variety of H₁ ligands to this point-mutated receptor. Instead of continuing experiments involving high levels of expensive radioligands, competitive binding assays using ³H-Mepyramine, whose binding affinity is unaffected by this mutation, were performed. The logical starting compounds were (-)-*trans*-PAT and the endogenous agonist histamine. A diverse series of HH₁R ligands were included in these experiments including: the inverse agonist mepyramine, the endogenous agonist histamine, and an enantiomer and a diastereomer of (-)-*trans*-PAT. The PAT

enantiomer and diastereomer are (+)-trans-PAT and (-)-cis-PAT, respectively. They represent the two most potent PAT stereoisomers, after the lead compound (-)-trans-PAT. Structures for these compounds are found below in figure 3-3.

The binding profile of histamine is altered when compared to the WT HH₁R. At the WT histamine has a K_i of about 3 μM, while at Y5.48A that value is reduced significantly to 15.8 ± 3 μM (P = 0.0067**). This reduction in affinity cannot be due to a direct interaction with the ligand as previously detailed, a more likely explanation is that the native conformation of TMD 5 is altered by this mutation. The critical binding residues K5.39, T5.42, and N5.46 are all very close to this mutation, and any perturbation to the helical structure is likely to cause a reduction in affinity. Competitive binding of mepyramine was affected as well, but only slightly. The WT K_i of 2nM, was reduced to 4.905 ± 1.2 nM (P = 0.026*). As expected for a ligand with minimal interactions with TMD 5, there is only a slight reduction in the ability of the Y5.48A HH₁R to bind mepyramine.

As expected from the saturation binding results, there is a significant reduction in the ability of (-)-trans-PAT to bind to the Y5.48A mutant. At the WT HH₁R, (-)-trans-PAT displaces ³H-mepyramine quite effectively, evidenced by its K_i value of 1.95 ± 0.51 nM. When Y5.48A is considered, the K_i value drops approximately 100-fold to 148.4 ± 5.4 nM, when a t-test was performed to determine significance the resulting value was P = 0.0014**. Indicating that this reduction in affinity is quite significant when compared to the WT receptor. The next ligands investigated were the two stereoisomers of PAT, (-)-cis-PAT and (+)-trans-PAT. K_i values at the WT receptor are 13.7 ± 0.2 nM and 29.8 ± 4.0nM, respectively. Data from Y5.48A, indicates that both stereoisomers drop in affinity

by about 10-fold. (-)-cis-PAT drops to 143.6 ± 0.6 nM at Y5.48A, with a P value of 0.0003***. Affinity of (+)-trans-PAT falls to 245.5 ± 19.2 nM, a t-test revealed $P = 0.021^*$. Each of the PAT isomers that were investigated showed a significant drop ($P < 0.05$) in their ability to displace the radioligand. The curves displaying this data are demonstrated below in figure 3-4, and data is tabulated in table 3-2.

These results indicate that (-)-trans-PAT possesses the largest drop in affinity for the Y5.48A point mutation. It is significant to note that if one considered only the P-values for each of these ligands, it would erroneously be concluded that (-)-cis-PAT is the ligand that is most affected by Y5.48A, since it has the lowest P-value for the WT Y5.48A comparison. P-values can be considered when evaluating the difference between two sample populations and are useful for determining how different two populations are, however they must be used carefully. They should not be used to make conclusions about anything beyond the two populations that are being directly compared.

For example, it can be concluded that there are significant differences between the binding of (-)-trans-PAT at the WT and Y5.48 HH₁R, and that the same is true for (-)-cis-PAT. However, the statement that (-)-cis-PAT is more strongly affected by Y5.48A than (-)-trans-PAT would be incorrect; despite the fact that (-)-cis-PAT has a smaller p-value (0.0003 vs. 0.0014). In fact, the affinity of (-)-trans-PAT is reduced 100-fold at Y5.48A, while (-)-cis-PAT affinity was lowered by a factor of 10. Therefore, when examining the trends between different compounds at differing receptors, one should consider not only the significance value that the data generates, but also the overall magnitude of affinity gain or reduction as well.

The smaller p-value generated by (-)-cis-PAT can be explained by the very small standard deviation values for those experiments. The t-value for a given data set is inversely proportional to the square of the standard deviations (S_{X1} and S_{X2} shown below). This gives standard deviation a very strong influence over the value generated by the t-test. Since the standard deviation values generated by the (-)-cis-PAT data are miniscule, there is less chance of the WT and Y5.48A data overlapping, and validating the null hypothesis. This results in an exaggerated significance value and explains the very low p-values observed in these experiments.

T-test for significance

$$t = \frac{\bar{X}_1 - \bar{X}_2}{\sqrt{\frac{2}{n} * \sqrt{\frac{S_{X1}^2 + S_{X2}^2}{2}}}}$$

Inositol Phosphate Production Mediated via $G_{\alpha Q}$

Interpreting these results with binding data alone proved quite difficult, so functional experiments were performed. The HH_1R displays functional selectivity, like many other GPCR's, signaling through both $G_{\alpha Q}/IP_3$ and $G_{\alpha S}/cAMP$. In the periphery of the body the $G_{\alpha Q}/IP_3$ signaling cascade, which has made HH_1R receptors synonymous with allergic responses, is the dominant pathway (Leurset et al., 1995; Moniri et al., 2004). Our investigation was begun at the $G_{\alpha Q}/IP_3$ pathway, using the endogenous agonist histamine. At the WT HH_1R , the function of histamine through $G_{\alpha Q}$ has been well established. From my work at the WT receptor, it has been established that histamine has an EC_{50} value of $0.159 \pm 0.024 \mu M$ with an E_{MAX} of $401.1 \pm 81\%$ basal. This value meshes closely with EC_{50} values found in the literature for the human H_1R (Seifert et al., 2003; Xie et al., 2006). It should be mentioned that histamine is an unusual ligand, since

it has a K_i value in the μM range, yet is able to activate its receptor easily at concentrations 10x lower than the K_i (Xie et al., 2006). This discrepancy highlights an important point that binding affinity (K_i) and functional activity (EC_{50} or IC_{50}) do not always correlate and should be analyzed separately.

When Y5.48A is examined in the $\text{IP}_3/\text{PLC}/\text{G}_{\alpha\text{Q}}$ assay with histamine, the receptor is clearly able to function. The EC_{50} value is reduced at least 50-fold to $8.028 \pm 0.66 \mu\text{M}$, resulting in a significant P-value of 0.0003^{***} . Interestingly, the E_{Max} for the receptor, $340.9 \pm 53.5\%$ basal, is unperturbed when compared to the WT ($P = 0.54$). To ensure that the difference observed between the WT and Y5.48A receptors was indeed significant, an ANOVA analysis was performed in GraphPad prism 5.0 to compare the entire curves. Similar to the t-test that was performed with the EC_{50} and E_{Max} values, the ANOVA analysis revealed a significant difference between the WT and Y5.48A functional curves and resulted in a P-value of 0.0042^{**} . The observed reduction in histamine efficacy indicates that there is some perturbation to the receptor caused by the Y5.48A mutation. This perturbation is unlikely to be caused by a direct residue-ligand interaction, because histamine is a rather small ligand and this mutation does not face into the binding pocket of the receptor. It is more likely the mutation alters the conformation, structure, or the stability of the receptor, to cause the observed reduction in efficacy. It should be noted that Y5.48A is located very near a series of residues that are known to be critical for histamine binding. K5.39, T5.42, and N5.46 are all located within two helical turns of Y5.48A. If position 5.48 is involved in stabilizing the helix, its removal could destabilize the helical structure, preventing dimerization from occurring and altering the binding of ligands that interact with TMDs 5 and 6.

The unchanged E_{Max} value between the WT and Y5.48A HH₁R's suggests that the receptor is still fully functional, but its ability to recognize and efficiently respond to its endogenous agonist is diminished. Compiled EC_{50} and IC_{50} for these IP₃ experiments can be seen for histamine and (-)-*trans*-PAT in table 3-3. Representative plots are shown below in figure 3-5.

(-)-*trans*-PAT, which is an inverse agonist at the WT HH₁R, was the next ligand examined in the IP assay (Travers, Fang, and Booth., 2009 pre-publication). Quantifying inverse agonism responses is a much more laborious process than evaluating agonist response. In order to measure a signal, a receptor must first demonstrate a basal activity that is significant enough to be measured and the ligand must be potent enough to bind and reduce the observed basal level of activity. For these experiments, sensitivity is crucial and any methodology that possesses a lower limit of detection (LOD) should be employed.

For example, ³H-IP/PLC activity can be quantified through anion exchange columns or by binding to Scintillation Proximity Assay (SPA) beads. It is possible to evaluate 4-12 times as many samples with the SPA methodology, but it has a much lower LOD than the columns. After many replicates and inconclusive experiments, IC_{50} values were obtained for mepyramine and (-)-*trans*-PAT. At the WT receptor, mepyramine yielded an IC_{50} of 2.51 ± 0.4 nM with an I_{max} of $61.4 \pm 1.3\%$ basal. At Y5.48A, the IC_{50} and I_{max} values were 3.35 ± 0.3 nM and $63.49 \pm 3.2\%$ of basal activity. When IC_{50} and I_{max} values were compared between the WT and Y5.48A receptors, neither the potency, nor the efficacy broke the significance limit of $P < 0.05$ giving values of 0.22 and 0.65 respectively. A further analysis using ANOVA to compare the full

functional curves between WT and Y5.48A confirmed that there is no significant difference for mepyramine, with a P-value of 0.63. These data confirm that mepyramine is still able to bind to and activate the Y5.48A mutated HH₁R.

For (-)-*trans*-PAT, an IC₅₀ of 251.7 ± 18.2 nM, along with an I_{max} of $63.8 \pm 2.2\%$ basal was obtained at the WT receptor. Similar experiments at Y5.48A, yielded no change from basal levels of activity, regardless of the PAT concentration. ANOVA analysis was then used to confirm that this loss of inverse agonism is significantly different from the WT receptor. The p-value resulting from the ANOVA test showed that there was a statistically significant loss of function across the entire curve between the WT and Y5.48A receptors, with a P-value of 0.0012**. Suggesting that, at Y5.48A (-)-*trans*-PAT appears to lose its ability to function as an inverse agonist. When this finding is contrasted with the ability of histamine to fully activate the Y5.48A receptor and the ability of mepyramine to bind and function, the result is a ligand specific loss of function for (-)-*trans*-PAT at Y5.48A.

Given the ligand-specific loss of binding and function of (-)-*trans*-PAT, and the reduction in affinity of histamine at Y5.48A, it is clear that this point mutation has caused some significant structural alterations to the WT HH₁R. Whatever these modifications may be, they are able to generate a fully functioning receptor. As evidenced by histamine's ability to produce a similar E_{Max} value as the WT and the unaltered binding profile and functional profile of mepyramine. These facts shift the focus away from these ligands and toward the unique properties of (-)-*trans*-PAT.

As mentioned above, (-)-*trans*-PAT is a ligand with unusual pharmacology. The functional selectivity at the two main HH₁R functional pathways, inverse agonism at

G_{αQ} antagonism at G_{αS}, has yet to be duplicated by any other ligand in our lab. Previous studies have shown that (-)-*trans*-PAT labels only one-seventh of the HH₁R population that is expressed and that this ligand binds to domain-swapped dimers (Booth et al., 2002; Bakker et al., 2004). These facts coupled with the location of Y5.48A away from the intrahelical ligand binding pocket, and its hypothesized role in receptor dimerization suggest that Y5.48A is somehow preventing and/or hindering the HH₁R from creating domain swapped dimers. The loss of these dimers prevents (-)-*trans*-PAT from binding in a natural manner and as a result the subsequent function that ligand exerts upon the receptor is lost.

BRET Studies Comparing dimerization of the WT and Y5.48A H₁ Receptors

In order to address the dimerization hypothesis, we contacted some of our colleagues in Amsterdam who are experts in FRET and BRET. Rob Leurs and Henry Vischer investigated dimerization at the WT HH₁R using BRET, and compared the results to the point mutated Y5.48A receptor. Before discussing the data, a brief overview of BRET should be detailed. BRET is an acronym for Bioluminescence Resonance Energy Transfer and is a technique that is used to determine the proximity of two proteins. In this case, we are examining the ability of two GPCRs to assemble into a homodimer. BRET depends upon two different proteins that are attached to the N- or C-terminus of GPCRs. In these experiments a luciferase enzyme, from *Renilla reniformis* is used as the donor. This enzyme catalyses the reaction found in the formula below.

R. luciferase catalysis:



The acceptor of the photon of light is yellow fluorescent protein (YFP), which is fused to a second GPCR. When the two tagged GPCRs are cotransfected and assemble into a dimer, a transfer of energy takes place between the two attached proteins. The photon of light emitted by luciferase is transferred via resonance to YFP, which emits energy pertaining to a unique wavelength. This wavelength is monitored and can be correlated to a proximity between the two tagged receptor, reflecting GPCR dimerization. This effect can be measured as long as the acceptor and donor proteins are within 10 nanometers of each other.

When this technique was used to compare the WT and Y5.48A receptors the results showed no change between the WT and point mutated receptor. It was hypothesized that domain-swapped dimer formation would be impaired and would be observable through BRET. Unfortunately, the data indicated only slight differences in dimerization at WT and Y5.48A H₁ receptors. The BRET_{Max} values, which are similar to the B_{max} in a saturation isotherm, indicated a value of 0.125 ± 0.008 for the WT/WT homodimer and 0.107 ± 0.11 for Y5.48A/Y5.48A. These values were not significantly different, running contrary to the original hypothesis. However, upon reexamination of the Bakker 2004 paper that demonstrated domain-swapping at the HH₁R, it was observed that domain-swapped dimers, represented by the coexpressed D3.32A and F6.52A receptors, are a small subset of the H₁ receptor population. Mepyramine is able to label all H₁ receptors with a B_{max} of 21 ± 4 pMol/mg of protein. In contrast, (-)-*trans*-PAT labels only 3.4 ± 1.0 pMol/mg of protein, about 1/7th of the overall receptor population. Intriguingly, if 1/7th of the reported BRET_{Max} value for the WT receptor is removed, the resultant value is 0.107. This is the exact experimental value for the

Y5.48A/Y5.48A homodimer. Despite being statistically insignificant, these results, coupled with the loss of saturation binding and function of (-)-*trans*-PAT, suggest that domain-swapped dimers are lost, while contact dimers remain at the Y5.48A point-mutated HH₁R.

Summary

When all of the data for these experiments is compiled, the data reveals that Y5.48A is playing a significant role in the functional role of the HH₁R. The ligand specific loss of binding up to 10 nM of (-)-*trans*-PAT, coupled with its loss of inverse agonism suggested a ligand specific effect. The unaltered binding and functional profile of mepyramine, and the reduced, but measurable accumulation of IP₃ produced by histamine incubation confirm that this is indeed a ligand-specific phenomenon. Given the unique nature of this alteration of function, and the previous knowledge that PAT binds preferentially to domain-swapped dimers the logical conclusion is that the formation of domain-swapped dimers is significantly impaired and/or abolished at the Y5.48A HH₁R. BRET results were unable to confirm this result directly, but did confirm the existence of contact dimers at Y5.48A; in addition to lending indirect evidence towards this conclusion.

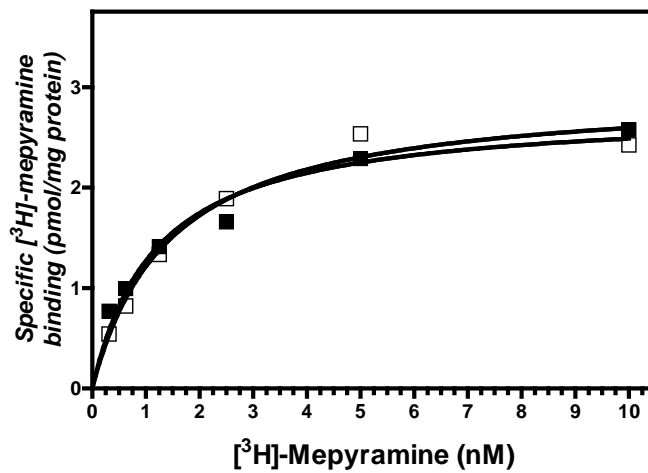


Figure 3-1. Saturation binding isotherms for ³H-mepyramine at the WT (■) and Y5.48A HH₁R (□) performed in transiently transfected HEK-293 cells

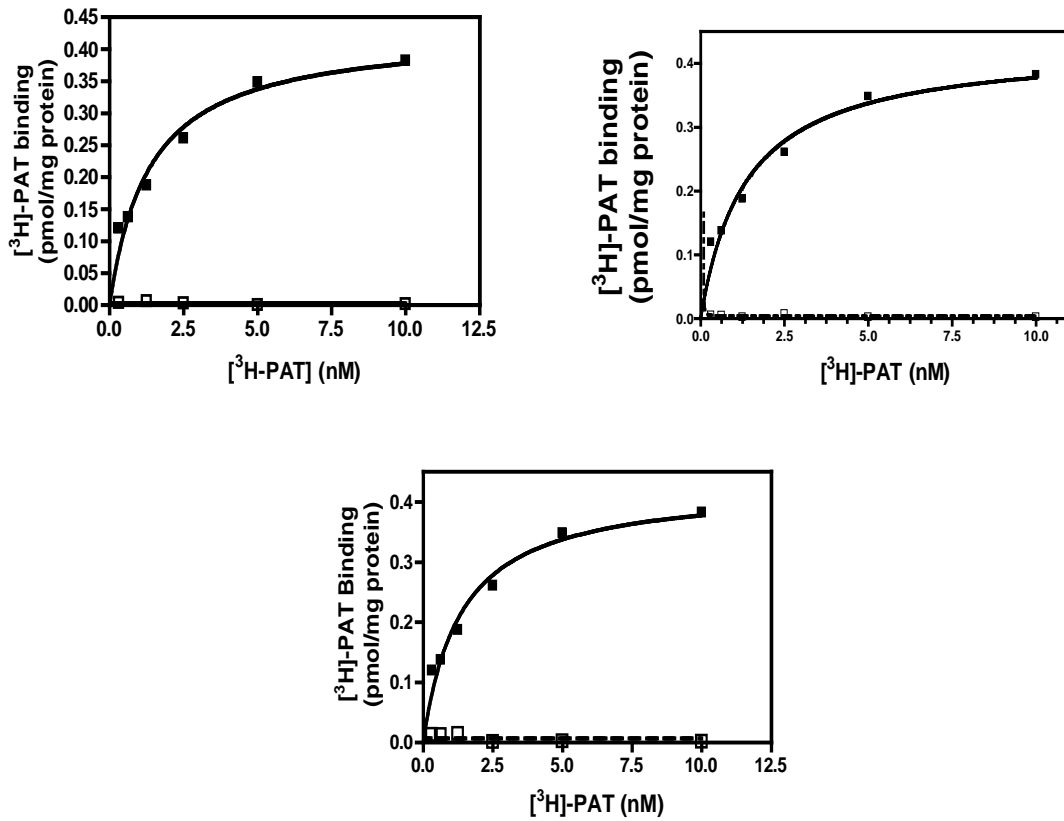


Figure 3-2. Saturation isotherms for ³H-(-)-*trans*-PAT labeled WT (■) and Y5.48A(□) HH₁ receptors. Transiently expressed in HEK-293 cells with varying protein concentrations. A) 0.01 mg/mL of protein. B) Depicts binding for Y5.48A at protein concentration of 0.02 mg/mL. C) Depicts binding for Y5.48A at protein concentration of 0.1 mg/mL

Figure 3-3. Structures of ligands examined in this section: (-)-*trans*-PAT (top left), mepyramine (top right), (-)-*cis*-PAT (left center), (+)-*trans*-PAT (right center), and histamine (bottom)

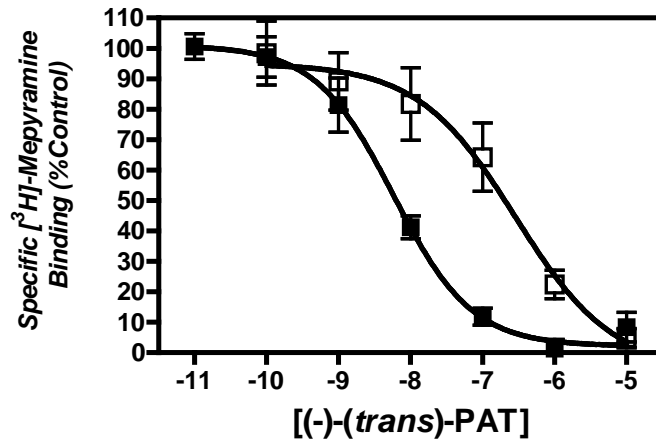


Figure 3-4. Competitive binding curves for (-)-*trans*-PAT at the WT (■) and Y5.48A (□)HH₁R

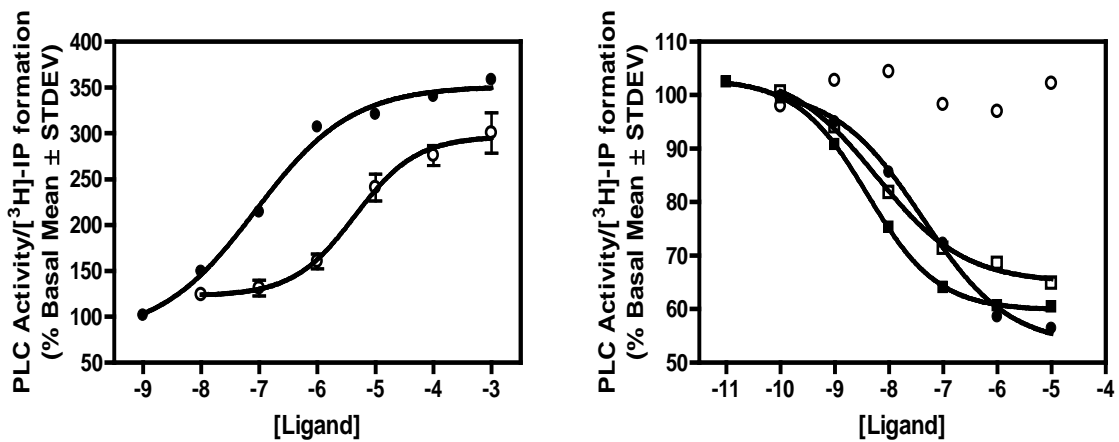


Figure 3-5. Ligand mediated PLC/IP₃ functional activity at WT vs. Y5.48A HH1 receptors. A) histamine at WT (●) and Y5.48A (○). B) (-)-*trans*-PAT at WT (●) and Y5.48A (○), and mepyramine at WT (■) and Y5.48A (□).

Table 3-1. Compiled K_D and B_{Max} values for 3H -mepyramine and (-)-trans-PAT at the WT and Y5.48A HH_1R .

HH_1R Receptor type	K_D value for 3H -mepyramine (nM)	B_{max} value for 3H -mepyramine (pMol/mg protein)	K_D value for 3H -(-)-trans-PAT (nM)	B_{max} value for 3H -(-)-trans-PAT (pMol/mg protein)
WT	1.024 ± 0.22	2.981 ± 0.5	1.34 ± 0.3	0.345 ± 0.06
Y5.48A	1.790 ± 0.18 (P=0.40)	3.085 ± 0.6 (P=0.89)	N/A	N/A

Table 3-2. Tabulated K_i values for the HH_1R ligands examined in this section at both the WT and Y5.48A point-mutated receptors.

Ligand	K_i value for WT HH_1R (nM)	K_i value for Y5.48A HH_1R (nM)	P-value comparing K_i at WT and Y5.48A
Histamine	3000 ± 280	15800 ± 3000	0.0067**
(-)-trans-PAT	1.95 ± 0.51	148.4 ± 5.4	0.0014**
(+)-trans-PAT	29.8 ± 4.0	245.5 ± 19.2	0.021*
Mepyramine	2.14 ± 0.4	4.905 ± 1.2	0.026*
(-)-cis-PAT	13.7 ± 0.2	143.6 ± 0.6	0.0003***

Table 3-3. Displays the correlated functional values for the ligands examined in the IP3/GαQ functional assay at the WT and Y5.48A HH_1R . The P-values that are listed with Y5.48A data compare that column to the WT HH_1R

Ligand	WT HH_1R EC/IC ₅₀ (nM)	WT HH_1R E/ I_{max} (% Basal response)	Y5.48A HH_1R EC/IC ₅₀ (nM)	Y5.48A HH_1R E/ I_{max} (% Basal response)
Histamine	159 ± 24	401.1 ± 80	8030 ± 660 (P=0.0003***)	340.9 ± 54 (P= 0.54)
(-)-trans-PAT	251 ± 0.77	63.8	N/A	N/A
Mepyramine	2.51 ± 0.4	61.4 ± 1.3	3.35 ± 0.4 (P=0.22)	63.49 ± 3.2 (P=0.65)

CHAPTER 4 PROBING THE ROLE OF RESIDUE Y7.53A IN THE LIGAND BINDING AND ACTIVATION OF THE HH₁R

Rationale for Undertaking These Studies and Literature Review

Contrary to the previous mutation Y5.48A, there is a litany of literature about position Y7.53A in aminergic GPCRs. In fact, Y7.53A has been investigated at α_{1B} and β_2 adrenergic receptors, and M₁ muscarinic receptors, all of which are closely related to the histamine H₁ receptor (Rosendorff et al., 2000). What makes this particular mutation so intriguing is the vast array of different results this mutation has produced. Everything from no change or slight increase in agonist affinity, to significant (150-fold) increase in agonist affinity has been observed when mutating this residue (Prioleau et al., 2002; Rosendorff et al., 2000). This result is rather surprising, given this residue is located at the cytoplasmic end of TMD 7 far away from the orthosteric binding pocket of class A GPCRs, this is demonstrated below in figure 4-1. Due to its location deep within TMD 7, this residue is going to have no direct effect on ligand binding, since it is too far away from the orthosteric binding pocket. Instead, any effects on ligand binding are likely to be due to alterations in the ability of G-protein to couple to the receptor, or alterations to the structure of TMD 7. If altered G-protein coupling were occurring, it would manifest itself as an alteration in affinity for agonists, with little to no change in inverse agonist affinity.

In addition to the effects on agonist affinity, Y7.53 has an incredible ability to influence GPCR signaling. A quick survey of current GPCR literature reveals Y7.53 mutations have been shown to produce constitutively active receptors with varying activities, a loss of G-protein coupling, and even receptor internalization (Rosendorff et

al., 2000 Prioleau et al., 2002). These results strongly suggest that Y7.53 is a critical residue in the activation processes of GPCRs that are closely related to the HH₁R.

A very interesting and novel concept with respect to the Y7.53A mutation is the concept of functional selectivity. Previous research has implicated this position as critical for GPCR function, G-protein coupling, and internalization (Rosendorff et al., 2000; Prioleau et al., 2002). To the best of my knowledge the concept of functional selectivity, and Y7.53A in general, has yet to be investigated at the HH₁R. Expanding these studies into the H₁ receptor will provide further information about the activation of class A GPCRs, while investigating a concept that is novel to the Y7.53 literature, functional selectivity. By making use of (-)-trans-PAT, (-)-cis-PAB, and histamine it will be possible to investigate ligands displaying functional selectivity at this residue.

By undertaking these studies, it is hypothesized that it will be possible to determine whether Y7.53 is critical to the activation of a single signaling pathway (G_{αQ} or G_{αS}), or is involved in the overall activation process of the human H₁ receptor (G_{αQ} and G_{αS}). Invoking the use of the library of PAT related compounds, in conjunction with traditional H₁ ligands like triprolidine and mepyramine, will allow the undertaking of a thorough Y7.53 study including the effects of inverse agonists, full agonists, and functionally selective ligands.

Materials and Methods

The techniques and chemicals described in chapters two and three were used in this chapter as well. PLC measurement and competitive binding assays were also used in the chapter. Any additional techniques that were employed are described below.

Measurement of AC activity/cAMP formation. HEK293 cells transfected and transiently expressing wild type and Y7.53A H₁ receptors were aliquoted into

microtubes, and preincubated for 5-10 minutes with 5 mM phosphodiesterase inhibitor 3-isobutyl-1-methylxanthine followed by treatments with drugs for 30 minutes in serum-free media. Cells were lysed by 0.1 M HCl for 20 minutes on ice and supernatants were used in the measurement of cAMP concentration with the Direct Cyclic AMP Enzyme Immunoassay Kit (Assay Designs Inc., Ann Arbor, MI). Data were expressed as mean percentage of control cAMP formation as obtained by linear standard curve extrapolation by GraphPad Prism version 5.02.

Experimental Results and Discussion

Competitive Binding Studies at Y7.53A

Competitive binding assays have been completed for (-) and (+)-*trans*-PAT, triprolidine, mepyramine, (-)-*cis*-PAB and histamine at WT and Y7.53A HH₁Rs. As was observed with other agonists, Y7.53A produced an increase in affinity for the endogenous agonist histamine. Its affinity was $1.0 \pm 0.1 \mu\text{M}$ at Y7.53A, increased 3-fold from a WT affinity of $2.99 \pm 0.28 \mu\text{M}$ at WT receptors. This increase in affinity was significant yielding a $P = 0.0014^{**}$. In contrast, (-) and (+)-*trans*-PAT both demonstrated a slight loss in affinity from WT, yielding K_i values of 2.6 ± 0.53 and $64 \pm 14 \text{ nM}$, respectively. When the K_i values for the PAT ligands were compared to the WT receptor via the T-test, it was observed that there were no differences ($P > 0.05$) between any of these ligands and the WT receptor. Representative binding curves can be found in figure 4-1, and the binding affinities for all compounds studied at WT and Y7.53A HH₁Rs, as well as their P-values can be found in table 4-1.

In addition to the ligands mentioned above, the affinities of the partial agonist (-)-*cis*-PAB and the inverse agonists mepyramine and triprolidine were assessed. Mepyramine and triprolidine yielded K_i values of 2.14 ± 0.6 and 1.25 ± 0.2

nM respectively. When compared to the WT values in the literature, these compounds yielded P-values greater than 0.05, indicating no significant differences in binding of these ligands between Y7.53A and the WT HH₁R. The last ligand that was investigated was the partial H₁ agonist, (-)-*cis*-PAB. At the Y7.53A point mutated receptor, PAB produced a reduced affinity of 233.3 ± 18 nM, which was significantly different from the WT yielding a p-value of 0.012*. Representative binding curves for these data can be found in figure 4-2.

Taken together these results mesh quite well with previous publications studying Y7.53 at receptors that are closely related to the HH₁R. An increase in agonist affinity was previously observed at Y7.53 point mutations in the M1 muscarinic receptor, as well as the 5HT_{2C} receptor (Rosendorff et al., 2000; Prioleau et al., 2002). Prioleau's paper showed a 2 to 6 fold increase in agonist affinity for 5HT_{2C} receptors, which is consistent with the findings observed for histamine (3-fold increase). In addition both papers demonstrated that inverse agonists for 5HT_{2C} receptors showed no change in affinity when Y7.53 is mutated. This result holds true for H₁ receptors as well, given that (-)-*trans*-PAT, (+)-*trans*-PAT, mepyramine, and triprolidine all show no statistical difference from their WT values. The perturbation to PAB's K_i is more puzzling, but is likely caused by perturbations to the native structure of TMD 7.

Inositol Phosphate Production Mediated via G_{αQ}

In order to investigate this hypothesis a thorough functional study was undertaken involving the functionally selective PAT ligands, traditional H₁ ligands, and the endogenous agonist histamine. These IP₃/G_{αQ} functional studies have been completed with histamine, traditional H₁ inverse agonists mepyramine and triprolidine, and several ligands from the PAT family including (-)-*trans*-PAT. Unfortunately, no response was

observed for the H₁ partial agonist (-)-*cis*-PAB after six separate experiments, where histamine produced a reproducible curve. This is likely due to the small window of activation for the Y7.53A receptor. Even the full IP₃ endogenous agonist histamine, produces only a 40% increase over basal, as opposed to a 400% increase at the WT receptor. Despite the high limit of detection for the column method of measuring inositol phosphates, accurately measuring a partial agonist response that is conservatively estimated at around 20% of basal proved to be too tall a task.

The EC₅₀ value for histamine at Y7.53A was $1.515 \pm 0.3 \mu\text{M}$ reduced approximately ten-fold from the WT value of 0.157 ± 0.012 . When these values are compared in a t-test the resultant P-Value is 0.0099**, indicating a significant dichotomy in the ability of histamine to activate G_{αQ}. Comparing the E_{max} signals between WT and Y7.53A revealed an even more interesting trend. As demonstrated in figure 4-2 below, a nearly five-fold reduction in efficacy is observed between Y7.53A and the WT receptor. The E_{max} at the WT receptor is $401.1 \pm 81\%$ basal, while Y7.53A gives an E_{max} of $143 \pm 8.0\%$, yielding a P < 0.0001***. These results indicate that histamine is less effective at activating the receptor, in terms of both efficacy and maximal response, despite having a higher binding affinity for the receptor. This is strongly suggestive of a reduction in the ability of G_{αQ} to couple to the receptor at the Y7.53A point mutation. Given the reduction of both efficacy and affinity at the HH₁R, the location of Y7.53 deep within TMD 7, and the previously reported works at closely related class A GPCR's, the Y7.53A point mutation drastically reduces the ability of the HH₁R to couple to G_{αQ}.

To build upon the binding results, mepyramine and (-)-*trans*-PAT, both of which act as inverse agonists, were examined in these functional experiments. (-)-*trans*-PAT

yielded an IC_{50} value of 225 ± 30 nM at Y7.53A and 251.7 ± 18 nM at the WT receptor, giving a $P = 0.62$. Mepyramine gave an IC_{50} of 2.2 ± 0.6 nM at Y7.53A, which was nearly identical to the WT value of 2.51 ± 0.8 nM. A t-test for significance yielded a p-value of 0.75. A t-test of the I_{max} values for both ligands revealed the values were unchanged from the WT HH_1R . At Y7.53A, mepyramine produced an I_{max} of $61.4 \pm 1.3\%$ basal ($P=0.75$), while (-)-*trans*-PAT yielded a value of 59.9 ± 6 ($P=0.51$). Representative functional curves for these data can be found in figure 4-3. These findings are identical to the established literature for Y7.53 mutations that demonstrate that the affinity of inverse agonists is unchanged when compared to the WT $5HT_{2C}$ receptor (Rosendorff et al., 2000; Prioleau et al., 2002).

To the best of my knowledge the comparison of the WT IC_{50} values for inverse agonists, to those at Y7.53A is a novel investigation at the H_1 receptor. The results of which shed light on the effects that reduced G-protein coupling has on the efficacy of inverse agonists. Based upon the findings listed above, the reduced G-protein coupling at Y7.53A has no effect on the functional response of inverse agonists at the HH_1R . This result fits well with our understanding of inverse agonists from current GPCR theory. Inverse agonists reduce the basal level of signalling by inducing, selecting, or stabilizing a conformation of the receptor that does not favor g-protein coupling. It seems that the reduced ability of Y7.53A to couple with $G_{\alpha Q}$ does not have an affect on the ability of inverse agonists to reduce basal signalling. It should also be noted that a similar effect was observed for the $5HT_{2C}$ inverse agonist, SB206553, hinting at strong similarities in the activation relays between the two closely related receptors (Rosendorff et al., 2000).

AC Activity/cAMP Formation Mediated via G_{αS}

To further investigate the effects of Y7.53A on HH₁R function, the ability of histamine to stimulate cAMP formation was assessed. At the WT HH₁R histamine has an EC₅₀ of 1.41 ± 0.14 μM and an E_{max} of 250 ± 33 % basal cAMP accumulation. When identical experiments were performed with the Y7.53A HH₁R there was no increase over basal signaling observed. Indicating the ability of G_{αS} to couple to the HH₁R has been abolished. Representative functional curves for WT and Y7.53A can be found in figure 4-4. The loss of the ability of histamine mediated cAMP production at Y7.53A stands in stark contrast to the reduced, yet measurable accumulation of IP₃ with the same ligand. Since the mutation is the same, there are no differences in binding of histamine to the receptor, and any change in ligand binding must be due to the binding of the G-protein. This strongly implicates the G-protein in the lack of cAMP production. Previous literature has suggested that Y7.53 mutations can uncouple the G-protein from the receptor and it appears that this is what is occurring with G_{αS}.

Summary

It has previously been suggested that this mutation can uncouple the G-protein from the receptor (Rosendorff et al., 2000). These experiments suggest that a similar result is taking place at the HH₁R and G_{αS}. This is supported by the fact that histamine is able to bind Y7.53A, and is able to function, albeit with reduced efficacy, via G_{αQ} to produce inositol phosphates. It is an intriguing finding that G_{αS} and G_{αQ} show unique results when examined at Y7.53A in functional assays. Previous literature suggested that G-proteins could not couple as effectively to the receptor when the tyrosine residue at Y7.53 was lost, but neglected to examine the concept of two different G-proteins coupling to the same receptor (Rosendorff et al., 2000; Prioleau et al., 2002). From

these experiments it can be inferred that $G_{\alpha S}$ and $G_{\alpha Q}$ have unique affinities for the Y7.53A mutation, and that these affinities differ from the native H_1R . $G_{\alpha Q}$ appears to have a reduced affinity for the Y7.53A receptor, indicated by its weakened ability to stimulate IP_3 formation; while all histamine signaling through $G_{\alpha S}$ is lost indicating a lack of receptor coupling. Since the Y7.53A receptor is going to have identical conformations presented to both G-proteins, it can be said that $G_{\alpha S}$ and $G_{\alpha Q}$ must have differing affinities. This concept fits well with our understanding of functional selectivity and hints that native receptor conformations preferred by $G_{\alpha S}$ and $G_{\alpha Q}$ should be distinct from one another. By extension, it would seem plausible that multiple binding modes could exist for the same ligand; and that the conformation selected/or induced by the ligand may be influenced by the G-protein to which the receptor is coupled. These distinct conformations would allow ligands to stabilize, induce, and/or select a receptor conformation that preferentially targets one G-protein over another, providing a possible molecular explanation for the phenomenon known as functional selectivity.

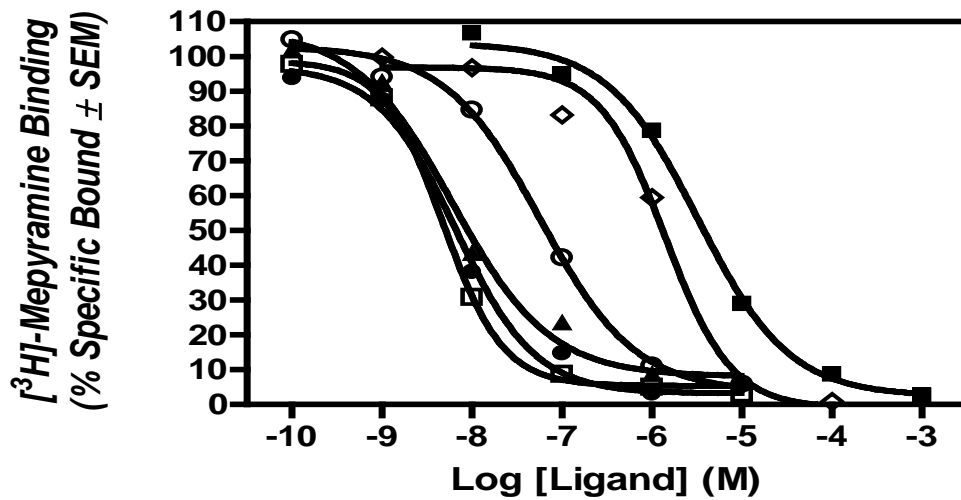


Figure 4-2. Representative competition binding curves for various H₁ ligands at the Y7.53A point mutated receptor: (-)-*trans*-PAT (●), (+)-*trans*-PAT (○), histamine (■), mepyramine (□), triprolidine (▲), and (-)-*cis*-PAB as (◇).

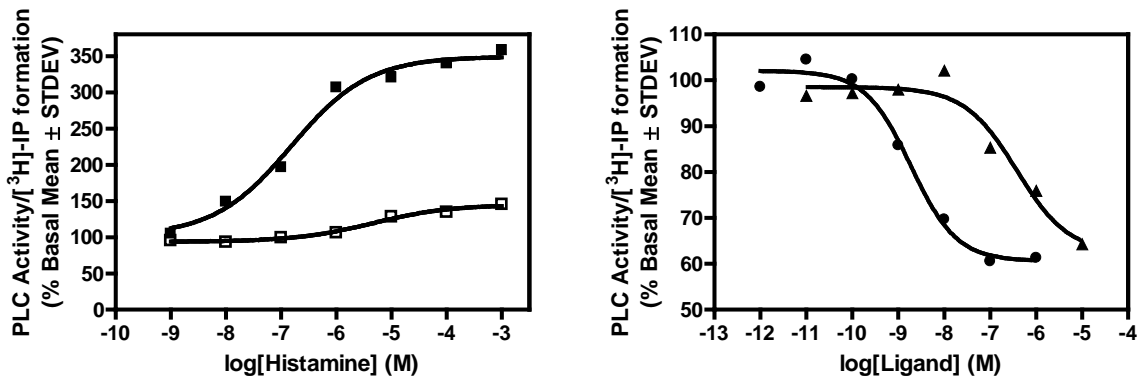


Figure 4-3. Representative G_{αQ}/PLC functional curves for H₁ ligands at the Y7.53A HH₁R. A) histamine at WT (■) and Y7.53A (□) receptors. B) mepyramine (●) and (-)-*trans*-PAT (▲).

Table 4-2. Tabulates the EC/IC₅₀ and E/I_{max} values of various ligands at the WT and Y7.53A point mutated receptors

Ligand	WT HH ₁ R EC/IC ₅₀ (nM)	WT HH ₁ R E _{max} /I _{max} (% Basal response)	Y7.53A HH ₁ R EC/IC ₅₀ (nM)	Y7.53A HH ₁ R E _{max} /I _{max} (% Basal response)
Histamine	159 ± 24	401.1 ± 81	1510 ± 300 (P=0.0003***)	143 ± 8.0 (P<0.0001***)
(-)- <i>trans</i> -PAT	251.8 ± 18	63.8 ± 2.2	225 ± 30 (P=0.62)	59.9 ± 6 (P=0.51)
Mepyramine	2.51 ± 0.4	61.4 ± 1.3	2.2 ± 0.46 (P=0.75)	61.4 ± 1.3 (P=0.65)

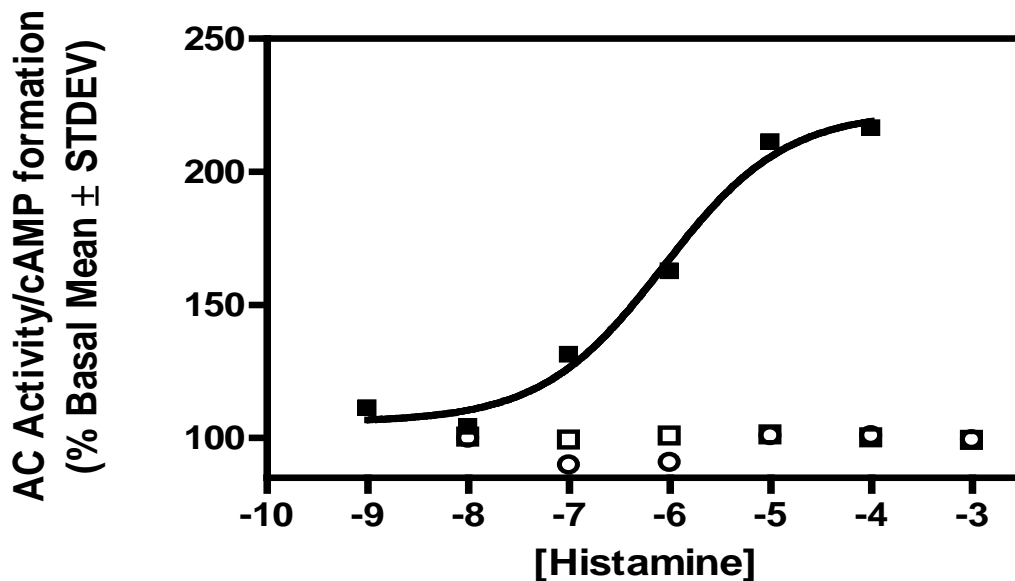


Figure 4-4. Representative cAMP/AC functional curves for histamine stimulation at WT (■) and Y7.53A (□ = assay 1) and (○ = assay 2) HH₁R.

CONCLUDING REMARKS

It is my hope that these studies of the HH₁R have advanced the understanding of how H₁ ligands bind to and activate the receptor. The unique binding and functional profile of (-)-*trans*-PAT represents a new class of ligand and understanding its subtle nuances will provide a basis for studying other ligands possessing functional selectivity at other GPCRs. The ability of this ligand to inhibit the PLC/IP signaling pathway and activate the AC/cAMP at the same receptor is a rare therapeutic quality. In this particular case, the unfavorable PLC/IP pathway that causes allergic responses is inhibited, while the pathway with therapeutic potential to stimulate neurotransmitter synthesis is activated. This unusual ability to activate the therapeutic pathway at the HH₁R and inhibit the pathway that causes side effects represents a significant step in GPCR therapeutics. By understanding the molecular basis for this particular effect it is hoped that additional ligands, at differing GPCRs, could be designed to exploit the concept of functional selectivity. In doing so, it should be possible to produce more specific drugs that activate only their desired functional property, while drastically reducing their non-specific side effects.

In my first specific aim I set out to better understand the binding of our lead compound (-)-*trans*-PAT and a series of similar analogues that were based off of this parent scaffold. My studies revealed that there are steric and electronic factors to consider around the amine region, which interacts ionically with D3.32A. This interaction is critical for the binding of all ligands to the HH₁R. When *meta* and *para*-substituted-PAT analogues were examined it was determined that each enantiomer seemed to bind to unique regions of the receptor. More specifically, the pendant phenyl ring of the ligand produces unique interactions with the HH₁R that lead the (-) and (+) enantiomers to bind

differently to the receptor. Through these studies it was also learned that larger substituents such as bromine and cyclooctyl rings are too large to be accommodated within the orthosteric binding pocket of the HH₁R. By better understanding the substitutions that cause high-affinity binding to the receptor it is hoped that our lab can produce more potent ligands that bind more specifically to the HH₁R.

The goal of my second aim was to understand what made (-)-*trans*-PAT such a unique ligand, meaning what was the root cause of its functional selectivity and its ability to label only a partial subset of the overall H₁ receptor population. This investigation began with a single amino acid residue (Y5.48A) that produced a loss of specific ³H-(-)-*trans*-PAT binding, but did not prohibit ³H-mepyramine from binding to the same mutation. From there, it was observed that PAT was unable to bind or function at Y5.48A, while histamine and mepyramine were able to function and bind to the receptor. This made the effects of Y5.48A on PAT ligand specific, and led to the conclusion that PAT exerts its effects through domain-swapped dimers. The mutation of this residue to alanine precluded the formation of these dimers and subsequently the loss of PAT binding and function. These results were supported by BRET studies and helped us arrive at the conclusion that PAT functioned exclusively through domain-swapped dimers.

In my last specific aim the goal was to investigate a particular residue, Y7.53 that was known to be involved in the functional processes of GPCRs that are closely phylogenically related to the HH₁R. The goal of these studies was to determine whether or not an alanine mutation at this particular position would have differing effects upon the pathways that the HH₁R can activate. My studies revealed a dichotomy between the

ability of the receptor to activate PLC/IP and AC/cAMP at Y7.53A. The overall response for histamine at AC/cAMP was ablated, while the PLC/IP pathway was still able to function, albeit in a significantly reduced manner. It was also observed that the inverse agonists (-)-*trans*-PAT and mepyramine were still able to function at Y7.53A. From these experiments it can be inferred that G_{αS} and G_{αQ} have unique affinities for the Y7.53A mutation, and that these affinities differ from the native HH₁R. G_{αQ} appears to have a reduced affinity for the Y7.53A receptor, indicated by its weakened ability to stimulate IP₃ formation; while all histamine signaling through G_{αS} is lost, indicating a lack of receptor coupling. Since the Y7.53A receptor is going to have identical conformations presented to both G-proteins, it can be said that G_{αS} and G_{αQ} must have differing affinities. This concept fits well with our understanding of functional selectivity and hints that native receptor conformations preferred by G_{αS} and G_{αQ} should be distinct from one another. By extension, it would seem plausible that multiple binding modes could exist for the same ligand; and that the conformation selected/or induced by the ligand may be influenced by the G-protein to which the receptor is coupled. These distinct conformations would allow ligands to stabilize, induce, and/or select a receptor conformation that preferentially targets one G-protein over another, providing a possible molecular explanation for the phenomenon known as functional selectivity.

Throughout these studies there were a couple shortcomings that warrant mentioning here. The inability to produce a double mutation for D3.32A/Y5.48A and Y5.48A/F6.52A would have allowed me to directly prove the domain-swapped dimer hypothesis for PAT. As things stand I had to use indirect evidence to prove this hypothesis, which while sufficient, was not ideal. If I had been able to produce these two

double mutations it would have been possible to demonstrate conclusively that Y5.48A prevents the receptor from forming domain-swapped dimers. I also wish I had more time to study Y7.53A, this particular mutation proved to be quite interesting and seemed to have a pronounced effect on the ability of the receptor to couple to the G-protein. My studies here illustrate for the first time that Y7.53A has differing effects on the ability of the HH₁R to activate two different G-proteins. If I had more time I would have loved to see if this phenomenon also occurred in receptors closely related to the HH₁R.

It is my hope that these studies have contributed to our overall understanding of GPCRs in general and more specifically the concept of functional selectivity. Ligand directed functional selectivity, as demonstrated with (-)-*trans*-PAT, possess significant potential for future drug design. Although this may not be realized in the near future, it is my sincere hope that my studies lay the groundwork for others to follow up on, and will further our understanding of these critical transmembrane receptors; leading to the design of more specific and efficacious drugs in the near future.

LIST OF REFERENCES

- Anthony et al. (2009). Dualsteric GPCR targeting: a novel route to binding and signaling pathway selectivity. *FASEB J.* , 442-450.
- Bakker et al. (2004). Domain swapping in the human histamine H₁receptor. *The Journal of Pharmacology and Experimental Therapeutics* , 131-138.
- Ballesteros et al. (2001). Structural mimicry in G-protein-coupled receptors: Implications of the high-resolution structure of rhodopsin for structure-function analysis of rhodopsin-like receptors. *Molecular Pharmacology* , 1-19.
- Bhattacharya et al. (2008). Ligand-stabilized conformational states of human beta-2-adrenergic receptor: insight into G-protein-coupled receptor activation. *Biophysical Journal* , 2027-2042.
- Booth et al. (2009). (1R, 3S)-(-)-Trans-PAT: A novel full-efficacy serotonin 5-HT_{2C} receptor agonist with 5-HT_{2A} and 5-HT_{2B} receptor inverse agonist/antagonist activity. *European Journal of Pharmacology* , 1-9.
- Booth et al. (2002). A novel phenylaminotetralin radioligand reveals a subpopulation of histamine H₁receptors. *The Journal of Pharmacology and Experimental Procedures* , 328-336.
- Booth et al. (2008). Molecular determinants of ligand-directed signaling for the histamine H₁ receptor. *Inflamm. Res.* , S01-S02.
- Booth et al. (1993). New sigma-like receptor recognized by novel phenylaminotetralins: ligand binding and functional studies. *The American Chemical Society for Pharmacology and Experimental Techniques* , 1232-1239.
- Booth, & Moniri. (2006). Role of PKA and PKC in histamine H₁ receptor-mediated activation of catecholamine neurotransmitter synthesis. *Neuroscience Letters* , 249-253.
- Brunton, Lazo, & Parker, a. (2006). Histamine, bradykinin, and their antagonists. In *The Pharmacological Basis of Therapeutics* (pp. 629-652). McGraw Hill.
- Bruysters et al. (2004). Mutational analysis of the histamine H₁-receptor binding pocket of histaprodifens. *European Journal of Pharmacology* , 55-63.
- Bucholtz et al. (1999). Synthesis, evaluation, and comparative molecular field analysis of 1-phenyl-3-amino-1,2,3,4-tetrahydronaphthalenes as ligands for the Histamine H₁receptor. *J. Med. Chem.* , 3041-3054.
- Chen et al. (2003). Chemical kindling induced by pentylenetetrazol in histamine H₁ receptor gene knockout mice (H₁KO), histidine decarboxylase deficient mice (HDC^{-/-}) and mast cell-deficient (W/W^v) mice. *Brain Research* , 162-166.

- Christopolous, & Kenakin. (2002). G-protein coupled receptor allostery and complexing. *Pharmacological Reviews* , 323-374.
- Fang, Travers, and Booth RG (2011) Pre-Publication
- Flanagan, C. (2005). A GPCR That Is Not “DRY”. *Molecular Pharmacology* , 1-3.
- Gillard et al. (2002). Binding characteristics of cetirizine and levocetirizine to human H₁histamine receptors: contribution of Lys (191) and Thr(194). *Molecular Pharmacology* , 391-399.
- Haas and Panula. (2003). The Role of histamine and the tuberomammillary nucleus in the nervous system. *Nature Reviews: Neuroscience* , 121-130.
- Haas et al. (2008). Histamine in the CNS. *Physiol Rev.* , 1183-1241.
- Hamm, H. (2001). How activated receptors couple to G proteins. *PNAS* , 4819-4821.
- Hermans, E. (2003). Biochemical and pharmacological control of the multiplicity of coupling at G-protein-coupled receptors. *Pharmacology and Therapeutics* , 25-44.
- Hoque, & Chesson. (2008). Zolpidem-induced sleepwalking, sleep related eating disorder, and sleep-driving: fluorine-18-fluorodeoxyglucose Positron Emission Tomography analysis, and a literature review of other unexpected clinical effects of zolpidem. *Journal of Clinical Sleep Medicine* , 471-476.
- Ito, C. (2009). Histamine H₃-receptor inverse agonists as novel antipsychotics. *Cent Nerv Syst Agents Med Chem* , 132-136.
- Johnston, & Siderovski. (2007). Receptor-mediated activation of heterotrimeric G-proteins: Current Structural Insights. *Molecular Pharmacology* , 219-230.
- Jongejan, & Leurs. (2005). Delineation of receptor-ligand interactions at the human histamine H₁receptor by a combined approach of site-directed mutagenesis and computational techniques - or - how to bind the H₁receptor. *Arch. Phram. Chem.* , 248-259.
- Kobilka, & Deupi. (2007). Conformational complexity of G-protein coupled receptors. *TRENDS in Pharmacological Sciences* , 397-406.
- Kobilka, & Rohrer. (1998). Insights from in vivo modification of adrenergic receptor gene expression. *Annu. Rev. Pharmacol. Toxicol* , 351-373.
- Kobilka, B. (2006). G protein coupled receptor structure and activation. *Biochimica et Biophysica Acta.* , 794–807.
- Leurs et al. (1995). Molecular pharmacological aspects of histamine receptors. *Pharmac. Ther.* , 413-463.

- Liang et al. (2003). Organization of the G-protein-coupled receptors rhodopsin and opsin in native membranes. *Journal of Biological Chemistry* , 21655–21662.
- Malfertheiner et al. (2009). Peptic ulcer disease. *Lancet* , 1449-1461.
- Meguro et al. (1995). Effects of thioperamide, a histamine H₃ Ligand. *Pharmacology Biochemistry and Behavior* , 321-325.
- Mirzadegan et al. (2003). Sequence analyses of G-protein coupled receptors: Similarities to rhodopsin. *Biochemistry* , 2759-2767.
- Moniri et al. (2004). Ligand-directed functional heterogeneity of histamine H₁ receptors: novel dual-function ligands selectively activate and block H₁-mediated phospholipase C and adenylyl cyclase signaling. *JPET* .274-281.
- Offermans, S. (2003). G-proteins as transducers in transmembrane signalling. *Biophysics and Molecular Biology* , 101-130.
- Panula et al. (1984). Histamine-containing neurons in the rat hypothalamus. *Proc. Natl. Acad. Sci.* , 2572-2576.
- Pin et al. (2004). Activation mechanism of the heterodimeric GABA_B receptor. *Biochemical Pharmacology* , 1565-1572.
- Prioleau et al. (2002). Conserved helix 7 tyrosine acts as a multistate conformational switch in the 5HT_{2C} receptor. *The Journal of Biological Chemistry* , 36577-6584.
- Rosendorff et al. (2000). Conserved helix 7 tyrosine functions as an activation relay at the serotonin 5HT_{2C} receptor. *Molecular Brain Research* , 90-96.
- Roth et al. (2007). Efficacy and safety of doxepin 1 mg, 3 mg, and 6 mg in adults with primary insomnia. *Sleep* , 1555-1561.
- Saxena, A., & Saxena, M. (1992). Developments in antihistamines (H₁). *Progress in Drug Research* , 35-125.
- Scharf et al. (2008). Efficacy and safety of doxepin 1 mg, 3 mg, and 6 mg in elderly patients with primary insomnia: arandomized, double-Blind, placebo-controlled crossover study. *J Clin Psychiatry* , 1557-64.
- Shi et al. (2002). Beta-2 Adrenergic receptor activation: modulation of the proline kink in transmembrane 6 by a rotamer toggle switch. *The Journal of Biological Chemistry* , 40989–40996.
- Smit et al. (1999). Molecular Propeties and signaling pathways of the H₁ receptor. *Clinical and Experimental Allergy* , 19-28.

- Spiegel, & Weinstein. (2004). Inherited diseases involving g proteins and g protein-coupled receptors. *Annu. Rev. Med.* , 27-39.
- Stahl. (2008). Selective histamine h₁ antagonism: novel hypnotic. *Trends in Psychopharmacology* , 1027-1038.
- Torrice et al. (2009). Probing the role of the cation- π interaction in the binding sites of GPCRs using unnatural amino acids. *Proceedings of the National Academy of Sciences PNAS*, 11919-11924.
- Urban et al. (2007). Functional Selectivity and Classical Concepts of Quantitative Pharmacology. *JPET* , 1-13.
- Van Rijn et al. (2006). Oligomerization of recombinant and endogenously expressed H₄receptors. *Mol Pharm* , 604-615.
- Visual Elements Group 17: The Halogens*. (n.d.). Retrieved June 28, 2010, from Royal Society of Chemistry:
http://www.rsc.org/chemsoc/visualelements/pages/data/intro_groupvii_data.html
- Wada et al. (1984). Distribution of the histaminergic neuron system in the central nervous system of rats; a fluorescent immunohistochemical analysis with histidine decarboxylase as a marker. *Brain Res* , 13-25.
- Whorton et al. (2007). A monomeric G protein-coupled receptor isolated in a high-density lipoprotein particle efficiently activates its G protein. *PNAS* , 7682-7687.
- Wieland et al. . (1999). Mutational Analysis of the Antagonist-binding Site of the Histamine H₁ Receptor . *Journal of Biological Chemistry* , 29994-30000.
- Yanai, & Toshiro. (2007). The physiological and pathophysiological roles of neuronal histamine: An insight from human PET Studies. *Pharmacology and Therapeutics* , 1-15.

BIOGRAPHICAL SKETCH

The author was born in 1984, to Bill and Linda Travers, in Baltimore, MD and was lucky enough to have a younger brother Garrett. He attended John Carroll High School in Bel Air, MD. After graduation, he attended Elon University in Elon, NC. He graduated with an American Chemical Society certified Bachelor of Science degree in chemistry and a minor in mathematics. Immediately after graduation, he started graduate school at the University of Florida, under the tutelage of Dr. Raymond Booth and completed his Doctor of Philosophy from University of Florida in August 2011.